UNIVERSITY OF CALIFORNIA, SAN DIEGO

Mechanisms integrating prior food experience to generate flexible behaviors

A dissertation submitted in partial satisfaction of the
requirements for the degree Doctor of Philosophy

in

Biology

by

Hiu Wing Lau

Committee in charge:

Professor Sreekanth Chalasani, Chair
Professor Stephan Anagnostaras
Professor Nicholas Spizter
Professor Lisa Stowers
Professor Jing Wang

2016

The Dissertation of Hiu Wing Lau is approved, and it is acceptable

in quality and form for publication on microfilm and electronically:

_____

_____

_____

_____

_____

Chair

University of California, San Diego

2016

DEDICATION

This is dedicated to my parents
for always 默默地支持和鼓勵我.

And to my incredible husband for
always being outrageously patient.

TABLE OF CONTENTS

LIST OF FIGURES

LIST OF TABLES

LIST OF SUPPLEMENTAL MOVIES

Chapter 2.

Movie S2.1. Sensory integration behavior of well-fed animals.
Well-fed wild-type animals in the sensory integration assay. Bracket indicates origin where animals are placed, spot shows position of 1:500 diacetyl odor, midline indicates repellent copper sulfate barrier.

Movie S2.2. Sensory integration behavior of food-deprived animals.
Wild-type animals food-deprived for three hours in sensory integration behavior assay. Bracket indicates origin where animals are placed, spot shows position of 1:500 diacetyl odor, midline indicates copper sulfate barrier.

Movie S2.3. Repellent-driven neural activity of ASI and ASH neurons in a well-fed animal.
Example video of well-fed animal with genetically encoded calcium indicator localized to the nuclei of ASI and ASH neurons stimulated with 50mM copper sulfate solution. Stimulus is presented as 1-second pulses starting at 10s and ending at 41s.

Movie S2.4. Repellent-driven neural activity of ASI and ASH neurons in a food-deprived animal.
Example video of food-deprived animal with genetically encoded calcium indicator localized to the nuclei of ASI and ASH neurons stimulated with 50mM copper sulfate solution. Stimulus is presented as 1-second pulses starting at 10s and ending at 41s,

ACKNOWLEDGEMENTS

I am grateful to all the mentors that have made this journey possible and enjoyable. Thank you to my thesis committee for being engaged and excited while offering constructive advice. My appreciation to Dr. Nick Spizter for being enthusiastic and supportive from my rotation until now, to Dr. Lisa Stowers and Dr. Jing Wang for critical input on our manuscript, and to Dr. Stephan Anagnostaras for your willingness to join my thesis committee and offering a unique point of view. The expertise and support from my committee has positively shaped my research and training.

I am incredibly thankful for my graduate advisor, Dr. Sreekanth Chalasani. Your commitment to mentoring comes through in numerous ways, whether it is in support of my research, career or personal growth. I appreciate your honesty, encouragement and support at every challenge and stage of this journey. Your enthusiasm for biology is contagious and your approach to solving complex biological problems is inspiring. I have learned more than I expected to and grown in unimaginable ways throughout this process. Most importantly, thank you for being mindful in putting together a lab that fosters a supportive and positive environment for learning and growing.

My appreciation also goes to past mentors at the University of Washington who helped me along the way to graduate school. My undergraduate mentor, Dr. David Parichy, gave me a chance to dive into research and discover my love for biology. Thank you to past members of the Parichy lab who contributed greatly to preparing me with countless lab skills, realistically portraying the life of academia and encouraging me to pursue this opportunity. I am also grateful for Dr. Scott Freeman's encouragement and

support. I am honored to have worked with you in biology education research and your approach to teaching inspired me to pursue invaluable experiences throughout graduate school.

The past and present members of the Chalasani lab have made this experience remarkable in countless ways. I appreciate Sarah Leinwand for teaching me basically everything *C. elegans* and for sharing many wonderful conversations. I am grateful for the company of Laura Hale, Chen-Min Yeh and Lauren Shipp, for being so caring, intelligent, inquisitive and supportive. I am fortunate to have been surrounded by incredible scientists and built lasting friendships from this journey. Many thanks to Ada Tong, Kathleen Quach, Adam Calhoun, Elizabeth DePasquale, Lou Tames, Uri Magaram for entertaining science and non-science conversations. Through the UCSD Biolgoical Sciences Ph.D. program, I gained the company of a wonderfully supportive group of friends. I am especially thankful for Leilani Cruz and Yvonne Pao, for being the best roommates, support system and filling this period with countless memories and laughs.

I am grateful for funding from National Science Foundation (NSF) Graduate Research Fellowship Program and a Socrates Fellowship from NSF GK-12 Program. It was a privilege to be paired with my partner high school teacher, Lenelle Wylie, who taught me priceless lessons in communicating science. Experiences in your classroom made the second year of graduate school unforgettable. Your dedication to teaching and mentoring continues to inspire me wherever I go.

Finally, thank you to my family for their patience, love, kindness, support and understanding. To my mom and dad, you taught me values that have gotten me through the most challenging times: to be humble, persistent and hard working. I owe my biggest

thanks to my husband, Shota Pearce, for moving to California with me and for always believing in my abilities. All the plates you made and labeled have contributed to this dissertation. You are a critical editor of my writing, an excellent audience for practice talks and my greatest supporter. For investing so much in me, this degree is as much yours as it is mine.

Chapter 1 includes a partial reprint of material in Lau, H.E., and Chalasani, S.H. (2014). Divergent and convergent roles for insulin-like peptides in the worm, fly and mammalian nervous systems. *Invert Neuroscience*.14 (2), 71-78 and is included with permission from the journal and all authors. The dissertation author is the primary author of this paper.

Chapter 2 is a reprint of the material as it appears in Lau, H. E., Cecere, Z.T., Liu, Z.,Yang, C.J., Sharpee, T.O., Chalasani, S.H. (2015). Neural mechanisms driving hunger-induced changes in sensory perception and behavior in *Caenorhabditis elegans* (in review) and is included with permission from all authors. It has been reformatted for this dissertation. The dissertation author was the primary author of this paper.

Chapter 3 is a reprint of the material as it appears in Lau, H. E., Liu, Z., Chalasani, S.H. (2015). Varying bacterial diet modifies chemosensory behavior via neuropeptide signaling in *Caenorhabditis elegans* (in preparation) and is included with permission from all authors. It has been reformatted for this dissertation. The dissertation author was the primary author of this paper.

VITA

Education

2016 Doctor of Philosophy, Biology, University of California, San Diego

2011 Bachelor of Science, Biology: Physiology; Neurobiology, University of Washington

Publications

Lau, H. E., Liu, Z., Chalasani, S.H. (2015). Bacterial diets modify chemosensory behaviors via neuropeptides in *Caenorhabditis elegans. In preparation*.

Lau, H. E., Cecere, Z.T., Liu, Z.,Yang, C.J., Sharpee, T.O., Chalasani, S.H. (2015). Neural mechanisms driving hunger-induced changes in sensory perception and behavior in *Caenorhabditis elegans*. *In review.*

Lau, H.E., and Chalasani, S.H. (2014). Divergent and convergent roles for insulin-like peptides in the worm, fly and mammalian nervous systems. *Invert Neuroscience*.14(2), 71-78.

Hamada, H., Watanabe, M., Kondo, S., Parichy, D.M., Lau, H.E., Nishida, T., Hasegawa, T. (2013). Involvement of Delta-Notch signaling in zebrafish adult pigment stripe patterning. *Development* 141(2), 318-324.

Larson, T.A., Gordon, T.N., Lau, H.E., Parichy, D.M. (2010). Defects in oligodendrocyte and Schwann cell development, pigment pattern, and craniofacial morphology in puma mutant zebrafish having an alpha tubulin mutation. *Developmental Biology* 346, 296–309.

ABSTRACT OF THE DISSERTATION

Mechanisms integrating prior food experience to generate flexible behaviors

by

Hiu Wing Lau

Doctor of Philosophy in Biology

University of California, San Diego, 2016

Professor Sreekanth Chalasani, Chair

To accommodate complex and changing environmental conditions, animals have evolved mechanisms to modify behaviors that maximize survival. Behavior can be modified by prior experiences that alter internal states such as hunger and external cues such as food signals. Despite the importance of this ability to evaluate and respond to environmental changes, it remains incompletely understood how animals accomplish this essential task. Using the *Caenorhabditis elegans* model system, the goal of this dissertation is to reveal mechanisms that allow animals to interpret the world around them and respond appropriately. Advantages of using *C. elegans* include a simple body

plan with a total of only 959 somatic cells, a complete nervous system wiring diagram and robust behavior readouts. Combining these advantages with powerful genetics and molecular manipulations, my dissertation presents mechanistic insight into how the nervous system generates flexible behaviors.

Chapter 1 introduces effects of environmental changes on neural circuits and how neuropeptides play an important role in linking food conditions with animal behavior responses. Insulin-like signaling is presented as an example of how conserved molecules play critical roles in modifying the nervous system. In Chapters 2 and 3, I use acute food experience paradigms to probe how prior experience modifies the nervous system resulting in altered animal behavior. Using acute food deprivation in Chapter 2, I show that internal state changes specifically and reversibly modify *C.elegans* behavioral responses to repellent signals. Lack of food status is sensed and relayed through multiple tissues using neuropeptides to modify downstream ASI chemosensory neurons altering repellent sensitivity. In Chapter 3, I show that transiently altering diet by changing food source modifies *C. elegans* behavioral responses to attractive signals. I also find that neuropeptide signals are used to relay diet changes modifying food-seeking behavior. In summary, my research links dietary changes with neuropeptide signals from multiple tissues modifying behaviors. Together, I have identified a role for neuropeptides and conserved signaling pathways in relaying changes in internal and external states. In sum, this dissertation unravels how prior experiences involving food signals modify the nervous system allowing animals to generate adaptive and appropriate behaviors.

CHAPTER 1.

Introduction

In response to complex environmental conditions that are constantly changing, animals generate adaptive and appropriate behaviors. In addition, prior experiences altering internal states can have profound effects on animal physiology and behavior. Numerous experiences in the environment can alter animals' internal and external states including information regarding temperature, mating, hunger and thirst, interactions with other animals and possible threats. In particular, food signals are crucial cues with direct impact on animal health and survival. A dissection of the mechanisms underlying prior experience modification of animal behavior requires revealing the underlying genes, molecules, cells and neural circuits. While previous studies have contributed to an understanding of the nervous system and how it is modified by prior experience, the inherent complexity within and beyond the nervous system presents a challenge for a comprehensive analysis of the underlying mechanisms. Utilizing the experimentally tractable *Caenorhabditis elegans* model system with advantages such as a simple body plan, nervous system and robust behavioral readouts, the research presented in my dissertation aims to address these important aspects of neurobiology linking prior states and behavioral outputs.

Prior food experience modifies neural circuits via neuropeptides

While animals respond to many different environmental cues, food signals are one of the most important cues with direct impact on physiology. Food signals and internal states are directly tied to metabolism and physiological homeostasis of the animal. Flexibility in behavior responses to both food quality and food quantity greatly aids survival. An important class of modulators that regulate responses to food related

conditions are small peptides and peptide hormones collectively called neuropeptides. In mammals, molecular signals that mediate energy homeostasis include a number of neuropeptides produced in the hypothalamus and peripheral signals such as leptin, cholecystokinin, ghrelin and insulin (Barsh and Schwartz, 2002). Studies in invertebrate model systems such as *C. elegans* and *D. melanogaster* have made progress in further dissecting the role of neuropeptides in modulating adaptive food related behaviors. In flies, It has been shown that dopamine, adipokinetic hormone, short neuropeptide F and neuropeptide F are involved in regulating olfactory and gustatory sensitivity (Su and Wang, 2014). *C. elegans* food related behaviors have been shown to be regulated by dopamine, the neuropeptide Y-related peptide receptor (NPR-1) and insulin signaling (Sengupta, 2013). One theme underlying modulation of food related behaviors is the conserved role of neuropeptides in relaying internal status, thereby linking environmental changes to the nervous system.

Neuropeptides have been shown to be important in modifying neural circuits and generating adaptive behaviors across many species (Taghert and Nitabach, 2012). The effect of internal states on behavior have been shown to be far reaching and can vary in strength, specificity, valence and persistence (Anderson and Adolphs, 2014). While some of these signals have been identified, the link between various environmental conditions, internal states and animal responses remains elusive. Furthermore, complexity in the function of neuropeptides relaying environmental conditions presents a challenge to understanding how specific internal states are encoded and how they interact with neural circuits driving behaviors. One hypothesis is that insulin signaling plays a major role in encoding food related prior experiences. Here, I will present research demonstrating the

role of insulin-like signaling as a conserved pathway with critical roles in modifying the nervous system. Beyond its classical role as an anorexigenic signal (Woods et al., 1996), insulin signaling modulates neural circuits and influences their output, as measured by behavior and neuronal activity in a number of model organisms (Ahmadian et al., 2004; Chalasani et al., 2010; Chen et al., 2013; Leinwand and Chalasani, 2013; Marks et al., 2009; Oda et al., 2011; Root et al., 2011). Beginning with an overview of the pathway, I will discuss the role of insulin signaling in regulating neuronal function across multiple organisms. By discussing the various roles of insulin signaling, this introduction aims to demonstrate an important and conserved role for neuropeptides in relaying internal state and external conditions of an animal to the nervous system where central physiological and behavioral processes are regulated.

Molecular components of the insulin-signaling cascade

The molecular components of the insulin-signaling pathway have been well characterized in worms, flies and mammals (Figure 1.1). Insulin or insulin-like peptides (ILPs) bind and activate a tyrosine kinase like insulin receptor (Massague et al., 1980). Upon activation, the insulin receptor phosphorylates a group of insulin receptor substrate (IRS) proteins, which in turn activate phosphoinositide 3-kinase (PI3K). When activated, PI3K regulates the activity of downstream kinases Akt/protein kinase B (PKB), leading to phosphorylation of the forkhead transcription factor, FOXO. Once phosphorylated, FOXO is unable to enter the nucleus, thereby reducing the transcription of target genes (Accili and Arden, 2004). In summary, one way in which insulin signaling regulates animal physiology is by inhibiting transcription of FOXO- dependent target genes.

The molecules involved in the canonical insulin-signaling cascade are highly conserved across both vertebrates and invertebrates. The *C. elegans* homologs of the insulin receptor, PI3K and FOXO are called DAF-2, AGE-1 and DAF-16, respectively (Figure 1.1, yellow) (Morris et al., 1996; Paradis et al., 1999; Paradis and Ruvkun, 1998; Pierce et al., 2001). However, the *C. elegans* homolog of IRS (IST-1) is proposed to function in a parallel pathway to the AGE-1/PI3K pathway (Wolkow et al., 2002). The other well-studied invertebrate model, *D. melanogaster*, has all components of the mammalian insulin-signaling pathway including an insulin receptor (dInR), IRS (CHICO and LNK) and FOXO (dFOXO) with similar functions (Figure 1.1, blue) (Leevers et al., 1996; Poltilove et al., 2000; Staveley et al., 1998; Werz et al., 2009). The homologs of insulin signaling molecules found across both vertebrates and invertebrates exemplify the remarkable conservation of this important pathway through evolution.

Modulation of neural function by ILPs in *C. elegans*

The well-studied nematode, *C. elegans*, has provided critical insights into insulin signaling and its role in regulating animal physiology, longevity and neuronal functions. Forty insulin-like peptide (ILP) genes, *ins-1* to *ins-39* and *daf-28,* have been identified in the *C. elegans* genome (Ritter et al., 2013). Characteristic of gene duplication events throughout evolution, these ILP genes are distributed across all six pairs of chromosomes in the worm (Figure 1.2). The expansive insulin gene family allows for both divergence and redundancy in the function of this crucial signaling network. INS-1 is most similar to the mammalian insulin peptide, but the other worm ILPs also show conserved structural domains with human insulin (Pierce et al., 2001).

Studies analyzing the role of ILPs in the *C. elegans* nervous system have shown that ILPs can have different effects on neural circuits in different contexts. *C. elegans* exposed to pathogenic bacteria can learn and avoid that pathogen upon a second exposure (Zhang et al., 2005). In the pathogen-avoidance learning paradigm, ASI chemosensory neuron-released INS-6 peptide inhibits transcription of INS-7 peptide in the oxygen-sensing URX neurons. In the absence of INS-6, INS-7 acts through the DAF-2 receptors to regulate the localization of DAF-16 in downstream RIA interneurons (Chen et al., 2013). This ILP-ILP loop demonstrates the complexity of signaling used to achieve specific changes in neural networks. Another study has demonstrated a separate role for INS-6 in regulating neural function. Here, INS-6 was shown to play a crucial role in coupling environmental conditions with development by inhibiting dauer entry and promoting dauer exit (Cornils et al., 2011). In response to harsh environmental conditions, *C. elegans* larvae enter a reversible stage of growth arrest (termed ‘‘dauer’’) wherein the animal arrests feeding and limits locomotion (Cassada and Russell, 1975). For regulating dauer arrest, the INS-6 signal is also released from ASI sensory neurons. Collectively, these results suggest that a high degree of spatial and temporal control of ILP function enables the same ligand to perform different roles based on context.

Insulin has also been shown to modulate neuronal activity in a transcription-independent manner that occurs on faster time-scales. In a salt chemotaxis learning paradigm, a 10–60 minute exposure to a particular concentration of salt in the absence of food leads to reduced attraction to that salt concentration (Tomioka et al., 2006). INS-1, DAF-2 and AGE-1 are all involved in altering neural activity of the salt-sensing ASE neurons based on associated food status (Oda et al., 2011). Importantly, this process does

not require DAF-16 or transcription. Similarly, INS-1 released from AIA interneurons has been shown to suppress AWC sensory neuron responses to food odors (Chalasani et al., 2010). In both of these examples, INS-1 acts on short timescales: less than a second in the case of AWC responses and a few minutes in ASE-associated behavior. In summary, modulation of neural function by insulin signaling in relation to food conditions is regulated at many levels: at the source, at the target, spatially and temporally.

Conservation of insulin signaling across species

Similar mechanisms and functions of insulin peptides have also been observed in the invertebrate model organism, *D. melanogaster*, and mammals. Orthologs to the mammalian and *C. elegans* insulin pathway have also been identified including a dInR (Drosophila insulin receptor), chico and lnk (IRS), PI3K and akt (Protein kinase B) (Figure 1.1) (Leevers et al., 1996; Poltilove et al., 2000; Staveley et al., 1998; Werz et al., 2009). Similar to results obtained using the *C. elegans* model, insulin signaling in *D. melanogaster* has also been shown to regulate multiple aspects of neuronal development. During development, a small cluster of median neurosecretory cells release insulin into the circulatory system in response to nutrients (Ikeya et al., 2002). Circulating insulin acts on neurons in the mushroom body and regulates the feeding behavior and growth of the fly larvae (Zhao and Campos, 2012). Insulins have also been shown to couple environmental conditions to physiology in the adult fly. *D. melanogaster* S6 kinase is involved in modulating hunger response by regulating the opposing effects of insulin and neuropeptide F signaling pathways (Wu et al., 2005). In addition, low levels of circulating insulin leads to the increase in the expression levels of the short neuropeptide

F receptor at the synapse between the olfactory receptor neuron and the projection neuron. This transcription-dependent event, which is inhibited by insulin signaling, enhances the attraction of adult flies to food (Root et al., 2011). These results show that dILPs produced in the brain couple nutritional status with neural circuit functions. In contrast to *C. elegans* findings of fast action of ILPs, the timescale of insulin action in flies can range from hours to days to accommodate changing nutrient availability. To summarize, these studies show that insulin represents a versatile signal that works with other peptide signaling systems to integrate nutritional status and regulate neuronal development and function.

In the mammalian system, peripheral insulin made by the pancreas can cross the blood brain barrier and influence the nervous system (Banks, 2004). Similar to the role of ILPs in invertebrates, ILPs in mammals also play a role in regulating neuronal growth and development (Chiu and Cline, 2010). In the brain, insulin mediates transcription-independent changes in specific neuronal populations on short timescales. Insulin in the olfactory bulb suppresses the activity of the shaker-like voltage-gated potassium channel, Kv1.3. Intranasal delivery of insulin resulted in increased phosphorylation of the Kv1.3 channel, leading to improved memory in recognition tasks and increased odor discrimination (Marks et al., 2009). Similarly, insulin and IGF1 both induce long-term depression and attenuate AMPA-mediated currents in the cerebellum through endocytosis of receptor subunits (Ahmadian et al., 2004; Wang and Linden, 1999). On the timescale of seconds, IGF1 also induces increases in calcium channel currents in a process that requires PI-3K (Blair and Marshall, 1997). On these fast timescales, insulin in the rodent brain modulates neuronal function by modulating the activity of ion channels (Blair and

Marshall, 1997; Marks et al., 2009). Apart from effects on ion channels, insulin signaling has also been shown to interact with other signaling pathways. In one study, insulin signaling acts in the hypothalamus to regulate the activity of another forkhead transcription factor, FOXA2 (Silva et al., 2009). Insulin signaling inhibits activity of FOXA2, reducing expression of neuropeptide genes orexin and melanin-concentrating hormone. Changes in orexin and melanin-concentrating hormone modify insulin sensitivity, body fat content and glucose metabolism of the animal (Silva et al., 2009). In the mammalian system, it is likely that a complex network of many different hormones and signaling peptides takes the place of an elaborately evolved insulin system observed in worms. Yet, the conserved role of the insulin-signaling pathway in coupling nutritional status with neuronal function and regulation is evident.

CONCLUSIONS

With the highlighted examples of insulin regulating neuronal function across species, a recurring theme is the critical role that insulin signaling plays in coupling different aspects of physiology to changing environmental conditions. Beyond insulin-like signaling, a broader network of peptide signaling pathways is also used to communicate internal state. In mammals, molecules such as neuropeptide Y, leptin, ghrelin, corticotropin-releasing hormone and melanin-concentrating hormone are used to modify specific target neurons in the hypothalamus for encoding nutritional status (Gao and Horvath, 2007). In *C. elegans*, there have been 122 neuropeptide genes identified including 42 neuropeptide-like proteins, 40 FMRFamine-related peptides and 40 insulin-like peptides (Hobert, 2013). I propose that this multitude of signals allows the animal to

encode and integrate various internal and external conditions effectively. Findings of neuropeptide signaling in *C. elegans* have and continue to reveal novel functions and mechanisms underlying the complexity in neuropeptide function. This thesis aims to provide critical links between prior food experiences, signaling molecules and neural function. Understanding peptide regulation and function is critical to deciphering the complex mammalian brain (Bargmann, 2012). Importantly, gaining a deeper understanding of peptide action further contributes to knowledge of how various tissues and organ systems individually and collectively respond to complex environmental changes.

The goal of this dissertation is to present my findings of molecular and cellular mechanisms underlying prior experience modification of behaviors in *C. elegans*. In Chapter 2, I will present evidence that in the context of hunger, multiple tissues sense lack of food and relay internal state using neuropeptides and non-canoncial insulin signaling. Here, neuropeptide signals from multiple tissues converge on a pair of chemosensory neurons to specifically modify repellent-driven behaviors. Chapter 3 will demonstrate how altering an animal's diet can lead to changes in peptide signals between tissues resulting in modified attractant-driven behaviors. Chapter 4 will further discuss how my research provides insight into understanding interactions between environmental signals and animal nervous systems. Lastly, I will highlight directions where future studies can expand upon the findings presented here.

ACKNOWLEDGEMENTS

This chapter includes a partial reprint of material in Lau H.E. and Chalasani, S.H.

(2014). Divergent and convergent roles for insulin-like peptides in the worm, fly and mammalian nervous systems. Invert Neuroscience.14(2), 71-78 and is included with permission from the journal and all authors. It has been reformatted for this dissertation. The dissertation author is the primary author of this paper.

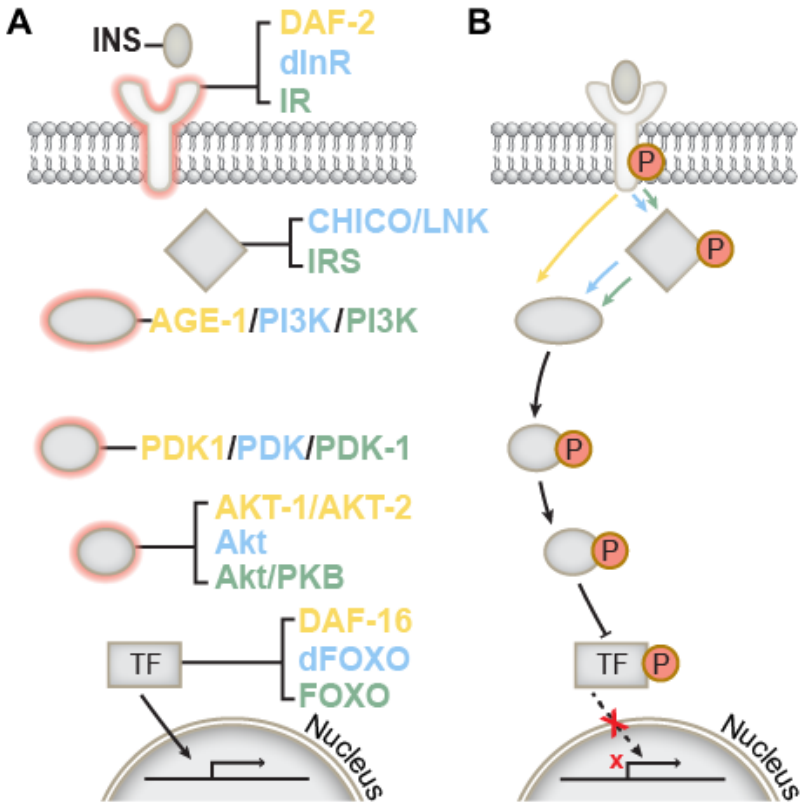

Figure 1.1. Insulin signaling pathway components.
(A) Basal state of the insulin signaling pathway. Mammalian insulin signaling components are labeled in green. *C. elegans* and *D. melanogaster* homologs of these molecules are shown in yellow and blue, respectively. Insulin receptors are conserved receptor tyrosine kinases. Upon ligand binding, insulin receptors phosphorylate their substrate, IRS, which in turn activates PI3K. In contrast to flies and mammals, the worm IRS (called IST-1) seems to work in parallel to the AGE-1/PI3K pathway shown here. Two kinases PDK-1 and AKT act downstream of PI3K and phosphorylate the forkhead transcription factor, FOXO, preventing it from activating target genes. In the absence of insulin, FOXO enters the nucleus and promotes the transcription of target genes. (B) Activation of insulin signaling pathway inhibits transcription of target genes. Activation of the insulin receptor results in phosphorylation of the insulin receptor substrates (CHICO and LNK in *D. melanogaster*). Phosphorylation of IRS activates downstream kinases PI3K, PDK and AKT, leading to the inhibition of FOXO, thereby reducing the transcription of target genes.

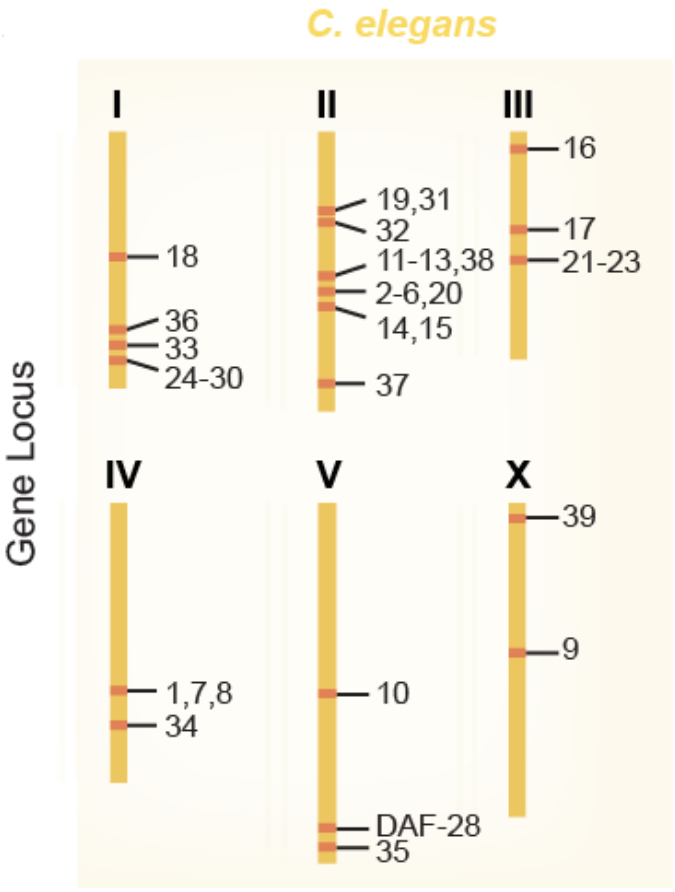

Figure 1.2 Chromosomal location of insulin-like peptide genes in *C. elegans*.
C. elegans genome has 40 ILP genes spread across all six chromosomes.

REFERENCES

Accili, D., and Arden, K.C. (2004). FoxOs at the crossroads of cellular metabolism, differentiation, and transformation. Cell *117*, 421-426.

Ahmadian, G., Ju, W., Liu, L., Wyszynski, M., Lee, S., Dunah, A., Taghibiglou, C., Wang, Y., Lu, J., Wong, T., Sheng, M., and Wang, Y. (2004). Tyrosine phosphorylation of GluR2 is required for insulin-stimulated AMPA receptor endocytosis and LTD. The EMBO journal *23*, 1040-1050.

Anderson, D.J., and Adolphs, R. (2014). A framework for studying emotions across species. Cell *157*, 187-200.

Banks, W. (2004). The source of cerebral insulin. European journal of pharmacology *490*, 5-12.

Bargmann, C.I. (2012). Beyond the connectome: how neuromodulators shape neural circuits. BioEssays : news and reviews in molecular, cellular and developmental biology *34*, 458-465.

Barsh, G.S., and Schwartz, M.W. (2002). Genetic approaches to studying energy balance: perception and integration. Nature reviews Genetics *3*, 589-600.

Blair, L., and Marshall, J. (1997). IGF-1 Modulates N and L Calcium Channels in a PI 3-Kinase-Dependent Manner. Neuron *19*.

Cassada, R.C., and Russell, R.L. (1975). The dauerlarva, a post-embryonic developmental variant of the nematode Caenorhabditis elegans. Dev Biol *46*, 326-342.

Chalasani, S.H., Kato, S., Albrecht, D.R., Nakagawa, T., Abbott, L.F., and Bargmann, C.I. (2010). Neuropeptide feedback modifies odor-evoked dynamics in Caenorhabditis elegans olfactory neurons. Nat Neurosci *13*, 615-621.

Chen, Z., Hendricks, M., Cornils, A., Maier, W., Alcedo, J., and Zhang, Y. (2013). Two insulin-like peptides antagonistically regulate aversive olfactory learning in C. elegans. Neuron *77*, 572-585.

Chiu, S.-L., and Cline, H.T. (2010). Insulin receptor signaling in the development of neuronal structure and function. Neural Development *5*, 7.

Cornils, A., Gloeck, M., Chen, Z., Zhang, Y., and Alcedo, J. (2011). Specific insulin-like peptides encode sensory information to regulate distinct developmental processes. Development (Cambridge, England) *138*, 1183-1193.

Gao, Q., and Horvath, T.L. (2007). Neurobiology of Feeding and Energy Expenditure. Neuroscience *30*, 367-398.

Hobert, O. (2013). The neuronal genome of Caenorhabditis elegans. WormBook, 1-106.

Ikeya, T., Galic, M., Belawat, P., Nairz, K., and Hafen, E. (2002). Nutrient-dependent expression of insulin-like peptides from neuroendocrine cells in the CNS contributes to growth regulation in Drosophila. Current biology : CB *12*, 1293-1300.

Leevers, S., Weinkove, D., MacDougall, L., Hafen, E., and Waterfield, M. (1996). The Drosophila phosphoinositide 3-kinase Dp110 promotes cell growth. The EMBO journal *15*, 6584-6594.

Leinwand, S.G., and Chalasani, S.H. (2013). Neuropeptide signaling remodels chemosensory circuit composition in Caenorhabditis elegans. Nature Neuroscience *16*, 1461-1467.

Marks, D., Tucker, K., Cavallin, M., Mast, T., and Fadool, D. (2009). Awake intranasal insulin delivery modifies protein complexes and alters memory, anxiety, and olfactory behaviors. The Journal of neuroscience : the official journal of the Society for Neuroscience *29*, 6734-6751.

Massague, J., Pilch, P.F., and Czech, M.P. (1980). Electrophoretic resolution of three major insulin receptor structures with unique subunit stoichiometries. Proceedings of the National Academy of Sciences *77*, 7137-7141.

Morris, J.Z., Tissenbaum, H.A., and Ruvkun, G. (1996). A phosphatidylinositol-3-OH kinase family member regulating longevity and diapause in Caenorhabditis elegans. Nature *382*, 536-539.

Oda, S., Tomioka, M., and Iino, Y. (2011). Neuronal plasticity regulated by the insulin-like signaling pathway underlies salt chemotaxis learning in Caenorhabditis elegans. Journal of neurophysiology *106*, 301-308.

Paradis, S., Ailion, M., Toker, A., Thomas, J., and Ruvkun, G. (1999). A PDK1 homolog is necessary and sufficient to transduce AGE-1 PI3 kinase signals that regulate diapause in Caenorhabditis elegans. Genes & development *13*, 1438-1452.

Paradis, S., and Ruvkun, G. (1998). Caenorhabditis elegans Akt/PKB transduces insulin receptor-like signals from AGE-1 PI3 kinase to the DAF-16 transcription factor. Genes & development *12*, 2488-2498.

Pierce, S.B., Costa, M., Wisotzkey, R., Devadhar, S., Homburger, S.A., Buchman, A.R., Ferguson, K.C., Heller, J., Platt, D.M., Pasquinelli, A.A., Liu, L.X., Doberstein, S.K., and Ruvkun, G. (2001). Regulation of DAF-2 receptor signaling by human insulin and ins-1, a member of the unusually large and diverse C. elegans insulin gene family. Genes Dev *15*, 672-686.

Poltilove, R., Jacobs, A., Haft, C., Xu, P., and Taylor, S. (2000). Characterization of Drosophila insulin receptor substrate. The Journal of biological chemistry *275*, 23346-23354.

Ritter, A., Shen, Y., Fuxman Bass, J., Jeyaraj, S., Deplancke, B., Mukhopadhyay, A., Xu, J., Driscoll, M., Tissenbaum, H., and Walhout, A. (2013). Complex expression dynamics and robustness in C. elegans insulin networks. Genome research *23*, 954-965.

Root, C.M., Ko, K.I., Jafari, A., and Wang, J.W. (2011). Presynaptic facilitation by neuropeptide signaling mediates odor-driven food search. Cell *145*, 133-144.

Sengupta, P. (2013). The belly rules the nose: feeding state-dependent modulation of peripheral chemosensory responses. Curr Opin Neurobiol *23*, 68-75.

Silva, J.P., von Meyenn, F., Howell, J., Thorens, B., Wolfrum, C., and Stoffel, M. (2009). Regulation of adaptive behaviour during fasting by hypothalamic Foxa2. Nature *462*, 646-650.

Staveley, B., Ruel, L., Jin, J., Stambolic, V., Mastronardi, F., Heitzler, P., Woodgett, J., and Manoukian, A. (1998). Genetic analysis of protein kinase B (AKT) in Drosophila. Current biology : CB *8*, 599-602.

Su, C.-Y., and Wang, J., W. (2014). Modulation of neural circuits: how stimulus context shapes innate behavior in Drosophila. Current Opinion in Neurobiology.

Taghert, P.H., and Nitabach, M.N. (2012). Peptide neuromodulation in invertebrate model systems. Neuron *76*, 82-97.

Tomioka, M., Adachi, T., Suzuki, H., Kunitomo, H., Schafer, W.R., and Iino, Y. (2006). The insulin/PI 3-kinase pathway regulates salt chemotaxis learning in Caenorhabditis elegans. Neuron *51*, 613-625.

Wang, Y., and Linden, D.J. (1999). Expression of Cerebellar Long-Term Depression Requires Postsynaptic Clathrin-Mediated Endocytosis. Neuron *25*.

Werz, C., Köhler, K., Hafen, E., and Stocker, H. (2009). The Drosophila SH2B Family Adaptor Lnk Acts in Parallel to Chico in the Insulin Signaling Pathway. PLoS Genetics *5*.

Wolkow, C.A., Munoz, M.J., Riddle, D.L., and Ruvkun, G. (2002). Insulin receptor substrate and p55 orthologous adaptor proteins function in the Caenorhabditis elegans daf-2/insulin-like signaling pathway. J Biol Chem *277*, 49591-49597.

Woods, S., Chavez, M., Park, C., Riedy, C., Kaiyala, K., Richardson, R., Figlewicz, D., Schwartz, M., Porte, D., and Seeley, R. (1996). The evaluation of insulin as a metabolic signal influencing behavior via the brain. Neuroscience and biobehavioral reviews *20*, 139-144.

Wu, Q., Zhang, Y., Xu, J., and Shen, P. (2005). Regulation of hunger-driven behaviors by neural ribosomal S6 kinase in Drosophila. Proceedings of the National Academy of Sciences of the United States of America *102*, 13289-13294.

Zhang, Y., Lu, H., and Bargmann, C.I. (2005). Pathogenic bacteria induce aversive olfactory learning in Caenorhabditis elegans. Nature *438*, 179-184.

Zhao, X., and Campos, A. (2012). Insulin signalling in mushroom body neurons regulates feeding behaviour in Drosophila larvae. The Journal of experimental biology *215*, 2696-2702.

CHAPTER 2.

Neural mechanisms driving hunger-induced changes in sensory perception and behavior in *Caenorhabditis elegans*

ABSTRACT

While much is known about how external cues affect neural circuits, less is known about how internal states modify their function. We acutely food deprived *C. elegans* and analyzed its responses in integrating attractant and repellent signals. We show that food deprivation leads to a reversible decline in repellent sensitivity with no effect on appetitive behavior allowing animals to engage in higher risk behavior. Multiple tissues including the intestine and body wall muscles use a conserved transcription factor, MondoA, to detect the lack of food and release AEX-5 convertase processed peptides from dense core vesicles. Subsequently, ASI chemosensory neurons use the DAF-2 insulin receptor and non-canonical signaling to integrate the tissue-released peptide signals modifying their stimulus-evoked adaptation rate. We suggest that altering ASI neuronal dynamics affects its function and modifies behavior. Together, these studies show how internal state signals modify sensory perception and risk assessment to generate flexible behaviors.

INTRODUCTION

Animals have evolved intricate mechanisms to detect relevant environmental cues as well as integrate information about various internal states including hunger and sleep (Sternson et al., 2013; Taghert and Nitabach, 2012). While progress has been made in decoding the neural circuits processing environmental changes, less is known about the machinery that integrates information about internal states. Of particular importance is nutritional status, which has a profound effect on animal survival and elicits dramatic changes in food-seeking behaviors (Atasoy et al., 2012). Moreover, multiple species have

been shown to alter their behavior during periods of starvation (Gillette et al., 2000; Inagaki et al., 2014; Kawai et al., 2000; Sengupta, 2013). This is thought to be achieved by constant crosstalk between the central nervous system and the various peripheral organs (Dietrich and Horvath, 2013).

In mammals, signals from peripheral tissues (hormones and nutrients), most notably the gut-released polypeptide ghrelin, trigger neuronal changes and affect behaviors (Kojima et al., 1999; Tschop et al., 2000). Ghrelin acts on hypothalamic neurons that express agouti-related protein (AGRP) and neuropeptide Y (NPY) (Andrews et al., 2008; Cowley et al., 2003), as well as other brain regions to increase food intake (Carlini et al., 2004; Malik et al., 2008). In contrast, leptin and insulin peptides released from adipose tissue and the pancreas respectively, act to suppress feeding behavior (Air et al., 2002). Apart from feeding behaviors, these peptide signals also influence neural circuits regulating anxiety (Dietrich et al., 2015), indicating that this signaling has a broader role in modulating brain function. Moreover, malfunction of peripheral organ-nervous system communication axis results in a number of metabolic disorders, including diabetes and obesity (Dietrich and Horvath, 2012; Muller et al., 2015). Despite the importance of this physiological process, the precise neuronal machinery integrating metabolic signals and modifying behaviors remains unknown.

The nematode *Caenorhabditis elegans* with just 302 neurons (White et al., 1986), 20 cells in its intestine (McGhee, 2007) and 95 body wall muscle cells (Moerman and Williams, 2006) provides a unique opportunity for a high-resolution analysis of how the nervous system integrates internal signals. Previous studies have shown that *C. elegans*, similar to mammals, exhibits a number of behavioral, physiological and metabolic

changes in response to altered nutritional status. When worms are removed from food, they exhibit a 50% reduction in their feeding rate (Avery, 1993). When returned to food, starved animals temporarily feed faster than well-fed animals (Avery and Horvitz, 1990), suggesting that feeding is not a simple reflex to food stimulus but can be modified by experience. Moreover, upon food deprivation, *C. elegans* hermaphrodites will retain eggs (Trent et al., 1983), are unlikely to mate with males (Lipton et al., 2004) and initiate altered foraging behaviors (Gray et al., 2005; Hills et al., 2004; Sawin et al., 2000). Moreover, many molecules that signal hunger are conserved between *C. elegans* and vertebrates. For example, neuropeptide Y (NPY) signaling influences feeding behaviors in nematodes and mammals (de Bono and Bargmann, 1998; Mercer et al., 2011; Nassel and Wegener, 2011). Similar effects are also seen with insulin and dopamine signaling, which seem to act via modifying chemosensory activity and behavior in nematodes (Chalasani et al., 2010; Ezcurra et al., 2011) and on mammalian hypothalamic and mid-brain circuits respectively (Air et al., 2002; Berthoud, 2011; Figlewicz and Sipols, 2010) to modify feeding behavior.

Here we use *C. elegans* to dissect the machinery integrating internal food signals and modifying behaviors. We combined acute food deprivation with a behavioral assay that quantifies the animal's ability to integrate both toxic and food-related signals, mimicking a simplified real world scenario. In this sensory integration assay, animals cross a toxic copper barrier (repellent) and chemotax towards a point source of a volatile odor, diacetyl (attractant) (Ishihara et al., 2002). We show that food-deprived animals have reduced sensitivity to the repellent and cross the copper barrier more readily than well-fed animals. Moreover, we find that multiple internal tissues sense the lack of food,

release peptides and use non-canonical insulin signaling to alter the adaptation rate of chemosensory neurons. This altered neuronal state allows animals to reduce their avoidance to repellents and undertake a higher risk strategy in their search for food.

RESULTS

Acute food deprivation specifically alters repellent-driven behaviors

Animals simultaneously integrate both attractant and repellent signals from their environment to generate appropriate behavioral readouts. To mimic these interactions, animals are exposed to a copper repellent barrier and a gradient of a volatile attractant, diacetyl (Ishihara et al., 2002). The proportion of animals that cross the copper barrier are counted and expressed as an integration index (Figure 2.1A). We analyzed the behavior of well-fed wild-type animals and found that few cross the copper barrier and locomote towards the spot of the diacetyl (white bar, Figure 2.1B, Table S2.1 and Movie S2.1). In contrast, when animals are food deprived for 3 hours, we observe an ~100% increase in the number of animals crossing the copper barrier (dark bar, Figure 2.1B, Table S2.1 and Movie S2.2). Moreover, we found that food-deprived animals cross the repellent barrier throughout the entire 45-minute assay suggesting a broad change in behavior (Figure S2.1A). Food-deprived animals also do not alter locomotory speed indicating that their general movement is not modified (Figure S2.1B). Also, this effect is not specific to diacetyl, as food-deprived animals also cross the copper barrier more when paired with other volatile attractants, isoamyl alcohol or benzaldehyde (Figure S2.1C). The proportion of animals crossing the copper barrier in both well-fed and food-deprived states is a function of both attractant and repellent concentrations (Figures S2.1D-E and

Table S2.1). Together, our results show that food-deprived animals cross the repellent barrier more readily than well-fed animals.

Next, we tested whether food deprivation affects the sensitivity to repellents or attractants independently. We analyzed the behavior of well-fed and food-deprived animals on assay plates with either copper or odor gradients alone. We found that food-deprived animals crossed the copper barrier more readily than well-fed animals, suggesting that their responsiveness to copper is reduced (Figure 2.1C, Figure S2.1F and Table S2.1). In contrast, food-deprived animals did not alter their attraction to diacetyl or other volatile attractants (Figure 2.1C and Figure S2.1G). Given the small number of animals that cross the copper barrier alone (Figure 2.1B, a high % increase from well-fed value results from low integration index in the well-fed condition, Table S2.1), we continued to pair copper with the diacetyl attractant for further analysis. We found that food-deprived animals have reduced sensitivity to copper, intermediate concentrations of fructose and salt, but not quinine, 2-nonanone and other concentrations of fructose and salt (Figure S2.1H). We suggest that copper and these intermediate concentrations of salt and fructose are environmental cues that *C. elegans* might have evolved to detect and reducing sensitivity to these cues enables the animal to use a higher risk food search strategy.

Food deprivation reversibly modifies animal behavior

We probed the time course of the food-deprivation effect on animal behavior. We found that animals need to be food deprived for at least 2 hours before they showed a reduction in their copper sensitivity with a maximum effect at 3 hours (Figure 2.1D). We

also found that animals did not deplete their fat stores during the 3-hour food deprivation (Figure S2.2A-D), suggesting that this behavior change is likely to be independent of fat metabolism. Next, we asked whether the food-deprivation effect was reversible. We food-deprived animals for 3 hours and then returned them to food for different durations and analyzed animal behavior after the food experience. We found that food-deprived animals that had been returned to food for 5 hours reverted their copper avoidance behavior to well-fed behavior (Figure 2.1E). These results indicate that food deprivation reversibly reduces copper avoidance.

C. elegans has been shown to evaluate multiple aspects of the food experience, including changes in food distribution, oxygen and carbon dioxide concentrations, small molecule metabolites and others (Calhoun et al., 2015; Carrillo and Hallem, 2015; Ludewig and Schroeder, 2013). To uncouple the tactile and chemosensory input of the bacteria [*C. elegans* consume *E. coli* (Brenner, 1974)] from the nutritional value of ingesting bacteria, we analyzed the effect of modified bacteria on animal behavior. Aztreonam is a drug that inhibits bacterial cell wall synthesis and results in long filaments of bacteria that do not divide and cannot pass through the grinder into the *C. elegans* intestine (Gruninger et al., 2008). Animals exposed to aztreonam-treated bacteria experience the tactile and chemosensory input, but are unlikely to derive nutritional value from the food. We found that exposing animals to drug-treated bacteria for 3 hours was sufficient to reduce their sensitivity to copper, suggesting that the lack of food in the animal alters copper sensitivity (Figure 2.1F). Together, these results show that the lack of food in the *C. elegans* intestine, but not the absence of sensory cues, reduces the animal's sensitivity to copper.

Food deprivation reduces reorientations enabling more animals to cross the repellent barrier

To analyze how food deprivation modifies animal behavior, we developed a new multi-worm tracker. This tracker enables us to identify individual animals and their trajectories over many minutes as they integrate repellent and attractant signals in the sensory integration assay (see Extended Experimental Procedures for details of the tracker). We tracked animals in both well-fed and food-deprived conditions and filtered the tracking data to consider a time window between 3 and 15 minutes in the assay. Additionally, we included events executed by animals moving towards the copper barrier. We found that food-deprived animals are more likely to cross the repellent barrier when compared to well-fed animals as shown by the increased density of well-fed animal tracks before the copper barrier (Figure 2.2A, 2.2B). We performed a similar analysis on animals moving away from the copper barrier and found no significant differences between well-fed and food-deprived conditions (data not shown). We then fit a Laplace mixture model for the distribution of turn events observed at different distances from the copper barrier (Figure S2.3A-D). This allows us to precisely quantify the reorientations and small turns as the animals approached the copper barrier and after crossing the barrier (see Extended Experimental Procedures for quantification details). While a large reorientation allows the animal to reverse its direction of movement, small turns generate smaller changes in the direction (Figure S2.3A-D). These large reorientations and small turns are similar to the previously described “pirouettes” and “small turns” respectively (Iino and Yoshida, 2009; Pierce-Shimomura et al., 1999). Compared to food-deprived animals, we found that well-fed animals make significantly more reorientations as they

approach the copper barrier (Figure 2.2C). In contrast, there is no difference between well-fed and food-deprived animals in their relative small turn probabilities (Figure 2.2D). Since our assays included a paralytic, we were unable to obtain movement data from animals close to diacetyl. Together, these results suggest that well-fed animals reorient more, thus avoiding the copper barrier, while food-deprived animals reorient less and cross the copper barrier more frequently. Moreover, these data also suggest that food-deprived animals are unlikely to avoid toxic copper compounds in their environment allowing them to execute food search strategies with higher risk.

Intestine and body wall muscles use MML-1, but not MXL-2 to sense the lack of food and releases peptides to signal to the neurons

Our studies show that the lack of food inside the animal is responsible for the transient reduction in copper sensitivity. We hypothesized that internal tissues sense this lack of food and signal to the nervous system to modify neuronal function and behavior. To gain insights into how these tissues sense the absence of food, we used a candidate gene approach. In mammalian cells, glucose is rapidly converted to glucose-6-phostphate, whose levels are sensed by a two basic-helix-loop-helix-leucine zipper transcription factors, MondoA and ChREBP (Carbohydrate Response Element Binding Protein). In well-fed conditions, MondoA binds the excess glucose-6-phosphate and Mlx (Max-like protein X) and translocates to the nucleus where it activates transcription of glucose-responsive genes. In the absence of glucose, MondoA remains in the cytoplasm (Havula and Hietakangas, 2012; Stoltzman et al., 2008). *C. elegans* homologs for MondoA and Mlx have been identified as MML-1 and MXL-2 respectively (Grove et al.,

2009). Furthermore, MML-1 has also been shown to translocate into the intestinal nuclei under well-fed conditions (Johnson et al., 2014). We predicted that *mml-1* mutants would be unable to sense the lack of food and thereby unable to reduce copper sensitivity after food deprivation. Consistently, we found that *mml-1*, but not *mxl-2* mutants are defective in their integration responses after food deprivation (Figure 2.3A). To localize the MML-1 function to a specific tissue, we expressed the full-length coding sequence under specific promoter elements and analyzed its effect on behavior. We used promoter elements that drive expression in all neurons (*H20*), intestine (*gly-19*) or body wall muscles (*myo-3*) (Figure 2.3B) (Okkema et al., 1993; Shioi et al., 2001; Warren et al., 2001). We find that expressing the full-length cDNA encoding MML-1 specifically in the intestine and body wall muscles, but not neurons is sufficient to restore normal behavior to *mml-1* mutants (Figure 2.3A). We suggest that in the absence of food, MML-1 remains in the cytoplasm of intestinal and body wall muscle cells and speculate that the cytosolic MML-1 reduces copper sensitivity by modifying signaling between tissues.

Next, we hypothesized that the intestine and body wall muscles release peptide signals to relay the lack of food signal to the nervous system. To identify the relevant class of peptides, we analyzed gene mutants in peptide processing. The *C. elegans* genome encodes four known pro-protein covertases (AEX-5, EGL-3, BLI-4, and KPC-1) that cleave an overlapping subset of pro-peptides to generate mature peptides, which are further modified and packed into dense core vesicles (Li and Kim, 2008). Upon activation, dense core vesicles are released using the CAPS protein (calcium activated protein for secretion, *unc-31*) (Figure 2.3C) (Speese et al., 2007). We found that *aex-5* mutants were specifically defective in their sensory integration response under food-

deprived, but not well-fed condition (Figure 2.3D, Table S2.1). In contrast, *egl-3* mutants were defective in their sensory integration behavior in both well-fed and food-deprived conditions, while *bli-4* and *kpc-1* were defective only in the well-fed state (Figure 2.3D and Table S2.1). Previously, neuropeptide signaling has been shown to play a role in modifying sensory integration behavior (Ishihara et al., 2002) and we suggest that peptides processed by EGL-3, BLI-4 and KPC-1 might be involved. Together these results show that AEX-5-processed peptides are specifically required for animals to reduce their copper sensitivity after food deprivation.

To localize AEX-5 function to a specific tissue, we expressed the full-length coding sequence under specific promoter elements that drive expression in all neurons (*unc-119*), intestine (*gly-19*), body wall muscles (*myo-3*), pharynx (*myo-2*) and tail (*lin-44*) in the null mutant background and analyzed its effects on behavior (Figure 2.3B) (Hilliard and Bargmann, 2006; Maduro and Pilgrim, 1995; Okkema et al., 1993; Warren et al., 2001). We found that restoring AEX-5 to either the intestine, body wall muscles or neurons but not the pharynx or tail was sufficient to revert *aex-5* null mutants to normal modulation after food deprivation (Figure 2.3E). To confirm AEX-5 function in intestine, body wall muscles and neurons, we knocked down this gene specifically in those tissues and analyzed the effects on integration behavior. Expressing sense and anti-sense transcripts under cell-selective promoters has been shown to knock down the gene of interest in the target cells (Esposito et al., 2007; Leinwand and Chalasani, 2013). Using this approach, we found that knocking down *aex-5* in the intestine, body wall muscles or neurons generated animals that were defective in altering behavior after food-deprivation (Figure 2.3F). Previously, AEX-5 was shown to function in the intestine to modulate

defecation behavior and body wall muscles to affect neuromuscular junction function (Mahoney et al., 2008; Sheng et al., 2015). However, our results showing AEX-5 activity in neurons are novel. Also, we found that knocking down UNC-31 [CAPS protein required for peptide release (Speese et al., 2007)] in the intestine, body wall muscles or neurons also rendered animals unable to modify their response in the integration assay after food deprivation (Figure 2.3G). Taken together, these results suggest that while AEX-5 processing is required in the intestine, body wall muscles and neurons, release of AEX-5 processed peptides from any of those tissues is sufficient to reduce copper sensitivity after food deprivation. Moreover, our results also show that the intestine and body wall muscles also use dense core vesicles to release peptides, a novel mechanism.

ASI chemosensory neurons use DAF-2 receptors to integrate intestine-released AEX-5 processed peptide(s)

To gain insights into the nature of the intestine-released peptide signal, we analyzed mutants in downstream receptors. The *C. elegans* genome encodes at least 122 neuropeptide genes including 42 neuropeptide like proteins (NLPs), FMRFamine-related peptides (FLPs) and 40 insulin-like peptides (ILPs) (Hobert, 2013). Many of the NLPs and FLPs are thought to act on G-protein coupled receptors (GPCRs), while ILPs bind the receptor tyrosine kinase, DAF-2 to influence cellular functions (Chen et al., 2013b; Hobert, 2013; Leinwand and Chalasani, 2013; Pierce et al., 2001). Upon binding cognate ligand(s), GPCRs use heterotrimeric Gαβγ proteins to activate signal transduction (Hamm, 1998). There are two Gγ subunits, *gpc-1* and *gpc-2* in the *C. elegans* genome, both with viable null mutants (Jansen et al., 1999). We found that mutants in the insulin

receptor, DAF-2, were defective in their response to food deprivation, suggesting that the intestine and other tissues might release insulin-like peptide(s) to modify integration response after food deprivation (Figure 2.4A). In contrast, mutants in the two Gγ subunits or the carboxypeptidase, EGL-21, which is required to generate mature NLPs and FLPs (Husson et al., 2007) are not defective in their responsivity to copper after food deprivation (Figure S2.4A). Together, these data suggest that insulin signaling might be involved in reducing copper sensitivity after food deprivation.

To localize the site of DAF-2 action, we analyzed the effect of rescuing this receptor in different tissues. We found that expressing *daf-2* under the neuronal, but not intestine or body wall muscle promoters (Hung et al., 2014) restored normal behavior to the *daf-2* mutants (Figure 2.4A). These results implied that AEX-5 convertase might process an insulin-like peptide(s) in the various internal tissues. To identify the cognate ligand(s), we analyzed null mutants or RNA interference knockdowns against each of the 40 insulin-like peptides (Hobert, 2013). However, we found that none of the gene mutants or knockdowns in these peptides affected the altered integration response upon food deprivation (Table S2.2). We speculate that a combination of insulin-like or other peptide(s) might relay the lack of food signal from the intestine and other tissues. Taken together, these results suggest that neuronally expressed DAF-2 receptors might detect AEX-5 processed peptides that are released from multiple internal tissues.

To localize DAF-2 function to individual neurons, we used cell-selective promoters and generated transgenic animals. Previous studies have shown that three pairs of chemosensory neurons ASI, ASH and ADL detect copper ions and generate avoidance response (Hilliard et al., 2002). Given that food deprivation alters the animal's response

to copper ions specifically, we tested whether DAF-2 was required in any of these sensory neurons. We found that restoring DAF-2 to ASI, but not ASH or ADL was sufficient to restore normal behavior to *daf-2* mutants (Figure 2.4B, Table S2.1). ASI-specific expression does not completely rescue the food-deprivation driven *daf-2* mutant behavioral phenotype suggesting that DAF-2 might also be required in additional neurons. Together, these results suggest that ASI neurons use DAF-2 receptors to detect internal tissue-released peptide(s) to modify integration behavior.

ASI neurons use non-canonical insulin signaling to integrate AEX-5 processed peptide signals

To identify the components of the DAF-2 signaling in ASI neurons that integrate food status signals, we analyzed gene mutants in candidate pathway components (Figure 2.4C). We observed that mutants in the canonical insulin-signaling pathway components phosphoinositide 3-kinase (PI3K, *age-1*), serine/threonine kinases AKT-1, AKT-2 (*akt-1*, *akt-2*), 3-phosphoinositide-dependent kinase 1 (*pdk-1*) and lipid phosphatase (*daf-18*, PTEN suppressor) performed normally in the sensory integration assay after food deprivation (Figure S2.4B) (Lapierre and Hansen, 2012). In contrast, mutants in serum and glucocorticoid inducible kinase-1 (*sgk-1*) are defective in their copper sensitivity after food deprivation (Figure 2.4D). We found that restoring SGK-1 function to ASI neurons specifically was sufficient for normal integration response in food-deprived *sgk-1* mutants (Figure 2.4D). SGK-1 has been previously shown to interact with the mTORC2 complex including Rictor (Jones et al., 2009; Mizunuma et al., 2014). We also tested mutants in *rict-1* (*C. elegans* Rictor) in our sensory integration assay and found

that these mutants are also unable to alter their behavior after food deprivation (Figure 2.4D). Similar to SGK-1, we found that RICT-1 was also required in ASI neurons to restore normal food-deprivation behavior to *rict-1* mutants (Figure 2.4D). These results suggest that SGK-1 and RICT-1 might function in the same pathway downstream of DAF-2 receptors in ASI neurons. These results are consistent with previous studies showing that SGK-1 and mTORC2 act parallel to the canonical insulin-signaling pathway to regulate stress responses and animal lifespan (Hertweck et al., 2004). Collectively, these results show that both SGK-1 and RICT-1 function in ASI neurons downstream of DAF-2 receptors to reduce copper sensitivity after food deprivation.

To test whether AEX-5 and DAF-2 function in the same pathway, we performed genetic epistasis experiments. We generated an *aex-5;daf-2* double mutant, which did not show any additional defects when compared to either *aex-5* or *daf-2* single mutant (Figure 2.4E). We also found that expressing AEX-5 in the intestine and DAF-2 in ASI sensory neurons restored normal integration response after food deprivation (Figure 2.4E). Together, these data show that the intestine released AEX-5 processed peptides are detected by ASI neurons using the DAF-2 receptors. These results suggest the following order for these signaling events: food deprivation leads to lack of food within the animal, which is detected by the intestine and body wall muscles using cytosolic MML-1 leading to the release of AEX-5 processed peptides that bind DAF-2 receptors and are processed by downstream SGK-1 and RICT-1 in ASI and other neurons to reduce copper sensitivity and alter behavior.

Food deprivation alters ASI neuronal adaptation rate

To test how food deprivation modifies neural function, we probed the activity of copper-sensitive neurons using calcium imaging. We localized a genetically encoded calcium indicator (Akerboom et al., 2012) to the nuclei of ASI and ASH neurons, allowing us to measure neural activity in both neurons simultaneously. We also expressed the fluorescent mCherry protein under an ASI-selective promoter in the same transgenic animal enabling us to specifically identify ASI neuronal nuclei (Figure S2.5A-C). Recently, nuclear calcium dynamics have been shown to be similar to those measured from the cytoplasm (Schrodel et al., 2013), validating our approach. We presented the repellent copper solution to the nose of an animal constrained in a microfluidic device and recorded neural activity as previously described (Chalasani et al., 2007) in both well-fed and food-deprived conditions. We found that both well-fed and food-deprived animals responded similarly to long pulses (30 seconds) of repellent stimuli (data not shown). We then presented the repellent stimulus as 1-second pulses (1 second on, 1 second off) for 30 seconds. This protocol allows us to probe the activity of ASI and ASH neurons to repeated pulses of copper solution, a regimen that animals might experience as they encounter the copper barrier (see Experimental Procedures). We found that well-fed ASI neurons responded to the removal of copper stimuli with increasing fluorescence changes until a maximal fluorescence change (peak). Subsequently, the ASI calcium signals dropped suggesting that this neuron had adapted to the copper stimuli (black line indicates average, Figure 2.5A). This result is consistent with previous studies showing that adapted chemosensory neurons do not respond to stimuli (Chalasani et al., 2010). In contrast, under food-deprived conditions, ASI neurons had a higher threshold requiring additional stimulus pulses to observe a calcium change. Moreover, we did not observe a

distinct maximal fluorescence or a decline in the calcium signal, suggesting that ASI neurons did not adapt (green line indicates average, Figure 2.5A). Moreover, in both well-fed and food-deprived conditions, we observe an ASI calcium response to the removal of last copper stimulus suggesting that there are additional calcium dynamics. Given that we observe food-deprivation modifies animal behavior as the animal experiences the copper barrier, we focused our analysis on the calcium dynamics obtained in response to the repeated stimuli. We quantified the average change in fluorescence in an 8-second window both before and after the peak in well-fed conditions and compared the data to a similar time window in the food-deprived conditions (Figure 2.5B). We also tested ASI responses to additional copper stimulus concentrations and observed similar dynamics at 25 mM and 100 mM, but not at 10 mM (Figure S2.6A, S2.6C and S2.6E). These data suggest that ASI neurons show a dose-dependent response to the removal of copper stimuli and can adapt to repeat stimulus pulses, which is altered by food deprivation. Together, these data show that food deprivation increases the stimulus threshold and transforms ASI from an adapting to a non-adapting state.

Next, we analyzed ASH activity data in both well-fed and food-deprived conditions. We found that ASH neurons responded to both the addition and removal of copper stimuli. Under well-fed conditions, we observed complex dynamics including an increase in calcium signal to the initial stimulus pulses followed by responses without change in baseline through the middle stimulus pulses and finally, a smaller decline in the baseline response to the last few stimulus pulses (black line indicates average, Figure 2.5C). We also find that food deprivation lowers the ASH threshold (higher response to the initial stimulus pulses), which is followed by responses without change in baseline

through the middle stimulus pulses and no decline in the baseline response to the last few stimulus pulses (green line indicates average, Figure 2.5C). Similar to ASI dynamics, we also observe ASH responses to removal of the last copper stimulus pulses suggesting additional dynamics. We performed a similar analysis on the ASH calcium data and found that food deprivation reduces the stimulus threshold and had a smaller effect on the ASH adaptation rate (Figure 2.5D). We also tested additional copper stimulus concentrations and found that ASH neurons also show dose-dependent responses to both addition and removal, but are not significantly affected by food deprivation. Together, these data show that food deprivation reduces the stimulus threshold of ASH neurons and likely affects additional stimulus dynamics.

Our genetic experiments showed that food-deprivation effects are lost in *daf-2* mutants. To test whether the changes in ASI neural activity also use the same genetic pathway, we performed a similar analysis of their copper-evoked responses in *daf-2* mutants. Consistent with our genetic analysis, we found that the ASI-specific neural activity changes after food deprivation are lost in the *daf-2* mutants (Figure 2.6A-2.6D). We also compared the ratio of change in food-deprived to well-fed conditions in both wild-type and *daf-2* mutants and found that the insulin-receptor mutant had a significant effect on ASI, but not ASH activity (Figure 2.7A). Collectively, these results show that food deprivation affects ASI threshold and adaptation kinetics in a DAF-2 dependent manner.

DISCUSSION

We used food deprivation in *C. elegans* as a model to understand how changes in internal states modify behavior. We show that food-deprived animals reversibly alter their behavior by reducing their repellent responsiveness, allowing them to traverse potentially toxic environments in their search for food. Multiple tissues including the intestine, body wall muscles and neurons independently sense the lack of food and release peptide signals that are integrated by DAF-2 receptors on ASI neurons (Figure 2.7B). This novel, non-neuronal, dense core vesicle release dependent peptide signaling transforms ASI neurons from a rapidly adapting to a non-adapting neuron modifying animal behavior. We suggest that altering the state of sensory neurons affords greater dynamic range of control over behavioral decisions. More generally, we demonstrate how neuronal activity is regulated by internal state signals to modify behaviors lasting many minutes.

Multiple tissues release peptide(s) to signal "lack of food"

Multicellular animals sense and regulate glucose homeostasis at several levels. While insulin and glucagon maintain constant levels of circulating glucose, the Myc-family transcription factors are used within cells. Glucose uses cell membrane localized transporters to enter cells, where it is rapidly converted into glucose-6-phosphate (Jordan et al., 2010). This intermediate metabolite is sensed by the Myc-Max complex, which binds glucose-6-phosphate and translocates to the nucleus where it regulates the transcription of glucose-responsive genes (Havula and Hietakangas, 2012). While the role of ChREBP/MondoA-Mlx-glucose-6-phosphate complex in regulating the gene transcription is well studied (Li et al., 2010; Stoeckman et al., 2004; Stoltzman et al.,

2008), the role of these proteins in the cytoplasm remains poorly understood. We show a specific role for MML-1 (MondoA homolog), but not MXL-2 (Mlx homolog) in the intestine and body wall muscles in reducing copper sensitivity after food deprivation. We suggest that in the absence of MML-1, these two tissues are unable to detect the lack of glucose and do not relay signals to modify the downstream neuronal circuits. Moreover, we also speculate that MML-1 (MondoA) accumulation in the cytoplasm (in the absence of glucose) enables the intestine and body wall muscle cells to release peptide(s) relaying a "lack of glucose" signal to other tissues.

Our analysis describes a role for the pro-protein convertases in modifying behavior upon food deprivation. We show that while *egl-3, bli-4* and *kpc-1* mutants are defective in their sensory integration response, *aex-5* mutants are specifically affected in their response to food deprivation. Moreover, we show that AEX-5 functions in the intestine, body wall muscles and neurons to process relevant peptide(s). Previously, *aex-5* has been shown to function in both the body wall muscle cells and the intestine to regulate exocytosis at the neuromuscular junction and the defecation motor program respectively (Doi and Iwasaki, 2002; Sheng et al., 2015). However, our studies confirming a role for AEX-5 in neurons are novel. We suggest that *C. elegans* neurons use a MML-1 independent mechanism to detect the lack of glucose and release AEX-5 processed peptide(s). Surprisingly, we find that restoring AEX-5 function to the intestine, the body wall muscles or neurons is sufficient to restore normal behavior to *aex-5* mutants, while knocking down this gene in any of these three tissues disrupts wild-type behavior. Together, these results suggest that intestine, body wall muscle or neuronal release of AEX-5 processed peptide(s) alone is sufficient to relay food status signals and

this signaling is required in all three tissues in wild-type animals. Given that our transgenic rescue experiments involve expressing more than one copy of the AEX-5 protease in the three tissues (see Extended Experimental Procedures), we speculate that this "food status" signaling is regulated at the level of pro-peptide cleavage such that excess mature peptide(s) from the intestine, body wall muscles or neurons can compensate for the lack of signal from the other two tissues.

Moreover, we also identify a role for the dense core vesicle release machinery in non-neuronal tissues including the intestine and body wall muscles. Interestingly, in mammals a second CAPS protein (CAPS2) that is expressed in non-neuronal tissues has been identified (Speidel et al., 2003). These results suggest that peptide release from non-neuronal tissues might also involve dense core vesicles across multiple species from worms to mammals. Collectively, we show that multiple tissues including the intestine, body wall muscles and neurons process precursors using the AEX-5 protease and release mature peptide(s) using the CAPS protein relaying "food status" signals to downstream neurons.

ASI chemosensory neurons integrate "food status" signals

Our studies show that while the intestine, body wall muscles and neurons release AEX-5 processed peptide(s), ASI chemosensory neurons use the tyrosine kinase insulin receptor (DAF-2) to integrate these signals. Three lines of evidence suggest that the internal tissues are releasing insulin-like peptide(s)- first, the food-deprivation effect does not require G-protein receptor signaling, second, the insulin receptor (DAF-2) integrates these signals and third, DAF-2 and AEX-5 function in the same pathway. Although our

efforts to identify the cognate insulin-like peptide (ILP) have been unsuccessful, we suggest that combination of ILPs might relay "food status" signals from the intestine, body wall muscles and neurons to ASI sensory neurons. We also find that non-canonical signaling pathway components are used downstream of DAF-2 to integrate these peptide signals. Our results show that while PI-3Kinase, AKT kinase -1 and -2, PDK-1 and PTEN are not required, SGK-1 (serum and glucocorticoid inducible kinase) and its binding partner Rictor (a component of the mTORC2 complex) are required to integrate AEX-5 processed peptide signals. Although SGK-1 has been shown to phosphorylate DAF-16 (FOXO) in vitro (Hertweck et al., 2004), it might also indirectly regulate a subset of the DAF-16 target genes (Chen et al., 2013a; Murphy and Hu, 2013). We suggest that this SGK-1-Rictor (mTORC2) complex might integrate signals from multiple pathways including DAF-2 signaling to regulate DAF-16-target genes (Mizunuma et al., 2014) and modify neuronal functions and animal behavior.

Our genetic analysis shows that ASI chemosensory neurons integrate peptide signals and modify integration response after food deprivation. ASI neurons have been previously shown to detect food signals to modify animal behavior (Calhoun et al., 2015; Gallagher et al., 2013). However, our results showing that ASI integrates internal food status signals are novel.

Food-deprivation alters the ASI neural adaptation rate

Our imaging experiments show that ASH neurons respond to the copper pulses, before ASI neurons, suggesting that ASH might be a low-threshold, while ASI is a high-threshold copper detector. This is consistent with previous results showing that ASH is

crucial for copper avoidance (Hilliard et al., 2005; Hilliard et al., 2002) and with data showing that ASI is a high-threshold detector for food (Calhoun et al., 2015). This dual coding strategy with high and low-threshold neurons is commonly used across *C. elegans* and others species to efficiently encode stimulus information (Calhoun et al., 2015; McGlone and Reilly, 2010). Moreover, our analysis of ASH and ASI neural activity in *daf-2* mutants reveals a surprising feature. We find that ASH responses are greatly reduced in the *daf-2* mutants, but spare some neural dynamics, particularly in the early stimulus pulses. In contrast, the dynamics of the high-threshold ASI neurons are significantly altered. We suggest that the food-deprivation signal has a stronger influence on the high-threshold ASI, while sparing some of the signaling from the low threshold ASH neurons. These results are also consistent with our genetic experiments showing that DAF-2 is specifically required in ASI, but not ASH neurons to integrate internal food status signals.

We also show that food deprivation alters the adaptation kinetics in ASI sensory neurons and reduces its responsiveness to copper stimuli. Adaptation is a fundamental property of many sensory systems, enabling neurons to extract relevant information from background noise (Mease et al., 2013; Wark et al., 2009). Sensory neurons have been shown to adapt to a variety of stimulus distributions and efficiently encode information (Wark et al., 2007). Indeed, individual neurons in the rodent sensorimotor cortex and retinal ganglion cells and others have been shown to alter their input-output properties based on the size of the input stimulus and local statistical context (Mease et al., 2013; Wark et al., 2009). We observe a similar change in the ASI neural activity, where it adapts to repeated stimulus pulses allowing them to read local concentration gradients

more effectively. In contrast, under food-deprived conditions, the adaptation rate is reduced making these neurons insensitive to changes in copper stimuli. Moreover, we also show that non-canonical insulin signaling mediates some aspects of food deprivation by altering neural adaptation rates leading to flexible behaviors. We suggest that similar peptide signaling pathways might exist across different animal species allowing their nervous systems to integrate internal information like food deprivation, stress and others.

We speculate that changes in ASI neuronal properties might underlie altered animal behavior. We observe that food-deprived animals have fewer reorientations as they approach the copper barrier allowing them cross the repellent and approach the attractant. In contrast, well-fed animals have higher number of reorientations allow them to avoid the copper barrier. We suggest that transforming ASI from a rapidly adapting to a non-adapting neuron prevents this neuron from detecting local changes in copper leading to fewer reorientations and allowing the food-deprived animals to cross the copper barrier. These data are also consistent with previous studies showing that ASI neurons suppress reorientations indicating that animals with high ASI activity will re-orient less (Gray et al., 2005). These studies link metabolite sensing by internal tissues with non-canonical insulin signaling that alters neuronal adaptation rate to modify chemosensory behavior, a mechanism likely conserved across species.

METHODS

Strains and Molecular Biology

C. elegans strains were grown and maintained under standard conditions (Brenner, 1974). All strains used are listed in Supplemental Table S2.3.

The following primers were used for amplifying full-length cDNAs:

aex-5

forward 5'TATTTAGCTAGCATGAAATTAATTTTCCTG

reverse 5'TATTTAGGTACCTTATGACATTGTTCCCAC

mml-1

forward 5'TATTTAGCTAGCATGTCGCGCGGGCAGATTATACACAG

reverse 5'CGGGGTACCGAGCAGTTCAAAATGGATTTTTGAGTTGTTGC

sgk-1

forward5'TATTTAGCTAGCATGGTGAGGAAAGATGAGGTGACATGC

reverse 5'CGGGGTACCTCAGACCAAAACGCGATTGGTGTCGAC

rict-1

forward5'TATTTAGCTAGCATGGACACTCGTCGAAAAGTGTATCAC

reverse 5'CGGGGTACCTAAAAGATTTGCTGCAGGAATGCTCTCG

cDNAs corresponding to the entire coding sequences of *aex-5, mml-1, sgk-1 and rict-1,* genomic region was amplified by PCR using primers above and expressed under tissue or cell selective promoters. *aex-5* antisense DNA was synthesized (Genewiz) and expressed under tissue-selective promoters for knockdown experiments. Cell and tissue selective RNAi transgenes were created as previously described by co-injection of equal concentrations of sense and antisense oriented gene fragments driven by cell or tissue specific promoters (Esposito et al., 2007). Tissue specific expression was achieved with *unc-119* or *H20* for all neurons, *gly-19* for the intestine, *myo-3* for body wall muscles, *myo-2* for pharynx, and *lin-44* for hypodermal cells of the tail (Hilliard and Bargmann, 2006; Maduro and Pilgrim, 1995; Okkema et al., 1993; Shioi et al., 2001; Warren et al.,

2001). Cell-specific expression used *sre-1* for ADL, *sra-6* for ASH, and *str-3* for ASI neurons (Troemel et al., 1995). For all experiments, a splice leader (SL2) fused to *m-Cherry* or *gfp* transgene was used to confirm expression of the gene of interest in either specific cells or tissues.

Germline transformations were performed by microinjection of plasmids (Mello and Fire, 1995) at concentrations between 50 and 100 ng/μl with 10 ng/μl of *unc-122::rfp*, *unc-122::gfp* or *elt-2::gfp* as co-injection markers. For rescue experiments, DNA was injected into mutant *C. elegans*. For tissue-specific RNAi knockdown experiments, sense and antisense DNA was injected into wild type *C. elegans*.

Behavior Assays

Control and food-deprived animals were grown to adulthood on regular nematode growth medium (NGM) plates before they were washed and transferred to new food or food-free plates respectively for the indicated duration. Sensory integration assay was performed on 1.6% agar plates containing 5mM potassium phosphate (pH 6), 1mM $CaCl_2$ and 1mM $MgSO_4$. Repellent gradients (including $CuSO_4$, glycerol, NaCl, and quinine) were established by dripping 25μl of solution across the midline of the plate (Ishihara et al., 2002). Prior to the assay, the animals were washed from the food or food-free plates before being transferred to the assay plates. After 45 minutes or at indicated times, the integration index was computed as the number of worms in the odor half of the plate minus the worms in origin half of the plate divided by the total number of worms that moved beyond the origin. The percent increase of food-deprived animals from well-fed controls was calculated by subtracting the averaged well-fed integration indices from

each food-deprived integration index, divided by the averaged well-fed integration index. Nine or more assays were performed on at least three different days. Two-tailed unpaired *t* tests (for Figure 2.1B only) and one sample *t* tests were used to obtain statistical information across food conditions. An ordinary one-way ANOVA test was used to compare all conditions in Figures 2.1D-E. To compare across strains for genetic rescue or knock down experiments, unpaired *t* test with Welch's correction was used.

Aztreonam-treated bacteria were prepared as previously described (Gruninger et al., 2008). *E. coli* was grown at 37°C overnight while shaking vigorously to an optical density (OD) of less than 0.6 to avoid log phase. This culture was treated with aztreonam antibiotic (Sigma) at a final concentration of 10 μg/ml and incubated at 37°C for 3 hours with minimal shaking at 70 RPM. Aztreonam-treated bacteria were immediately spread on plates also with 10μg/ml aztreonam, dried and used that day for behavior experiments.

Calcium Imaging

C. elegans expressing nuclear-localized GCaMP5K calcium indicators (Akerboom et al., 2012) under an ASH and ASI selective promoter are trapped and imaged using a PDMS based microfluidic device (Chalasani et al., 2007). Expressing mCherry protein in the cytoplasm under an ASI-specific promoter identified ASI neurons. Both ASI and ASH neurons were imaged simultaneously. M13 buffer (30mM Tris-HCl pH 7.0, 100mM NaCl and 10 mM KCl) were used in all imaging experiments to prevent $CuSO_4$ from precipitating. Prior to data collection, ASH neurons were exposed to blue light for two minutes as previously published (Hilliard et al., 2005). Each animal was only imaged once using the 1-second on, 1-second off pulse protocol. Images were

captured using Metamorph software on an inverted microscope using a Photometrics EMCCD camera. Baseline F_0 was measured as average fluorescence during a three-second window (1s-4.4s). The ratio of change in fluorescence to the baseline F_0 is plotted using custom MATLAB scripts.

Fat quantification

Oil red O staining was conducted as previously described (Soukas et al., 2009). Briefly, synchronized animals under well-fed or food-deprived animals were kept on ice for 10 minutes to stop pharyngeal activity. After fixation, animals were taken through three freeze-thaw cycles and exposed to a working solution of Oil red O stain (40% water: 60% oil red O in isopropanol). Animals were imaged with a 20X objective on a Zeiss Axio Imager and an Orca Flash 4.0 camera. In all cases, staining in the intestine within 500 pixels from the bulb was quantified using ImageJ (NIH). Percent of stained pixels was calculated using ImageJ, which assigned every pixel a value on a gray scale of 0 (Black) – 255 (white), values of less than 50 correspond to staining. We estimated a ratio by calculating the sum of these 50 pixels and dividing it by the total number of pixels (150,000 pixels). Within each experiment, 14 animals from each condition were quantified and all experiments were repeated at least three times on different days. Data were analyzed for significance using Student's *t* test and error bars represent SEM.

Speed analysis

The movement of the animals was tracked over 30 minutes using a Pixelink camera and speed was analyzed with Matlab to track the centroid of the animal (Ramot et

al., 2008). Five worms were placed on a NGM plate to prevent collisions. The results from 12 plates collected over 3 days were averaged for each food condition.

Visualizing Copper Gradients

Copper sulfate gradients visualized using 1-(2-Pyridylazo)-2-naphthol (PAN, Sigma). Plates with 5mM, 25mM, 50mM and 100mM copper sulfate were dried overnight. 1ml of 0.01% PAN indicator was added to plates the next day and allowed to dry. The plates with PAN indicator were incubated overnight and imaged the following day to allow for saturation of the signal. Images and quantification of the copper barrier is shown in Figure S2.7.

Calcium Imaging Analysis

To quantify calcium responses of ASI and ASH neurons to copper concentrations 25-100mM, the stimulus pulse at which maximum fluorescence change (peak) occurs was determined (indicated by red arrows in Figures 2.5A, 2.5C, 2.6A, 2.6C and S2.6C-F). Changes in fluorescence in an eight-second window before and after the peak (indicated by red brackets to the left and right of the peak) are averaged for each food condition using MATLAB. To compare pre-peak and post-peak responses, unpaired *t* tests with Welch's correction were used. For Figure 2.7A, the percent increase of post-peak responses from pre-peak responses was calculated by subtracting the averaged pre-peak response from each post-peak response value, divided by the pre-peak response average. To compare across food conditions, unpaired *t* tests with Welch's correction was used.

Tracking

The movement of well-fed and food-deprived animals during sensory integration behavior assay (50mM copper sulfate barrier and 1:500 diacetyl) was tracked over 45 minutes using a Pixelink camera. The field of view captures the middle region of the plate (height 3.2 mm, width 40 mm). Six to twelve worms were placed on a chemotaxis plate to prevent collisions. Custom C++ software built on the OPENCV and dlib libraries was used to track the midpoints of large numbers of moving worms. Briefly, the user defines the initial positions of the animals using a mouse click. We then use a kalman filter to predict the location of animals in the next frame. Next, these predictions were paired with identified contours using a minimum distance algorithm, which is constrained to minimize the number of predictions paired to the same contour. We recorded the midpoint of the contour and used that information to update the kalman filter. We tested the efficacy of our tracker using its visual output. Due to the high frequency of worms leaving and reentering the frame, the tracker re-finds all worms every 200 frames and makes no attempt at tracking single worms for the duration of the movie.

Track Analysis and Model Fitting

Ten movies were tracked for animals in both well-fed and food-deprived conditions. Data from same condition movies were combined, yielding two time vs. midpoint datasets. The data was then downsampled so that time points were about 1.5 seconds apart. Downsampling removes the correlations in worm movements due to sinusoidal movements (data not shown). Changes in orientation were calculated for the downsampled data from sequences of movement tangent vectors. We filtered the tracking

data to consider a time window between 3 and 15 minutes in the assay and only analyzed the movements of animals that approached the attractant, diacetyl. We also filtered for other directions, but did not find a significant change in behavior after food deprivation. Change in orientation was calculated by comparing the movement vector entering the target point to the movement vector exiting the target point (Figure S2.3A, S2.3B). Finally, the change in orientation data was filtered using the time, x-position, and angle from the copper line at the beginning of each turn.

A Laplace mixture model was fit to each change in orientation distribution using the truncated Newton constrained optimization algorithm with multiple initial estimates:

$$p(x) = w * lap\left(x; \theta_{1,}\alpha_{1,}\beta_{1}\right) + (1 - w) * lap\left(x; \theta_{2,}\alpha_{2,}\beta_{2}\right)$$

where x refers to the change in orientation and each Laplace (lap) distribution is described by a skewed-Laplace formula:

$$lap(x; \theta, \alpha, \beta) = \begin{cases} \dfrac{exp\left(\dfrac{f(x,\theta)}{\alpha}\right)}{\alpha + \beta} \text{for} x \leq \theta \\ \dfrac{exp\left(\dfrac{g(x,\theta)}{\beta}\right)}{\alpha + \beta} \text{for} x > \theta \end{cases}$$

where function f calculates the angular increase from point x to mean θ, while function g calculates the angular decrease from x to θ. Since a peak always appeared at π, θ_2 was fixed at π. Moreover, the optimal θ_1 was found to always be near 0. Thus, the Laplace distribution with mean equal to θ_1 is considered the 'slight turn' Laplace. The second Laplace distribution is considered the 'reorientation' Laplace.

Since the integral from -inf to +inf of the skew Laplace is equal to 1, the weight parameter w describes the probability of a given sample falling in a given distribution.

Thus, the probability of reorientation can be estimated by 1-w. The $\alpha + \beta$ term serves as a pseudo variance term. Thus, $\alpha_1 + \beta_1$ describes the 'relative small turn probability'.

ACKNOWLEDGEMENTS

We thank A. Dillin, T. Ishihara, S. Lockery, A. Samuelson, E. Troemel, M. Zhen, the National BioResource Project (NBRP, Japan) and Caenorhabditis Genetics Center (CGC) for strains; C. Bargmann, E. Hallem, M. Hilliard, A. van der Linden, P. McGrath, D. Pilgrim and P. Sengupta for constructs; S. Srinivasan and lab members for RNAi clones and help with oil red O staining. We are also grateful to L. Stowers, J. Wang, S. Asinof, L. Hale, U. Magaram, L. Shipp, K. Quach, C. Yeh and members of the Chalasani lab for critical comments, advice, and insights. This work was funded by grants from The Rita Allen Foundation, The W.M. Keck Foundation and NIH R01MH096881-03 to S.H.C. H.E.L. was initially supported by the Socrates Program funded by NSF GK-12 STEM Fellows in Education (Award #NSF-742551) followed by a Graduate Research Fellowship also from the NSF.

Chapter 2 is a reprint of the material as it appears in Lau, H. E., Cecere, Z.T., Liu, Z.,Yang, C.J., Sharpee, T.O., Chalasani, S.H. (2015). Neural mechanisms driving hunger-induced changes in sensory perception and behavior in *Caenorhabditis elegans* (in review) and is included with permission from all authors. It has been reformatted for this dissertation. The dissertation author was the primary author of this paper.

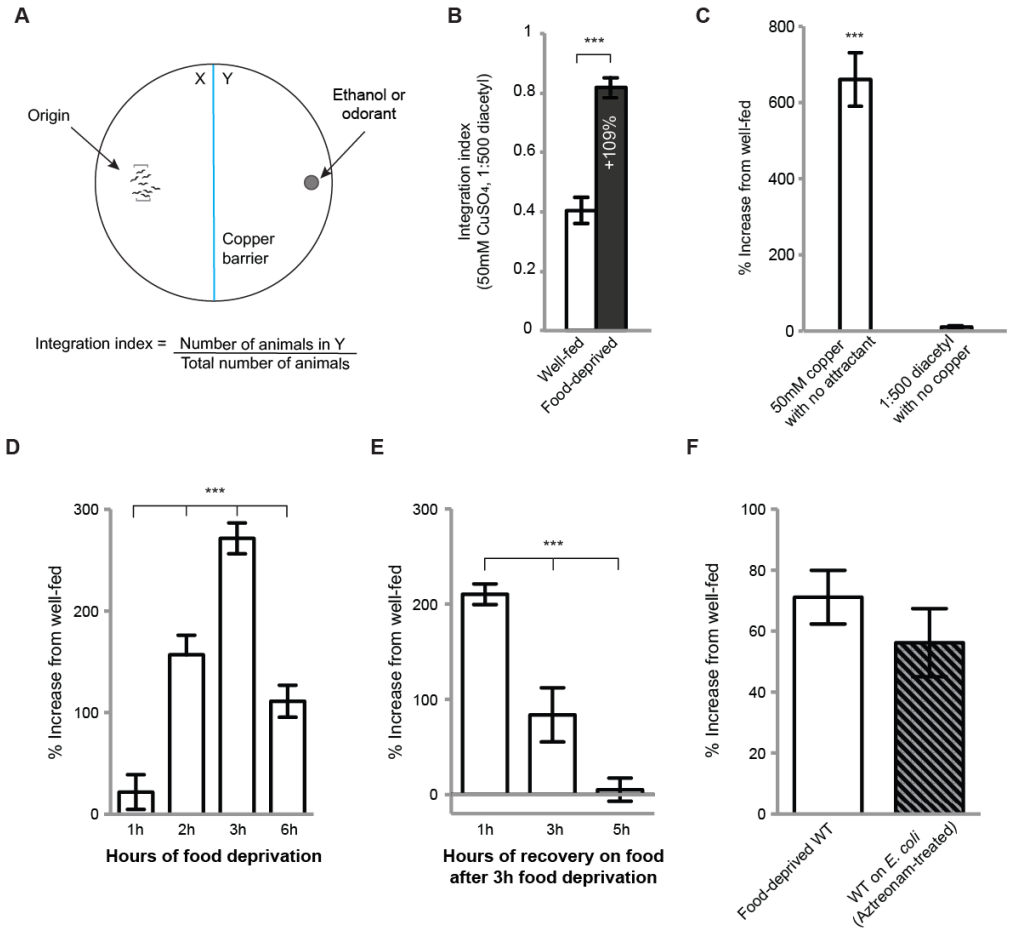

Figure 2.1. Food deprivation specifically and reversibly alters repellent-driven behaviors.

(A) Schematic of sensory integration assay with the copper barrier (blue) and animals at the origin and the attractant on the other side. (B) Food-deprived animals show increased integration index compared to well-fed animals integrating 50mM copper sulfate with 1:500 diacetyl. Two–tailed Student's *t* test ***$p < 0.0001$, $n \geq 9$. (C) Compared to well-fed animals, food-deprived animals cross the copper sulfate barrier significantly more even when no attractant is presented in the assay. Chemotaxis to diacetyl alone is not modified by food deprivation. One sample *t* test ***$p < 0.0001$, $n \geq 9$ per condition per assay. (D) Time course of food deprivation shows that a minimum two hours of food deprivation is required for modifying behavior. Maximum behavioral modification can be observed after three hours of food deprivation. One-way ANOVA ***$p < 0.0001$, $n \geq 9$ per condition per time point. (E) After three hours of food deprivation, five hours of recovery on food reverts sensory integration behavior to well-fed levels. One-way ANOVA ***$p < 0.0001$, $n \geq 9$ per condition per time point. (F) Animals exposed to aztreonam-treated *E. coli* for three hours show similar reduction in copper sensitivity as food-deprived animals. One sample *t* test $p < 0.05$, $n \geq 9$ per condition. All bars represent population means; error bars indicate SEM.

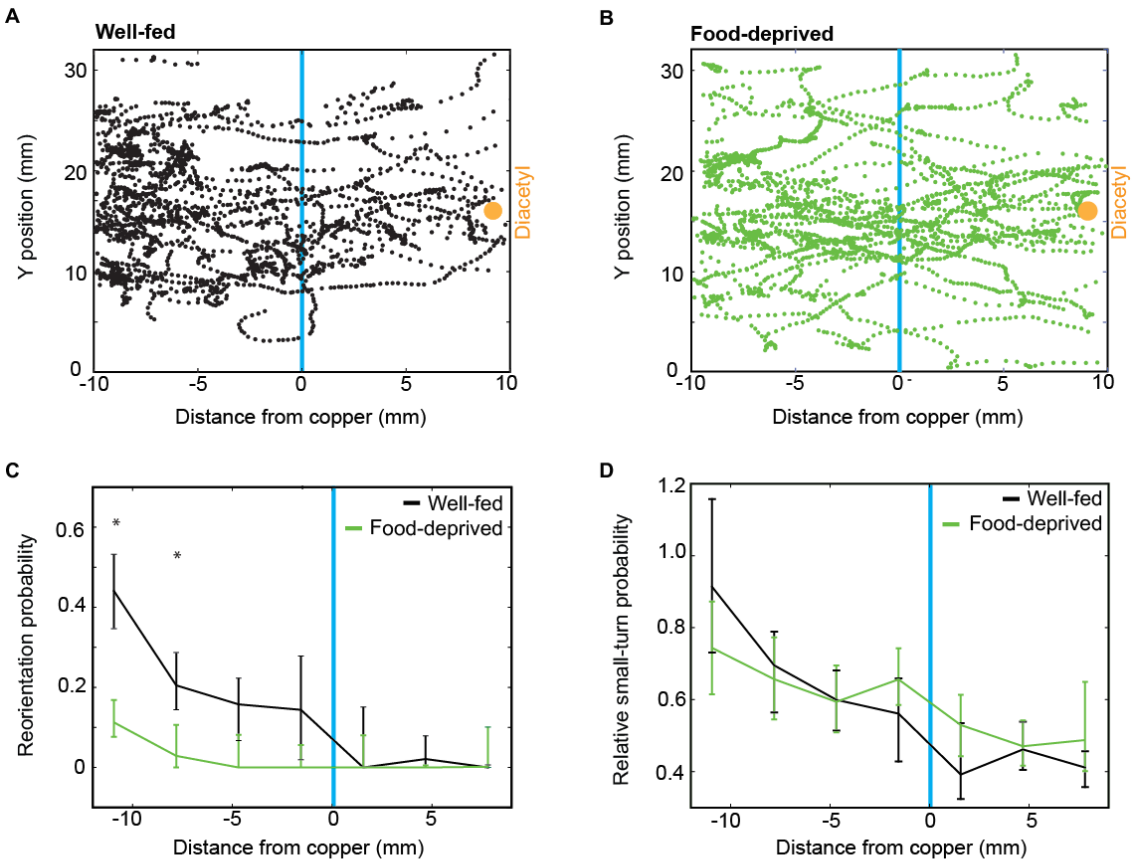

Figure 2.2. Food deprivation reduces reorientation events enabling increased repellent barrier crossing.
(A-B) Tracks of (A) well-fed and (B) food-deprived animals in sensory integration assay over 45 minutes. Blue line in the middle indicates the position of copper barrier. Animals begin -10 mm from copper barrier and diacetyl is positioned at 10mm from copper barrier at the orange spot. (n = 48 for each condition). (C) Reorientation probability of well-fed and food-deprived animals moving towards (left half) and away (right half) from the copper line during sensory integration assay. Well-fed animals exhibit increased reorientation probability approaching copper line. (D) Small-turn probability of well-fed and food-deprived animals moving towards (left half) and away (right half) from the copper line during sensory integration assay. Well-fed and food-deprived animals exhibit similar small-turn behaviors. All data points represent median of bootstrap reorientation probability estimates; error bars indicate 50% bootstrap bias-corrected confidence interval (n > 100, bootstraps = 1000, * 95% CI).

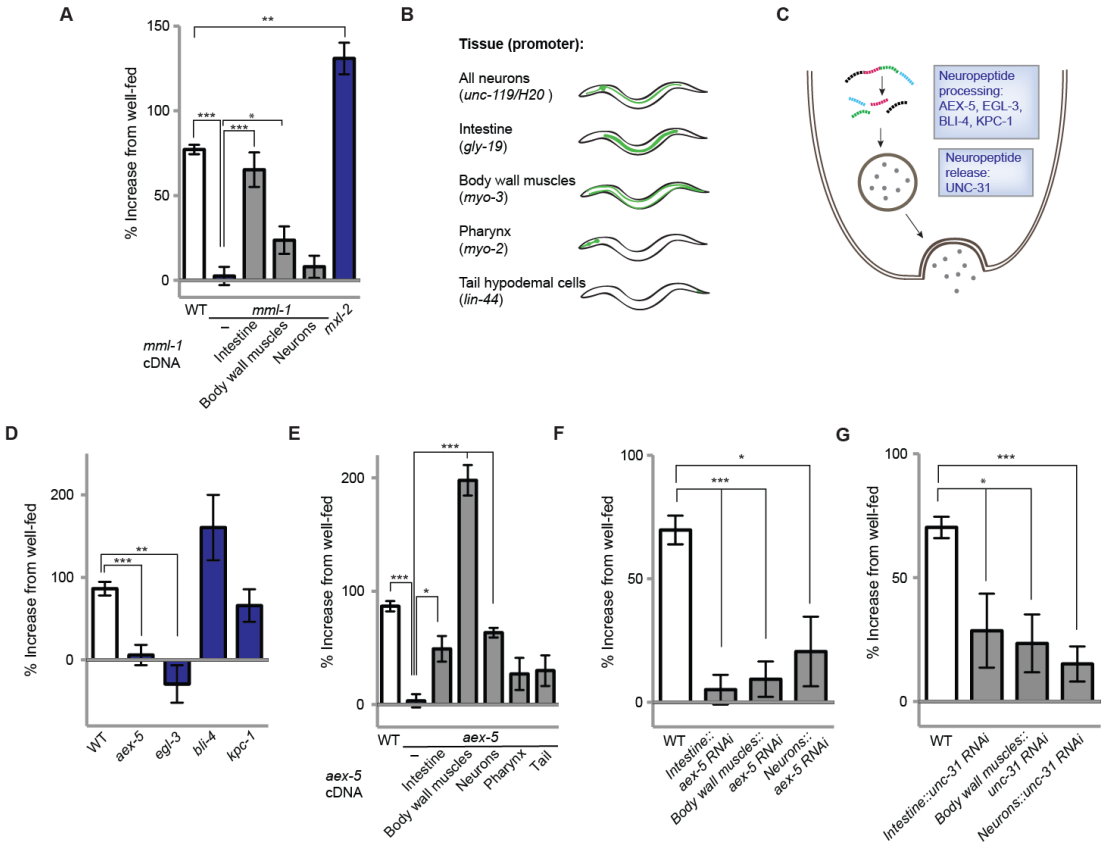

Figure 2.3. Multiple tissues sense lack of food with MML-1, process and release neuropeptides to modify behavior upon food deprivation.

(A) *mml-1*, but not *mxl-2* mutants are defective in modifying integration responses after food deprivation. Restoring *mml-1* cDNA in the intestine or body wall muscles but not neurons is sufficient to restore normal food deprivation behavior to *mml-1* mutants. (B) Schematic representation of promoters used for tissue-specific expression. (C) Schematic representation of proteins required for neuropeptide processing and release. Pro-peptides are cleaved by pro-protein convertases (AEX-5, EGL-3, BLI-4 and KPC-1) and further processed before they are packed into dense core vesicles and released using UNC-31 (CAPS protein). (D) AEX-5 and EGL-3, but not BLI-4 or KPC-1 processed peptides are required for sensory integration change after food deprivation. (E) Tissue-specific rescues of *aex-5* in either intestine, body wall muscles or neurons reverts *aex-5* null mutants to normal sensory integration response after food deprivation. (F-G) Tissue-specific knockdown of (F) *aex-5* or (G) *unc-31*in wild-type animals in intestine, body wall muscles or neurons resulted in animals that were defective in integration response after food deprivation., supporting a requirement for neuropeptide processing and release from these tissues. All bars represent population means; error bars indicate SEM. Unpaired *t* test with Welch's correction *p < 0.05; **p < 0.001; ***p < 0.0001, n ≥ 9 per condition per strain.

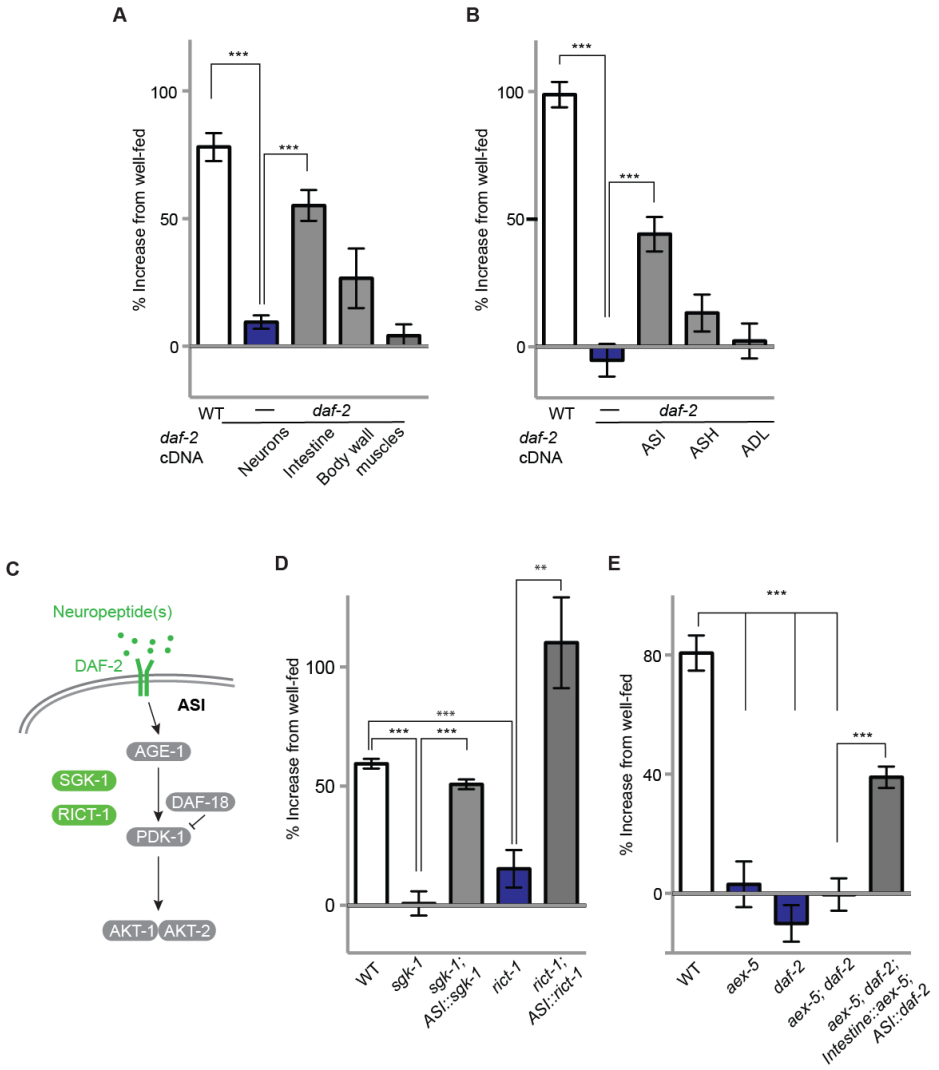

Figure 2.4. ASI chemosensory neurons use DAF-2 receptors to integrate intestine-released neuropeptides.

(A) *daf-2* mutants are defective in their sensory integration response after food deprivation. Rescue of *daf-2* in neurons, but not intestine or body wall muscles, is sufficient to restore wild-type food deprivation behavior. (B) Restoring DAF-2 to ASI, but not ASH or ADL neurons, is sufficient to partially restore integration response after food deprivation to *daf-2* mutants. (C) Schematic diagram of candidate pathway components downstream of DAF-2 activation. Components in green are required for behavioral modification upon food deprivation. (D) Animals with mutations in the *sgk-1* and *rict-1* genes are defective in integration response to food deprivation. Restoring *sgk-1* and *rict-1* to ASI neurons is sufficient to restore food-deprivation induced behavioral modification in s*gk-1 and rict-1* mutants, respectively. (E) Rescue of *aex-5* in the intestine and *daf-2* in ASI neurons of *aex-5;daf-2* double mutants is sufficient to restore sensory integration response after food deprivation. Unpaired *t* test with Welch's correction *$p < 0.05$; **$p < 0.001$; ***$p < 0.0001$, $n \geq 9$ per condition per strain.

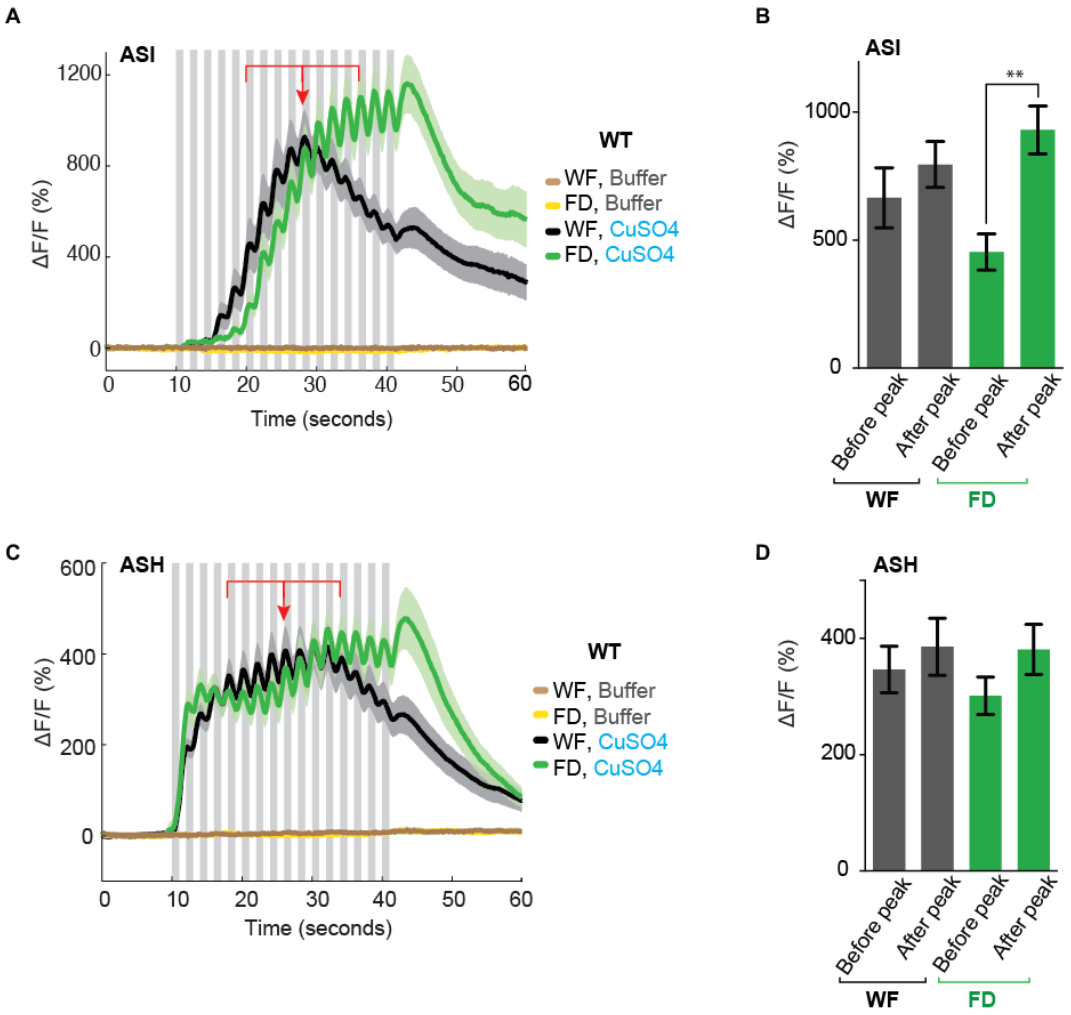

Figure 2.5. Food deprivation alters ASI neuronal adaptation rate.
(A) Responses of ASI neurons to 1-second pulses of 50mM copper solution in wild-type well-fed (WF) and food-deprived (FD) animals. Gray bars (16) represent stimulus pulses. Food-deprived animals do not readily adapt to repeated repellent pulses. Solid lines represent averaged traces, shading around each line indicate SEM ($n \geq 21$). (B) Bar graph of averaged fluorescence over a 8s-window before and after peak response (red arrow in (A) indicates peak). Well-fed animals respond to copper with an increase leading to the peak response followed by decay after the peak. In contrast, ASI responses in food-deprived animals continue to rise to subsequent pulses. Error bar indicates SEM (Unpaired *t* test with Welch's correction, $*p < 0.05$, $**p < 0.001$, $n \geq 21$). (C) Responses of ASH neurons to 1-second pulses of 50mM copper solution in well-fed and food-deprived animals. Solid lines represent averaged traces, shading around each line indicate SEM ($n \geq 21$). (D) Bar graph of averaged fluorescence over a 8s-window before and after peak response (red arrow in (C) indicates peak). ASH neurons in well-fed and food-deprived animals respond similarly to copper before and after the peak. Error bar indicates SEM (Unpaired *t* test with Welch's correction, $*p < 0.05$, $n \geq 21$).

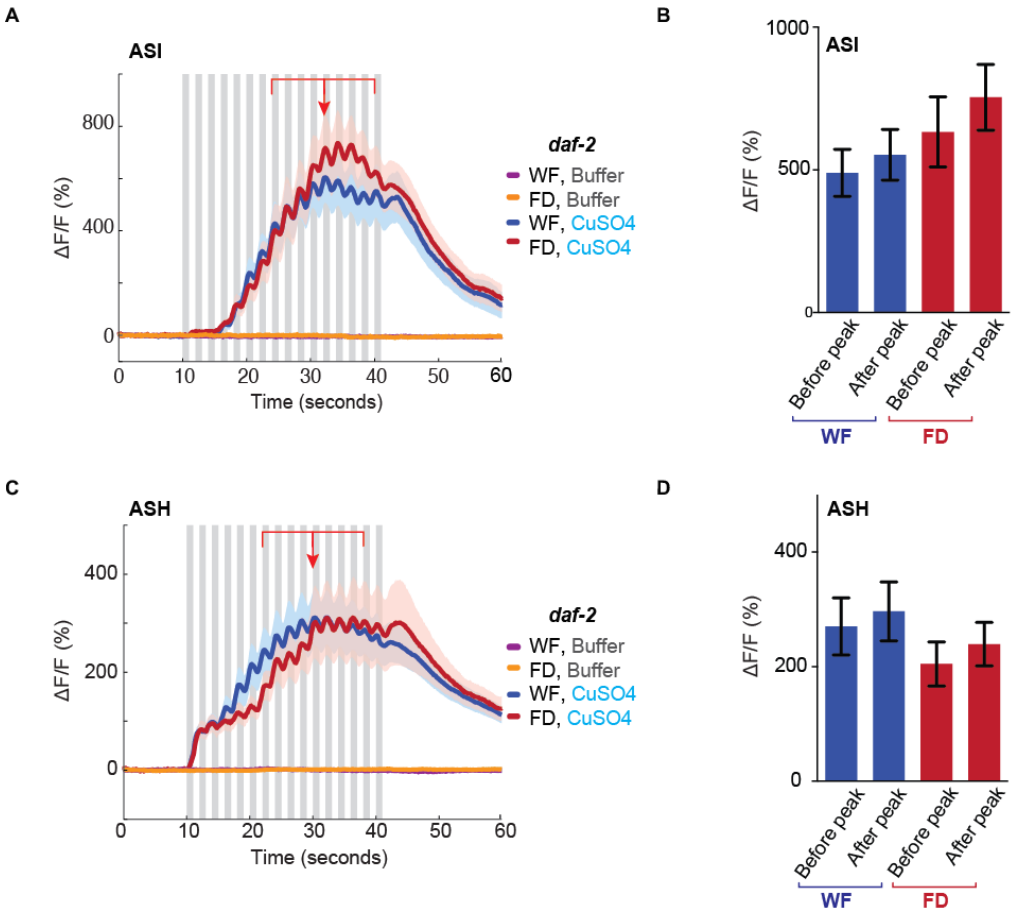

Figure 2.6. Modification of ASI neuronal adaptation rate after food deprivation requires DAF-2 signaling.
(A) Responses of ASI neurons to 1-second pulses of 50 mM copper solution in *daf-2* mutant animals under well-fed (WF) and food-deprived (FD) conditions. Gray bars (16) represent stimulus pulses. WF and FD *daf-2* animals respond similarly to copper stimuli. Solid lines represent averaged traces, shading around each line indicate SEM ($n \geq 13$). (B) Bar graph of averaged fluorescence over a 8s-window before and after peak response (red arrow in (A) indicates peak). Well-fed and food-deprived *daf-2* mutants respond to copper with an increase leading to the peak response followed by decrease after the peak. Error bar indicates SEM (Unpaired *t* test with Welch's correction, $*p < 0.05$, $n \geq 13$). (C) Responses of ASH neurons to 1-second pulses of 50mM copper solution in well-fed and food-deprived *daf-2* animals. Solid lines represent averaged traces, shading around each line indicate SEM ($n \geq 13$). (D) Bar graph of averaged fluorescence over a 8s-window before and after peak response (red arrow in (C) indicates peak). ASH neurons in well-fed and food-deprived animals respond similarly to copper before and after the peak. Error bar indicates SEM (Unpaired *t* test with Welch's correction, $*p < 0.05$, $n \geq 13$).

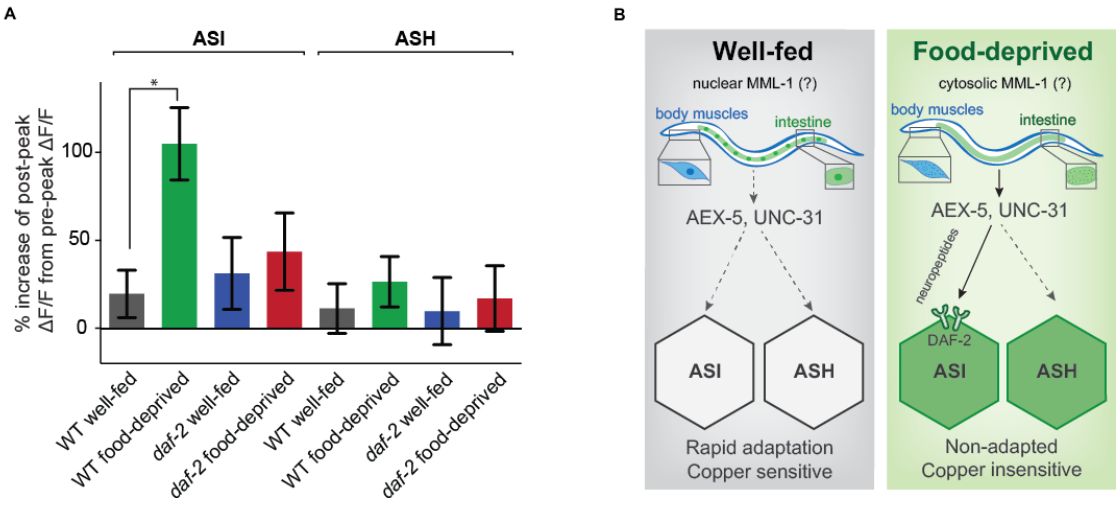

Figure 2.7. Food deprivation alters ASI adaptation rate via neuropeptide signaling. (A) Percent increase of post-peak response compared to pre-peak response. Wild-type food-deprived ASI, but not ASH neurons show a significant increase in their response to copper stimuli even as the responses decline in well-fed condition. Moreover, these food deprivation effects on ASI neurons are lost in *daf-2* mutants. (B) Model for food-deprivation induced modification of copper sensitivity.

SUPPLEMENTAL INFORMATION

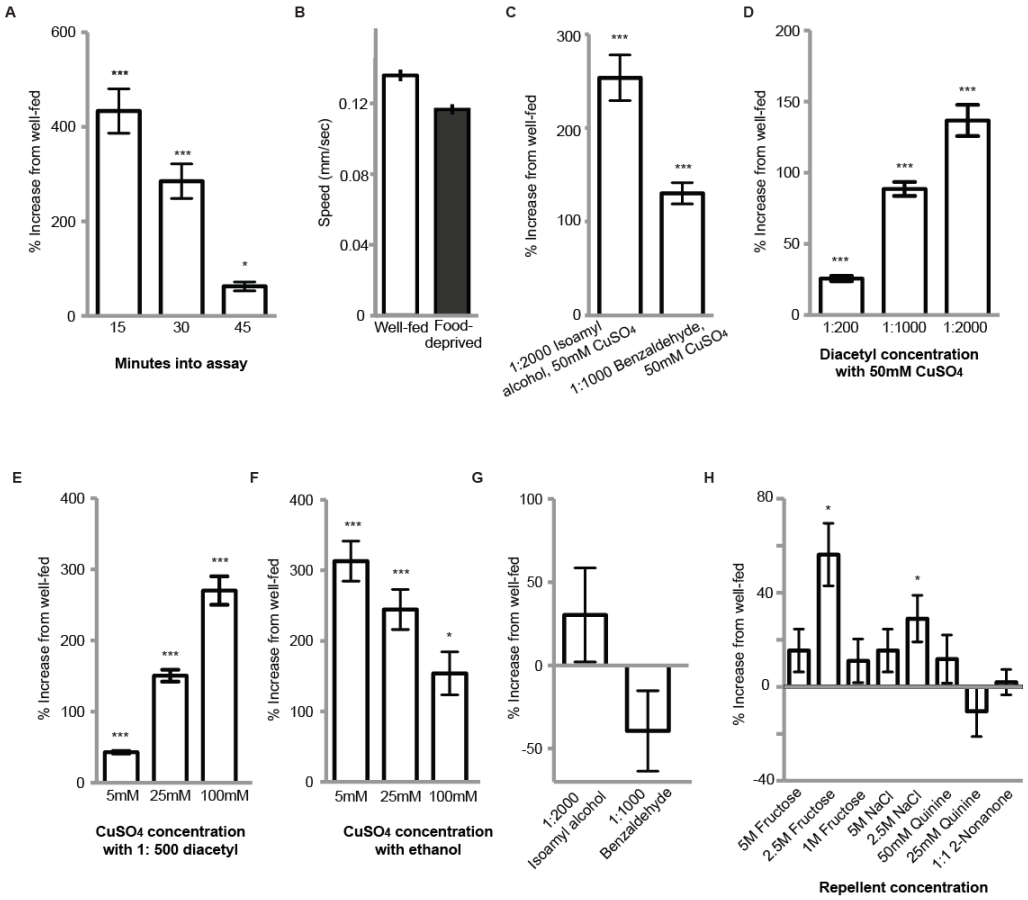

Figure S2.1. Food deprivation specifically alters repellent driven behaviors.
(A) Time course of sensory integration assay (1:500 diacetyl, 50mM $CuSO_4$) shows that food-deprived animals consistently crossed the copper barrier more readily at all three time points scored. (B) Speed of well-fed and food-deprived animals on an agar plate with no stimulus is not significantly different. Bars represent population means, errors bars indicate SEM, n = 12 plates. (C) Food-deprived animals show significant increases in integration index compared to well-fed animals in assays that pair copper with volatile attractants isoamyl alcohol or benzaldehyde. (D-E) Food-deprived animals cross the copper barrier significantly when presented with various concentrations of (D) copper and (E) diacetyl in sensory integration assay. (F) Food-deprived animals show increased integration index in behavior assays that present various concentrations of copper sulfate with ethanol (control). (G) Chemotaxis to isoamyl alcohol or benzaldehyde alone are not modified by food-deprivation. (H) Food-deprived animals show reduced sensitivity only to intermediate concentrations of fructose and salt. Soluble repellents (fructose, salt, quinine) are presented as a stripe in the integration assay with 1:2000 diacetyl. Volatile repellent 2-nonanone chemotaxis assay presents choice of ethanol (solvent control) and 2-nonanone. For A, C-H: All bars represent population means; error bars indicate SEM. One sample *t* test *p,0.05; **< 0.001; ***$p < 0.0001$, $n \geq 9$.

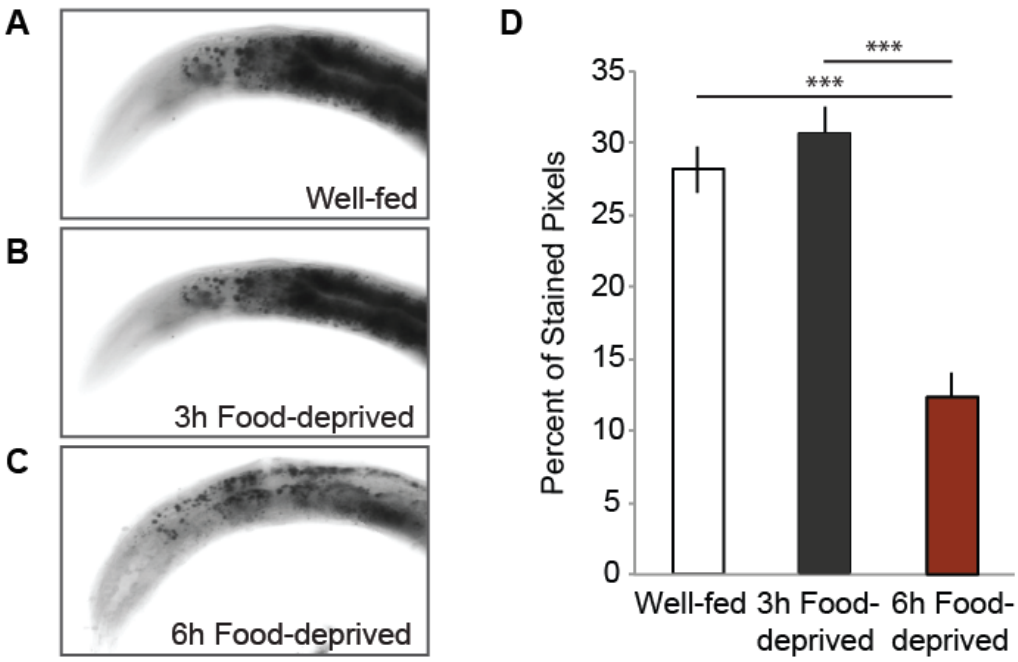

Figure S2.2. Fat stores are not depleted after three hours of food deprivation.
(A-C) Visualization of fat stores using Oil Red O staining of fixed (A) well-fed, (B) 3h food-deprived and (C) 6h food-deprived adult animals. (D) Quantification of Oil Red O staining shows depletion of fat stores after 6 hours of food deprivation. All bars represent population means; error bars indicate SEM. Two–tailed Student's *t* test ***$p < 0.0001$, $n \geq 44$.

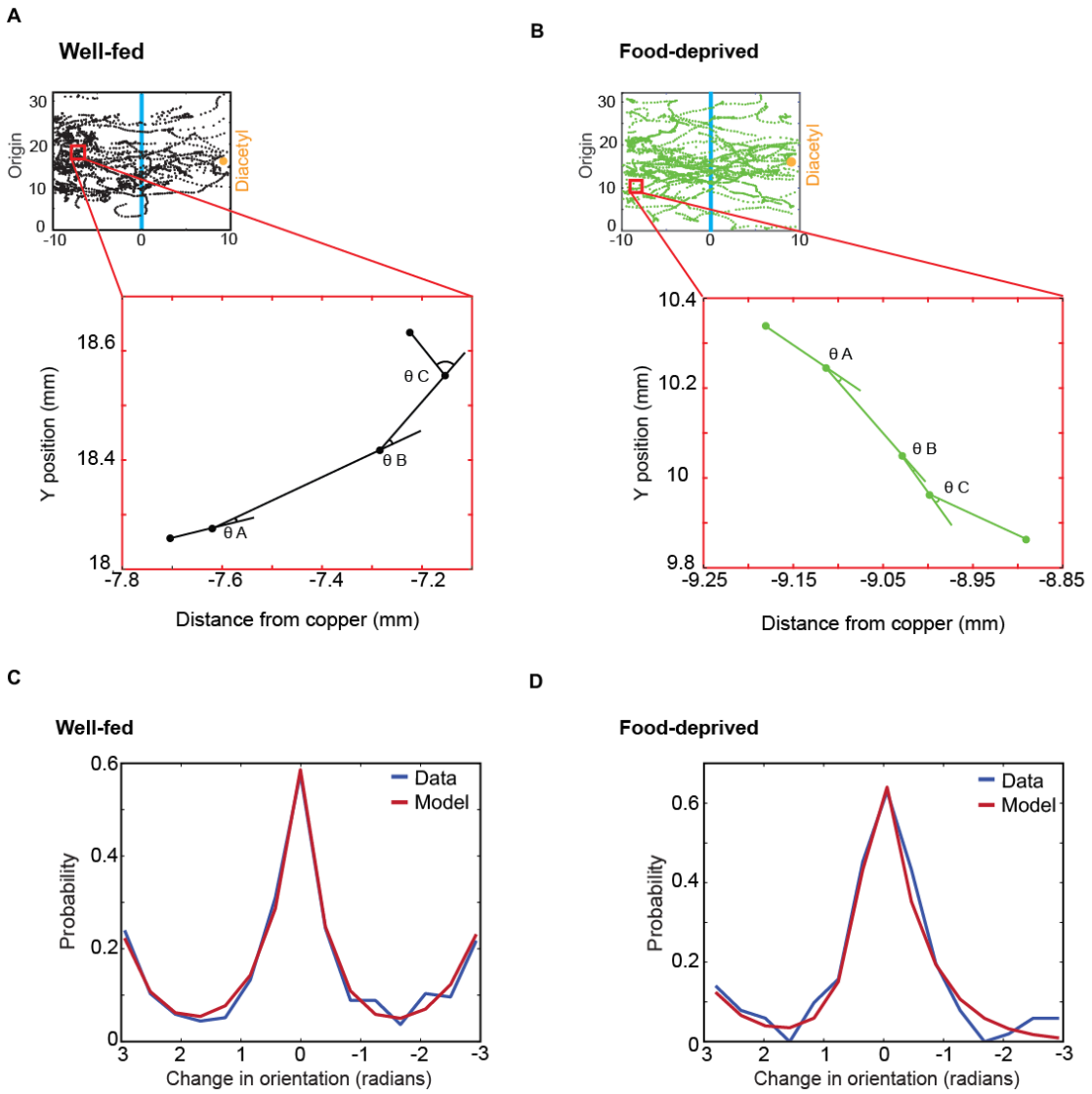

Figure S2.3. Analysis of well-fed and food-deprived tracks.
(A-B) Zoomed-in example of a (A) well-fed and (B) food-deprived worm track. Series of three points shown are midpoints for one worm 1.5 seconds apart in time. Vectors shown are movement vectors. Angles between movement vectors equal dθ/dt calculations at given points. (C-D) dθ/dt distribution of (C) well-fed and (D) food-deprived animals for midpoints between -7.5 mm and -10 mm and incoming orientation vector within π/4 of vector orthogonal to copper line (animals moving towards copper line).

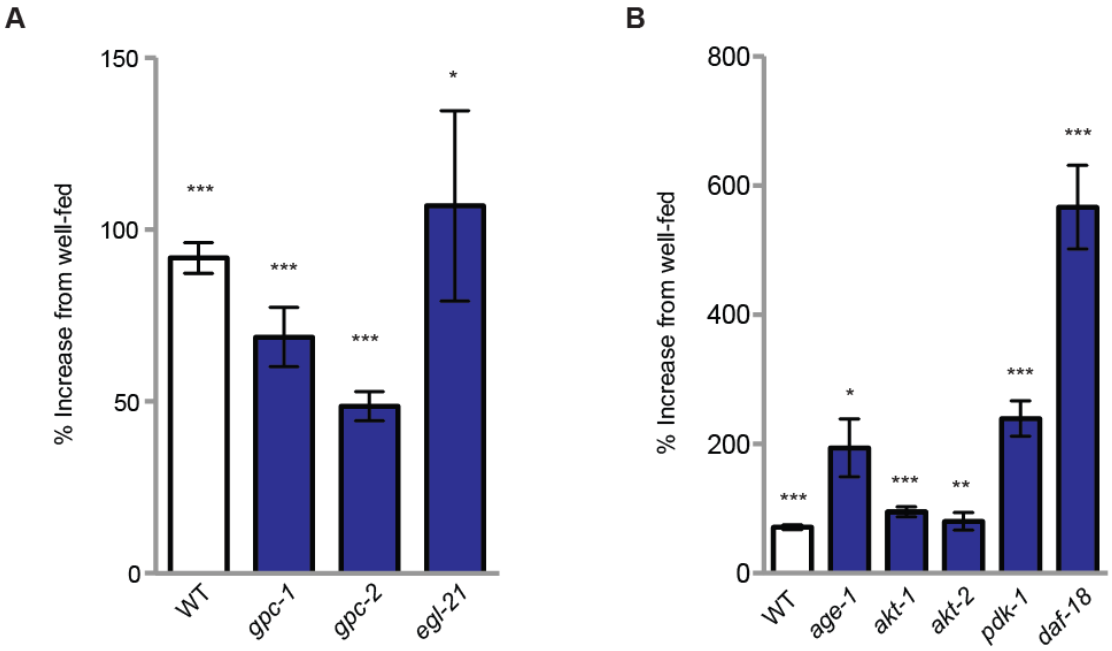

Figure S2.4. Mutants in neuropeptide processing and signaling and insulin-signaling transduction.
(A) Animals with null mutations in genes encoding Gγ subunits, *gpc-1* and *gpc-2*, show normal modification of integration behavior after food deprivation. Animals with mutations in *egl-21* also respond normally to food deprivation.(B) Animals with mutations in genes encoding insulin signaling pathway components are normal in modification of integration response after food deprivation. All bars represent population means; error bars indicate SEM. One sample *t* test *p < 0.05; **p < 0.001; ***p < 0.0001, n ≥ 9.

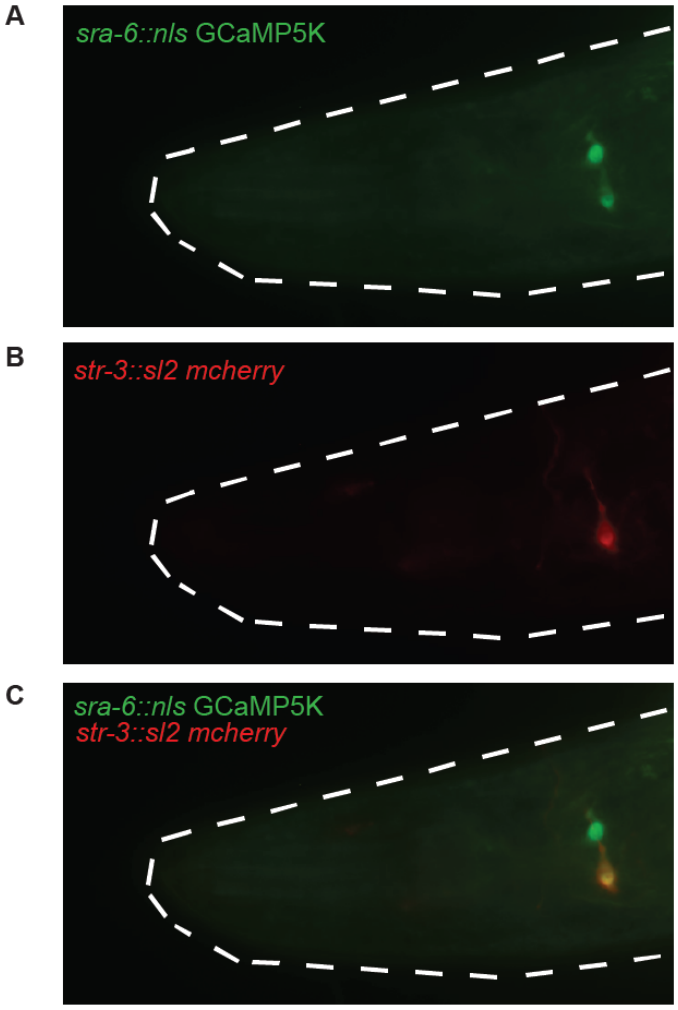

Figure S2.5. Nuclear localization of GCaMP5K to ASI and ASH neurons for calcium imaging.
(A) Genetically encoded calcium indicator GCaMP5K is expressed under the *sra-6* promoter in both ASI and ASH neurons. (B) Fluorescent mCherry protein is selectively expressed in ASI neurons under the *str-3* promoter. (C) Overlay shows the co-localization of mCherry and GCaMP5K allowing identification of ASI neurons.

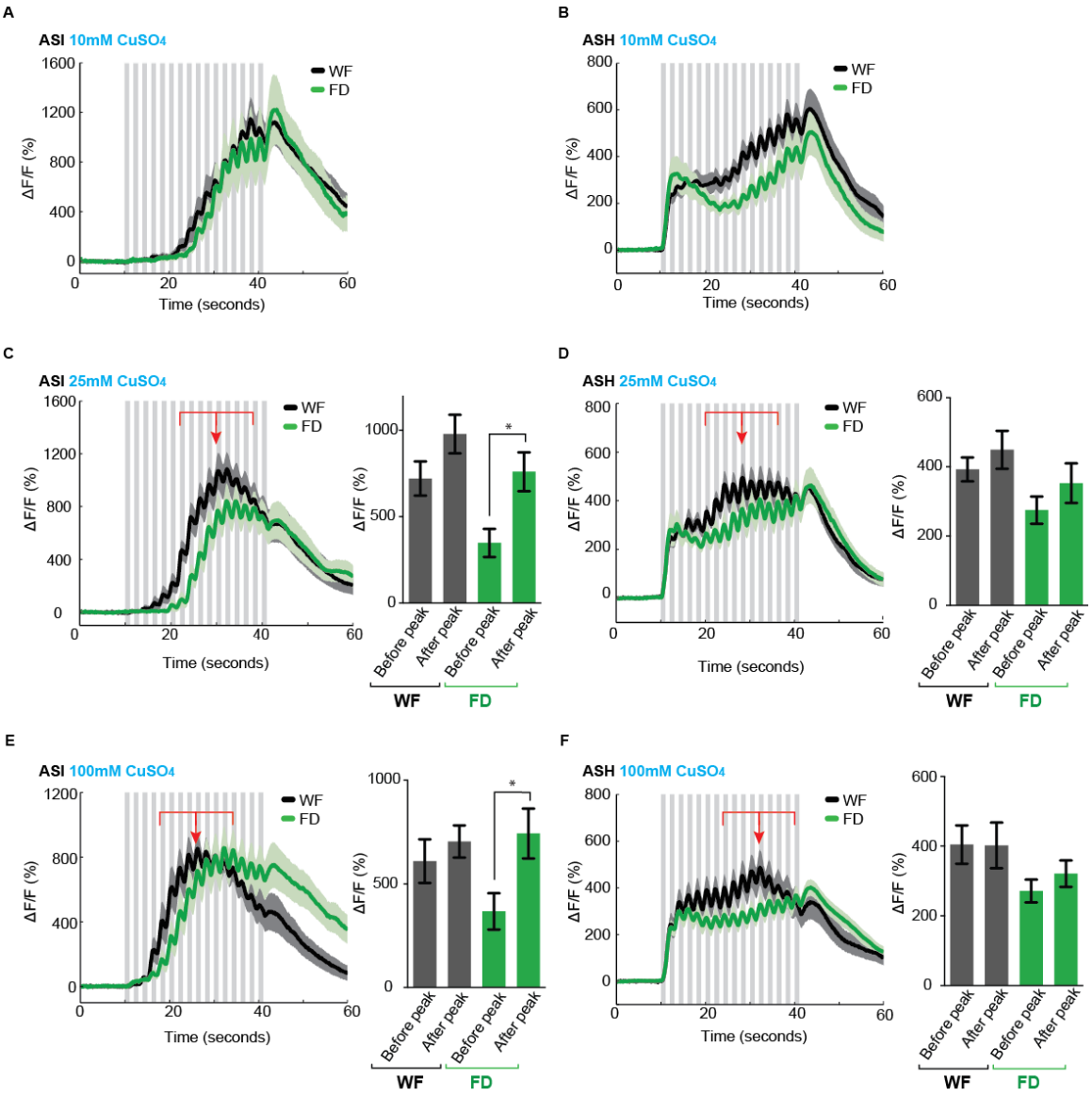

Figure S2.6. Calcium imaging of neuronal responses to various concentrations of copper sulfate stimulus.

(A-F) Responses of (A,C,E) ASI and (B,D,F) ASH neurons to 1-second pulses of (A,B)10mM (C,D) 25mM and (E,F) 100mM CuSO4 in well-fed and food-deprived animals. Gray bars represent presence of copper stimulus;16 pulses in total are delivered. Solid lines represent averaged traces, shading around each line and error bars in bar graphs indicate SEM. Average fluorescence over a 8s time window before and after the peak (red arrow) is represented in bar graphs. Peak response from 10mM copper occurs late after 14-15 pulses and therefore a bar graph comparing responses before and after the peak cannot be generated. Unpaired *t* test with Welch's correction *$p < 0.05$, $n \geq 14$.

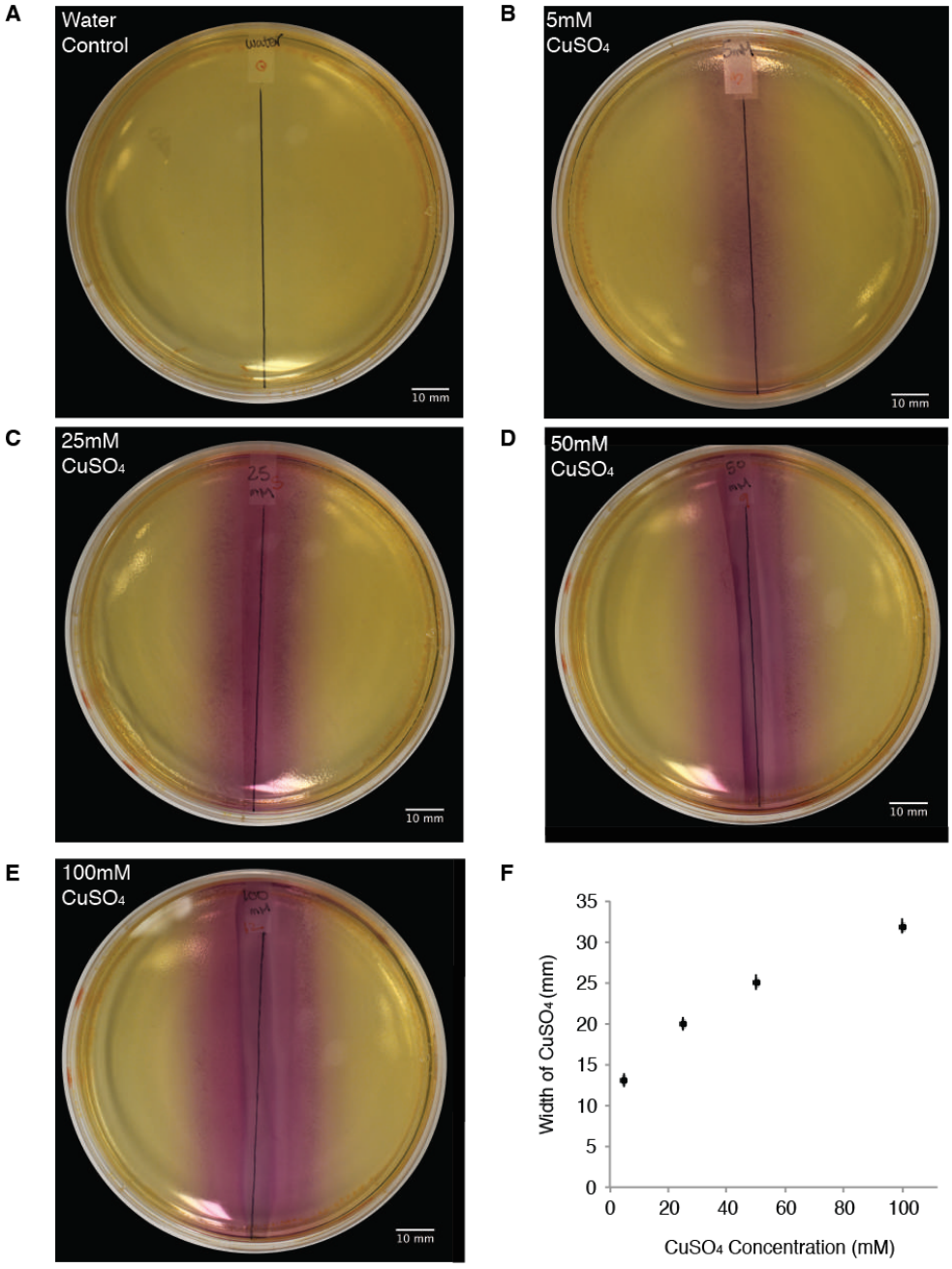

Figure S2.7. Spread of copper sulfate on agar plates visualized using (1-(2-pyridylazo)-2- naphthol) (PAN) indicator.
(A-E) 25ul of (A) water as control, (B) 5mM $CuSO_4$, (C) 25mM $CuSO_4$, (D) 50mM $CuSO_4$, and (E) 100mM $CuSO_4$ was dripped and dried along the midline of the plate to form a copper gradient. PAN indicator distributed over the entire plate shows a gradient of orange-red upon chelation with copper ions. (F) Measured width of copper area with each data point representing the average width, error bars indicate SEM. n = 9.

Table S2.1. Integration indexes for behavior assays. Integration index of well-fed and food-deprived animals used to calculate the percent increase of FD integration index from WF integration index is presented; one sample *t* test p value is also shown.

Strain	Type of assay	Well-fed Integration index	Food-deprived integration index	WF n	FD n	One-sample *t* test p value	Figure location
WT	Integration 1:500 diacetyl with 50mM copper sulfate	0.37	0.80	16	14	<0.0001	Figure 2.1B
WT	Integration 1:2000 isoamyl alcohol with 50mM copper sulfate	0.14	0.49	12	12	<0.0001	Figure S2.1C
WT	Integration 1:1000 benzaldehyde with 50mM copper sulfate	0.19	0.44	9	10	<0.0001	Figure S2.1C
WT	Integration 1:200 diacetyl with 50mM copper sulfate	0.73	0.92	10	10	<0.0001	Figure S2.1D
WT	Integration 1:1000 diacetyl with 50mM copper sulfate	0.41	0.78	10	10	<0.0001	Figure S2.1D
WT	Integration 1:2000 diacetyl with 50mM copper sulfate	0.30	0.72	10	10	<0.0001	Figure S2.1D
WT	Integration 1:500 diacetyl with 5mM copper sulfate	0.54	0.77	11	11	<0.0001	Figure S2.1E
WT	Integration 1:500 diacetyl with 25mM copper sulfate	0.30	0.74	9	9	<0.0001	Figure S2.1E
WT	Integration 1:500 diacetyl with 100mM copper sulfate	0.19	0.70	11	11	<0.0001	Figure S2.1E
WT	Integration ethanol with 5mM copper sulfate	0.12	0.48	9	9	<0.0001	Figure S2.1F
WT	Integration ethanol with 25mM copper sulfate	0.13	0.46	13	13	<0.0001	Figure S2.1F

Table S2.1. Integration indexes for behavior assays, continued.

Strain	Type of assay	Well-fed Integration index	Food-deprived integration index	WF n	FD n	One-sample *t* test p value	Figure location
WT	Integration ethanol with 50mM copper sulfate	0.05	0.40	10	10	<0.0001	Figure 2.1C
WT	Integration ethanol with 100mM copper sulfate	0.06	0.15	9	9	0.001	Figure S2.1F
WT	Chemotaxis with 1:500 diacetyl	0.70	0.77	9	9	0.0588	Figure 2.1C
WT	Chemotaxis with 1:2000 isoamyl alcohol	0.29	0.38	9	9	0.3149	Figure S2.1G
WT	Chemotaxis with 1:1000 benzaldehyde	0.34	0.20	9	9	0.1424	Figure S2.1G
WT	Integration 1:500 diacetyl with 50mM copper sulfate, 15 minute count	0.05	0.28	9	9	<0.0001	Figure S2.1A
WT	Integration 1:500 diacetyl with 50mM copper sulfate, 30 minute count	0.14	055	9	9	<0.0001	Figure S2.1A
WT	Integration 1:500 diacetyl with 50mM copper sulfate, 45 minute count	0.45	0.74	9	9	0.0002	Figure S2.1A
WT	Integration 1:500 diacetyl with 50mM copper sulfate (1 hr food condition)	0.35	0.43	13	14	0.2223	Figure 2.1D
WT	Integration 1:500 diacetyl with 50mM copper sulfate (2 hr food condition)	0.23	0.59	10	9	<0.0001	Figure 2.1D
WT	Integration 1:500 diacetyl with 50mM copper sulfate (3 hr food condition)	0.19	0.71	11	11	<0.0001	Figure 2.1D

Table S2.1. Integration indexes for behavior assays, continued.

Strain	Type of assay	Well-fed Integration index	Food-deprived integration index	WF n	FD n	One-sample t test p value	Figure location
WT	Integration 1:500 diacetyl with 50mM copper sulfate (6 hr food condition)	0.28	0.60	12	11	<0.0001	Figure 2.1D
WT	Integration 1:500 diacetyl with 50mM copper sulfate (1 hr recovery)	0.24	0.75	10	9	<0.0001	Figure 2.1E
WT	Integration 1:500 diacetyl with 50mM copper sulfate (3 hr recovery)	0.24	0.45	10	9	0.0187	Figure 2.1E
WT	Integration 1:500 diacetyl with 50mM copper sulfate (5 hr recovery)	0.42	0.44	9	10	0.6776	Figure 2.1E
WT	Integration 1:500 diacetyl with 50mM copper sulfate	0.39	0.66	9	9	<0.0001	Figure 2.1F
WT	Integration 1:500 diacetyl with 50mM copper sulfate	0.39	(Aztreonam treated) 0.60	9	9	0.001	Figure 2.1F
WT	Integration 1:500 diacetyl with 50mM copper sulfate	0.38	0.71	34	34	<0.0001	Figure 2.3D
aex-5	Integration 1:500 diacetyl with 50mM copper sulfate	0.46	0.48	12	11	0.6355	Figure 2.3D
egl-3	Integration 1:500 diacetyl with 50mM copper sulfate	0.20	0.14	10	9	0.2368	Figure 2.3D
bli-4	Integration 1:500 diacetyl with 50mM copper sulfate	0.24	0.63	9	9	0.0037	Figure 2.3D

Table S2.1. Integration indexes for behavior assays, continued.

Strain	Type of assay	Well-fed Integration index	Food-deprived integration index	WF n	FD n	One-sample t test p value	Figure location
kpc-1	Integration 1:500 diacetyl with 50mM copper sulfate	0.20	0.33	9	9	0.0104	Figure 2.3D
WT	Integration 1:500 diacetyl with 50mM copper sulfate	0.41	0.76	54	54	<0.0001	Figure 2.3E
aex-5	Integration 1:500 diacetyl with 50mM copper sulfate	0.55	0.56	27	28	0.5854	Figure 2.3E
aex-5; Intestine::aex-5 cDNA	Integration 1:500 diacetyl with 50mM copper sulfate	0.48	0.71	13	13	0.0009	Figure 2.3E
aex-5; Body wall muscle::aex-5 cDNA	Integration 1:500 diacetyl with 50mM copper sulfate	0.25	0.75	10	10	<0.0001	Figure 2.3E
aex-5; Neurons::aex-5 cDNA	Integration 1:500 diacetyl with 50mM copper sulfate	0.50	0.82	9	9	<0.0001	Figure 2.3E
aex-5; Pharynx::aex-5 cDNA	Integration 1:500 diacetyl with 50mM copper sulfate	0.35	0.44	9	10	0.0876	Figure 2.3E
aex-5; Tail::aex-5 cDNA	Integration 1:500 diacetyl with 50mM copper sulfate	0.34	0.44	10	9	0.0583	Figure 2.3E
WT	Integration 1:500 diacetyl with 50mM copper sulfate	0.48	0.82	22	22	<0.0001	Figure 2.3F
Intestine::aex-5 RNAi	Integration 1:500 diacetyl with 50mM copper sulfate	0.30	0.36	9	9	0.4201	Figure 2.3F
Body wall muscles::aex-5 RNAi	Integration 1:500 diacetyl with 50mM copper sulfate	0.53	0.56	10	10	0.2191	Figure 2.3F

Table S2.1. Integration indexes for behavior assays, continued.

Strain	Type of assay	Well-fed Integration index	Food-deprived integration index	WF n	FD n	One-sample t test p value	Figure location
Neurons::aex-5 RNAi	Integration 1:500 diacetyl with 50mM copper sulfate	0.45	0.49	9	9	0.1791	Figure 2.3F
WT	Integration 1:500 diacetyl with 50mM copper sulfate	0.49	0.83	14	14	<0.0001	Figure 2.3G
Intestine::unc-31 RNAi	Integration 1:500 diacetyl with 50mM copper sulfate	0.37	0.48	9	10	0.0882	Figure 2.3G
Body wall muscles::unc-31 RNAi	Integration 1:500 diacetyl with 50mM copper sulfate	0.39	0.48	11	11	0.0717	Figure 2.3G
Neurons::unc-31 RNAi	Integration 1:500 diacetyl with 50mM copper sulfate	0.39	0.45	9	9	0.0646	Figure 2.3G
WT	Integration 1:500 diacetyl with 50mM copper sulfate	0.49	0.88	32	33	<0.0001	Figure 2.3A
mml-1	Integration 1:500 diacetyl with 50mM copper sulfate	0.53	0.55	30	28	0.6318	Figure 2.3A
mxl-2	Integration 1:500 diacetyl with 50mM copper sulfate	0.32	0.74	9	9	<0.0001	Figure 2.3A
mml-1; Intestine::mml-1 cDNA	Integration 1:500 diacetyl with 50mM copper sulfate	0.48	0.80	11	11	<0.0001	Figure 2.3A
mml-1; Body wall muscles::mml-1 cDNA	Integration 1:500 diacetyl with 50mM copper sulfate	0.57	0.70	10	10	0.0167	Figure 2.3A
mml-1; Neurons::mml-1 cDNA	Integration 1:500 diacetyl with 50mM copper sulfate	0.54	0.59	11	11	0.2447	Figure 2.3A

Table S2.1. Integration indexes for behavior assays, continued.

Strain	Type of assay	Well-fed Integration index	Food-deprived integration index	WF n	FD n	One-sample t test p value	Figure location
WT	Integration 1:500 diacetyl with 50mM copper sulfate	0.40	0.76	18	18	<0.0001	Figure S2.4A
gpc-1	Integration 1:500 diacetyl with 50mM copper sulfate	0.51	0.86	9	9	<0.0001	Figure S2.4A
gpc-2	Integration 1:500 diacetyl with 50mM copper sulfate	0.57	0.84	9	9	<0.0001	Figure S2.4A
egl-21	Integration 1:500 diacetyl with 50mM copper sulfate	0.20	0.42	10	9	0.0048	Figure S2.4A
WT	Integration 1:500 diacetyl with 50mM copper sulfate	0.45	0.77	14	14	<0.0001	Figure 2.4A
daf-2;	Integration 1:500 diacetyl with 50mM copper sulfate	0.52	0.50	11	9	0.4245	Figure 2.4A
daf-2; Neurons::daf-2 cDNA	Integration 1:500 diacetyl with 50mM copper sulfate	0.47	0.73	10	10	<0.0001	Figure 2.4A
daf-2; Intestine::daf-2 cDNA	Integration 1:500 diacetyl with 50mM copper sulfate	0.43	0.55	9	9	0.0520	Figure 2.4A
daf-2; Body wall muscles::daf-2 cDNA	Integration 1:500 diacetyl with 50mM copper sulfate	0.54	0.56	10	9	0.3729	Figure 2.4A
WT	Integration 1:500 diacetyl with 50mM copper sulfate	0.39	0.78	25	24	<0.0001	Figure 2.4B

Table S2.1. Integration indexes for behavior assays, continued.

Strain	Type of assay	Well-fed Integration index	Food-deprived integration index	WF n	FD n	One-sample t test p value	Figure location
daf-2	Integration 1:500 diacetyl with 50mM copper sulfate	0.53	0.50	12	12	0.4311	Figure 2.4B
daf-2; ASI::daf-2 cDNA	Integration 1:500 diacetyl with 50mM copper sulfate	0.45	0.65	12	11	<0.0001	Figure 2.4B
daf-2; ASH::daf-2 cDNA	Integration 1:500 diacetyl with 50mM copper sulfate	0.45	0.52	10	10	0.1029	Figure 2.4B
daf-2; ADL::daf-2 cDNA	Integration 1:500 diacetyl with 50mM copper sulfate	0.50	0.51	10	10	0.7480	Figure 2.4B
WT	Integration 1:500 diacetyl with 50mM copper sulfate	0.45	0.78	32	32	<0.0001	Figure S2.4B
age-1	Integration 1:500 diacetyl with 50mM copper sulfate	0.15	0.45	9	9	0.0025	Figure S2.4B
akt-1	Integration 1:500 diacetyl with 50mM copper sulfate	0.40	0.77	11	10	<0.0001	Figure S2.4B
akt-2	Integration 1:500 diacetyl with 50mM copper sulfate	0.33	0.60	11	11	0.0002	Figure S2.4B
pdk-1	Integration 1:500 diacetyl with 50mM copper sulfate	0.20	0.70	9	9	<0.0001	Figure S2.4B
daf-18	Integration 1:500 diacetyl with 50mM copper sulfate	0.07	0.45	9	9	<0.0001	Figure S2.4B
WT	Integration 1:500 diacetyl with 50mM copper sulfate	0.56	0.90	18	18	<0.0001	Figure 2.4D

Table S2.1. Integration indexes for behavior assays, continued.

Strain	Type of assay	Well-fed Integration index	Food-deprived integration index	WF n	FD n	One-sample t test p value	Figure location
sgk-1	Integration 1:500 diacetyl with 50mM copper sulfate	0.59	0.60	9	9	0.8780	Figure 2.4D
sgk-1; ASI::sgk-1	Integration 1:500 diacetyl with 50mM copper sulfate	0.56	0.85	9	9	<0.0001	Figure 2.4D
rict-1	Integration 1:500 diacetyl with 50mM copper sulfate	0.34	0.42	18	18	0.1213	Figure 2.4D
rict-1; ASI::rict-1	Integration 1:500 diacetyl with 50mM copper sulfate	0.24	0.50	9	9	0.0004	Figure 2.4D
WT	Integration 1:500 diacetyl with 50mM copper sulfate	0.43	0.78	11	11	<0.0001	Figure 2.4E
aex-5	Integration 1:500 diacetyl with 50mM copper sulfate	0.54	0.56	11	9	0.7016	Figure 2.4E
daf-2	Integration 1:500 diacetyl with 50mM copper sulfate	0.62	0.56	9	9	0.1395	Figure 2.4E
aex-5; daf-2	Integration 1:500 diacetyl with 50mM copper sulfate	0.57	0.57	10	10	0.9438	Figure 2.4E
aex-5; daf-2; Intestine:: aex-5 cDNA; ASI::daf-2	Integration 1:500 diacetyl with 50mM copper sulfate	0.58	0.80	9	9	<0.0001	Figure 2.4E
WT	Chemotaxis 1:1 2-nonanone	-0.68	-0.69	9	9	0.7195	Figure S2.1H
WT	Integration 1:2000 diacetyl with 5M fructose	0.55	0.56	9	9	0.1343	Figure S1H
WT	Integration 1:2000 diacetyl with 2.5M fructose	0.41	0.65	9	9	0.0029	Figure S2.1H
WT	Integration 1:2000 diacetyl with 1M fructose	0.49	0.54	9	10	0.2635	Figure S2.1H

Table S2.1. Integration indexes for behavior assays, continued.

Strain	Type of assay	Well-fed Integration index	Food-deprived integration index	WF n	FD n	One-sample t test p value	Figure location
WT	Integration 1:2000 diacetyl with 5M sodium chloride	0.43	0.49	9	8	0.1343	Figure S2.1H
WT	Integration 1:2000 diacetyl with 2.5M sodium chloride	0.47	0.60	9	9	0.0190	Figure S2.1H
WT	Integration 1:2000 diacetyl with 50mM Quinine	0.26	0.29	9	9	0.2817	Figure S2.1H
WT	Integration 1:2000 diacetyl with 25mM Quinine	0.43	0.38	9	9	0.3633	Figure S2.1H

Table S2.2. Testing of insulin-like peptides (ILPs). Integration indexes of well-fed and food-deprived animals and corresponding standard deviations.

Strain	ILP	Well-fed (SD)	3h Food-deprived (SD)	Fold change
ILP mutants				
WT	-	0.35 (0.13)	0.94 (0.06)	2.67
CF1041	(DAF-2 receptor)	0.59 (0.18)	0.56 (0.24)	0.96
JT191	DAF-28	0.44 (0.08)	0.85 (0.09)	1.90
CX7155	INS-1	0.31 (0.08)	0.60 (0.12)	1.90
FX4467	INS-2	0.54 (0.12)	0.72 (0.12)	1.34
RB1915	INS-3	0.45 (0.13)	0.61 (0.11)	1.36
RB2544	INS-4	0.56 (0.12)	0.89 (0.07)	1.57
FX2560	INS-5	0.37 (0.16)	0.58 (0.16)	1.56
FX2416	INS-6	0.55 (0.06)	0.88 (0.01)	1.58
FX2001	INS-7	0.37 (0.05)	0.67 (0.06)	1.77
FX4144	INS-8	0.31 (0.09)	0.72 (0.13)	2.29
FX3618	INS-9	0.18 (0.10)	0.67 (0.04)	3.58
FX3498	INS-10	0.27 (0.03)	0.60 (0.03)	2.23
FX1053	INS-11	0.37 (0.10)	0.88 (0.04)	2.35
FX2918	INS-12	0.44 (0.07)	0.73 (0.00)	1.65
FX5129	INS-13	0.26 (0.08)	0.42 (0.08)	1.57
FX4886	INS-14	0.26 (0.16)	0.74 (0.07)	2.78
RB2489	INS-15	0.27 (0.13)	0.44 (0.06)	1.61
RB2159	INS-16	0.14 (NA)	0.37 (NA)	2.59
FX790	INS-17	0.55 (0.09)	0.93 (0.01)	1.69
VC1218 outcrossed	INS-18	0.23 (0.04)	0.65 (0.20)	2.83
FX5155	INS-19	0.46 (0.11)	0.63 (0.10)	1.35
FX5634	INS-20	0.34 (0.04)	0.63 (0.02)	1.82
FX5180	INS-21	0.28 (0.06)	0.49 (0.06)	1.76
RB2594	INS-22	0.32 (0.14)	0.64 (0.03)	1.97
FX1975	INS-23	0.42 (NA)	0.61 (0.15)	1.43
FX1983	INS-26	0.61 (0.07)	0.75 (0.09)	1.22
RB1911	INS-27	0.33 (0.01)	0.65 (0.03)	1.92
RB2059	INS-28	0.01 (0.00)	0.06 (0.02)	6.29
FX1922	INS-29	0.12 (0.11)	0.56 (0.05)	4.49
RB1809	INS-30	0.54 0.10)	0.82 (0.07)	1.51
RB2552	INS-31	0.36 (0.09)	0.66 (0.05)	1.82
FX6109	INS-32	0.54 (0.05)	0.87 (0.01)	1.59
FX2988	INS-33	0.29 (0.02)	0.45 (0.08)	1.51
FX3095	INS-34	0.03 (0.03)	0.55 (0.05)	15.50
RB2412	INS-35	0.06 (0.01)	0.24 (0.16)	3.73
FX6061	INS-37	0.42 (0.13)	0.85 (0.00)	2.00
ILP knockdown using feeding RNAi				
WT	(L4440 control)	0.34 (0.07)	0.94 (0.06)	2.07
WT	INS-24	0.39 (0.25)	0.59 (0.09)	1.49
WT	INS-25	0.27 (0.06)	0.64 (0.04)	2.30
WT	INS-36	0.36 (0.18)	0.64 (0.17)	1.75
WT	INS-39	0.43 (0.07)	0.66 (0.12)	1.55
ILP knockdown using intestine-specific RNAi				
WT	-	0.56 (0.12)	0.89 (0.07)	1.56
WT	INS-25	0.27 (0.06)	0.64 (0.04)	2.30

Table S2.3. Strain list. Table lists genotypes of all strains used.

Strain	Genotype	Name
Behavior		
N2	Bristol strain	"WT"
IV378	*aex-5(sa23) I,* JT23 outcrossed 4x	"*aex-5*" in Figure 2.3D, 3E, 4F
CB937	*bli-4(e937) I*	"*bli-4*" in Figure 2.3D
FX1377	*egl-3(tm1377) V*	"*egl-3*" in Figure 2.3D
VC48	*kpc-1(gk8) I*	"*kpc-1*" in Figure 2.3D
IV670	*aex-5(sa23) I; ueEx163 [unc-119::aex-5 sense:sl2mCherry, elt-2::gfp]*	"*aex-5; Neurons::aex-5*" in Figure 2.3E
IV290	*aex-5(sa23) I; ueEx182 [gly-19::aex-5 sense:sl2mCherry, elt-2::gfp]*	"*aex-5; Intestine::aex-5*" in Figure 2.3E
IV486	*aex-5(sa23) I; ueEx304 [myo-3::aex-5 sense:sl2gfp, unc122::rfp]*	"*aex-5; Body wall muscles::aex-5*" in Figure 2.3E
IV566	*aex-5(sa23) I; ueEx369 [myo-2::aex-5 sense:sl2gfp, elt-2::gfp]*	"*aex-5; Pharynx::aex-5*" in Figure 2.3E
IV568	*aex-5(sa23) I; ueEx371 [lin-44 aex-5 sense::sl2gfp, elt-2::gfp]*	"*aex-5; Tail::aex-5*" in Figure 3E
IV607	*ueEx402 [h20::aex-5sense:sl2mCherry, h20::aex-5 antisense:sl2gfp]*	"*Neurons::aex-5 RNAi*" in Figure 2.3F
IV617	*ueEx410[gly-19::aex-5 sense:sl2mcherry, elt-2::gfp]; ueEx422[gly-19::aex-5 antisense:sl2mcherry, unc-122::rfp]*	"*Intestine::aex-5 RNAi*" in Figure 2.3F
IV614	*ueEx408[myo-3::aex-5 sense:sl2gfp, myo-3::aex-5 antisense:sl2mCherry, elt-2::gfp]*	"*Body wall muscles::aex-5 RNAi*" in Figure 2.3F
IV616	*aex-5(sa21) I; daf-2(e1370) III*	"*aex-5; daf-2*" in Figure 2.4E

Table S2.3. Strain list, continued.

Strain	Genotype	Name
CF1041	*daf-2(e1370) III*	"*daf-2*" in Figure 2.4A, 2.4B, 2.4D, 2.4E
ZM8561	*daf-2(m596) III; hpEx2906 [myo-2p::RFP + rgef-1p::daf-2]*	"*daf-2; Neurons::daf-2*" in Figure 2.4A
ZM8562	*daf-2(m596) III; hpEx3369 [myo-2p::RFP + ges-1p(short)::daf-2]*	"*daf-2; Intestine::daf-2*" in Figure 2.4A
ZM9028	*daf-2(m596) III; hpEx2905 [myo-2p::RFP + myo-3::daf-2]*	"*daf-2; Body wall muscles::daf-2*" in Figure 2.4A
TJ1052	*age-1(hx546) II*	"*age-1*" in Figure S2.4B
CB1375	*daf-18(e1375) IV*	"*daf-18*" in Figure S2.4B
GR1318	*pdk-1(mg142) X*	"*pdk-1*" in Figure S2.4B
VC345	*sgk-1(ok538) X*	"*sgk-1*" in Figure 2.4D
RB759	*akt-1(ok525) V*	"*akt-1*" in Figure S2.4B
VC204	*akt-2(ok393) X*	"*akt-2*" in Figure S2.4B
IV665	*aex-5(sa23) I; daf-2(e1370) III; ueEx457 gly-19::aex-5 sense:sl2mCherry, str-3::daf-2sense:sl2mcherry, elt-2::gfp]*	*aex-5; daf-2; gly-19::aex-5; ASI::daf-2"* in Figure 2.4E
IV628	*daf-2(e1370) III; ueEx421[sra-6::daf-2 sense:sl2mcherry, elt-2::gfp]*	*"daf-2; ASH::daf-2"*in Figure 2.4B
IV650	*daf-2(e1370) III; ueEx444[str-3::daf-2 sense:sl2mcherry, elt-2::gfp]*	*"daf-2; ASI:: daf-2"* in Figure 2.4B
IV648	*daf-2(e1370) III; ueEx442[sre-1::daf-2 sense:sl2mcherry, elt-2::gfp]*	*"daf-2; ADL::daf-2"* in Figure 2.4B
IV620	*ueEx413[myo-3::unc-31 sense:sl2rmCherry, myo-3::unc-31 antisense:sl2mCherry, elt-2::gfp]*	*Body wall muscles::unc-31 RNAi* in Figure 2.3G

Table S2.3. Strain list, continued.

Strain	Genotype	Name
IV621	*ueEx415[h20::unc-31 sense:sl2rmCherry, h20::unc-31 antisense:sl2gfp, elt-2::gfp]*	*Neurons::unc-31 RNAi* in Figure 2.3G
IV623	*ueEx416[gly-19::unc-31 sense:sl2rmCherry, gly-19::unc-31 antisense:sl2gfp, unc-122::gfp]*	*Intestine::unc-31 RNAi* in Figure 2.3G
KP2018	*egl-21(n476) IV*	*"egl-21"*in Figure S2.4A
JN372	*gpc-1(pe372) X*	*"gpc-1"*in Figure S2.4A
FX14812	*gpc-2(tm4988) I*	*"gpc-2"* in Figure S2.4A
KQ1366	*rict-1(ft7) II*	*"rict-1"* in Figure 2.4D
IV676	*sgk-1(ok538) X; ueEX466 [str-3::sgk-1 sense:sl2gfp, elt-2::gfp]*	*"sgk-1; ASI::sgk-1"* in Figures 2.4D
IV674	*rict-1(ft7) II; ueEx464[str-3::rict-1 sense:sl2gfp, elt-2::gfp]*	*"rict-1; ASI::rict-1"* in Figure 2.4D
RB954	*mml-1(ok849) II*	*"mml-1"* in Figure 2.3A
IV681	*mml-1(ok849) II; ueEx471[gly-19::mml-1 sense:sl2mcherry, unc122::gfp]*	*"mml-1; Intestine::mml-1"* in Figure 2.3A
IV688	*mml-1(ok849) II; ueEx478[myo-3::mml-1 sense:sl2mcherry, elt-2::gfp]*	*"mml-1; Body wall muscles::mml-1"* in Figure 2.3A
IV690	*mml-1(ok849) II; ueEx480[H20::mml-1 sense:sl2mcherry, elt-2::gfp]*	*"mml-1; Neurons::mml-1"* in Figure 2.3A
SM1366	*mxl-2(tm1516) II*	*"mxl-2"* in Figure 2.3A
Mutants for insulin-like peptide screen		
JT191	*daf-28(sa191)V*	"DAF-28" in Table S2.2
CX7155	*ins-1(nr2091) IV*	"INS-1" in Table S2.2

Table S2.3. Strain list, continued.

Strain	Genotype	Name
FX4467	*ins-2(tm4467) I*	"INS-2" in Table S2.2
RB1915	*ins-3(ok2488) II*	"INS-3" in Table S2.2
RB2544	*ns-4(ok3534) II*	"INS-4" in Table S2.2
FX2560	*ins-5(tm2560) II*	"INS-5" in Table S2.2
FX2416	*ins-6(tm2416) II*	"INS-6" in Table S2.2
FX2001	*ins-7(tm2001) IV*	"INS-7" in Table S2.2
FX4144	*ins-8(tm4144) IV*	"INS-8" in Table S2.2
FX3618	*ins-9(tm3618) X*	"INS-9" in Table S2.2
FX3498	*ins-10(tm3498) V*	"INS-10" in Table S2.2
FX1053	*ins-11(tm1053) II*	"INS-11" in Table S2.2
FX2918	*ins-12(tm2918) II*	"INS-12" in Table S2.2
FX5129	*ins-13(tm5129) II*	"INS-13" in Table S2.2
FX4886	*ins-14(tm4886) II*	"INS-14" in Table S2.2
RB2489	*ins-15(ok3444) II*	"INS-15" in Table S2.2
RB2159	*ins-16(ok2919) III*	"INS-16" in Table S2.2
FX790	*ins-17(tm790) III*	"INS-17" in Table S2.2
IV420 (VC1218 outcrossed)	*ins-18(ok1672) I*	"INS-18" in Table S2.2
FX5155	*ins-19(tm5155) II*	"INS-19" in Table S2. 2.2
FX5634	*ins-20(tm5634) II*	"INS-20" in Table S2.2
FX05180	*ins-21(tm5180) III*	"INS-21" in Table S2.2

Table S2.3. Strain list, continued.

Strain	Genotype	Name
RB2594	*ins-22(ok3616) III*	"INS-22" in Table S2.2
FX1975	*ins-23(tm1875) III*	"INS-23" in Table S2.2
FX1983	*ins-26(tm1983) I*	"INS-26" in Table S2.2
RB1911	*ins-27(ok2474) I*	"INS-27" in Table S2.2
RB2059	*ins-28(ok2722) I*	"INS-28" in Table S2.2
FX1922	*ins-29 (tm1922) I*	"INS-29" in Table S2.2
RB1809	*ins-30(ok2343) I*	"INS-30" in Table S2.2
RB2552	*ins-31(ok3543) II*	"INS-31" in Table S2.2
FX6109	*ins-32(tm6109) II*	"INS-32" in Table S2.2
FX2988	*ins-33(tm2988) I*	"INS-33" in Table S2.2
FX3095	*ins-34(tm3095) IV*	"INS-34" in Table S2.2
RB2412	*ins-35(ok3297) V*	"INS-35" in Table S2.2
FX6061	*ins-37(tm6061) II*	"INS-37" in Table S2.2
Calcium Imaging		
IV664	*ueEx456[str-3::sl2mcherry, unc-122::rfp]; ueEx447[sra-6::NLS-GCaMP5K, unc-122::gfp]*	"ASI" or "ASH" in Figure 52.A-D, 2.7A, S2.6A-F.
IV672	*daf-2(e1370) III; ueEx456[str-3::sl2mcherry, unc-122::rfp]; ueEx447[sra-6::NLS-GCaMP5K, unc-122::gfp]*	"*daf-2* ASI" or "*daf-2* ASH" in Figure 6A-D, S2.7A

REFERENCES

Air, E.L., Benoit, S.C., Clegg, D.J., Seeley, R.J., and Woods, S.C. (2002). Insulin and leptin combine additively to reduce food intake and body weight in rats. Endocrinology *143*, 2449-2452.

Akerboom, J., Chen, T.W., Wardill, T.J., Tian, L., Marvin, J.S., Mutlu, S., Calderon, N.C., Esposti, F., Borghuis, B.G., Sun, X.R., Gordus, A., Orger, M.B., Portugues, R., Engert, F., Macklin, J.J., Filosa, A., Aggarwal, A., Kerr, R.A., Takagi, R., Kracun, S., Shigetomi, E., Khakh, B.S., Baier, H., Lagnado, L., Wang, S.S., Bargmann, C.I., Kimmel, B.E., Jayaraman, V., Svoboda, K., Kim, D.S., Schreiter, E.R., and Looger, L.L. (2012). Optimization of a GCaMP calcium indicator for neural activity imaging. J Neurosci *32*, 13819-13840.

Andrews, Z.B., Liu, Z.W., Walllingford, N., Erion, D.M., Borok, E., Friedman, J.M., Tschop, M.H., Shanabrough, M., Cline, G., Shulman, G.I., Coppola, A., Gao, X.B., Horvath, T.L., and Diano, S. (2008). UCP2 mediates ghrelin's action on NPY/AgRP neurons by lowering free radicals. Nature *454*, 846-851.

Atasoy, D., Betley, J.N., Su, H.H., and Sternson, S.M. (2012). Deconstruction of a neural circuit for hunger. Nature *488*, 172-177.

Avery, L. (1993). The genetics of feeding in Caenorhabditis elegans. Genetics *133*, 897-917.

Avery, L., and Horvitz, H.R. (1990). Effects of starvation and neuroactive drugs on feeding in Caenorhabditis elegans. J Exp Zool *253*, 263-270.

Berthoud, H.R. (2011). Metabolic and hedonic drives in the neural control of appetite: who is the boss? Curr Opin Neurobiol *21*, 888-896.

Brenner, S. (1974). The genetics of Caenorhabditis elegans. Genetics *77*, 71-94.

Calhoun, A.J., Tong, A., Pokala, N., Fitzpatrick, J.A., Sharpee, T.O., and Chalasani, S.H. (2015). Neural Mechanisms for Evaluating Environmental Variability in Caenorhabditis elegans. Neuron *86*, 428-441.

Carlini, V.P., Varas, M.M., Cragnolini, A.B., Schioth, H.B., Scimonelli, T.N., and de Barioglio, S.R. (2004). Differential role of the hippocampus, amygdala, and dorsal raphe nucleus in regulating feeding, memory, and anxiety-like behavioral responses to ghrelin. Biochem Biophys Res Commun *313*, 635-641.

Carrillo, M.A., and Hallem, E.A. (2015). Gas sensing in nematodes. Mol Neurobiol *51*, 919-931.

Chalasani, S.H., Chronis, N., Tsunozaki, M., Gray, J.M., Ramot, D., Goodman, M.B., and Bargmann, C.I. (2007). Dissecting a circuit for olfactory behaviour in Caenorhabditis elegans. Nature *450*, 63-70.

Chalasani, S.H., Kato, S., Albrecht, D.R., Nakagawa, T., Abbott, L.F., and Bargmann, C.I. (2010). Neuropeptide feedback modifies odor-evoked dynamics in Caenorhabditis elegans olfactory neurons. Nat Neurosci *13*, 615-621.

Chen, A.T., Guo, C., Dumas, K.J., Ashrafi, K., and Hu, P.J. (2013a). Effects of Caenorhabditis elegans sgk-1 mutations on lifespan, stress resistance, and DAF-16/FoxO regulation. Aging Cell *12*, 932-940.

Chen, Z., Hendricks, M., Cornils, A., Maier, W., Alcedo, J., and Zhang, Y. (2013b). Two insulin-like peptides antagonistically regulate aversive olfactory learning in C. elegans. Neuron *77*, 572-585.

Cowley, M.A., Smith, R.G., Diano, S., Tschop, M., Pronchuk, N., Grove, K.L., Strasburger, C.J., Bidlingmaier, M., Esterman, M., Heiman, M.L., Garcia-Segura, L.M., Nillni, E.A., Mendez, P., Low, M.J., Sotonyi, P., Friedman, J.M., Liu, H., Pinto, S., Colmers, W.F., Cone, R.D., and Horvath, T.L. (2003). The distribution and mechanism of action of ghrelin in the CNS demonstrates a novel hypothalamic circuit regulating energy homeostasis. Neuron *37*, 649-661.

de Bono, M., and Bargmann, C.I. (1998). Natural variation in a neuropeptide Y receptor homolog modifies social behavior and food response in C. elegans. Cell *94*, 679-689.

Dietrich, M.O., and Horvath, T.L. (2012). Limitations in anti-obesity drug development: the critical role of hunger-promoting neurons. Nat Rev Drug Discov *11*, 675-691.

Dietrich, M.O., and Horvath, T.L. (2013). Hypothalamic control of energy balance: insights into the role of synaptic plasticity. Trends Neurosci *36*, 65-73.

Dietrich, M.O., Zimmer, M.R., Bober, J., and Horvath, T.L. (2015). Hypothalamic Agrp neurons drive stereotypic behaviors beyond feeding. Cell *160*, 1222-1232.

Doi, M., and Iwasaki, K. (2002). Regulation of retrograde signaling at neuromuscular junctions by the novel C2 domain protein AEX-1. Neuron *33*, 249-259.

Esposito, G., Di Schiavi, E., Bergamasco, C., and Bazzicalupo, P. (2007). Efficient and cell specific knock-down of gene function in targeted C. elegans neurons. Gene *395*, 170-176.

Ezcurra, M., Tanizawa, Y., Swoboda, P., and Schafer, W.R. (2011). Food sensitizes C. elegans avoidance behaviours through acute dopamine signalling. Embo J *30*, 1110-1122.

Figlewicz, D.P., and Sipols, A.J. (2010). Energy regulatory signals and food reward. Pharmacol Biochem Behav *97*, 15-24.

Gallagher, T., Kim, J., Oldenbroek, M., Kerr, R., and You, Y.J. (2013). ASI regulates satiety quiescence in C. elegans. J Neurosci *33*, 9716-9724.

Gillette, R., Huang, R.C., Hatcher, N., and Moroz, L.L. (2000). Cost-benefit analysis potential in feeding behavior of a predatory snail by integration of hunger, taste, and pain. Proc Natl Acad Sci U S A *97*, 3585-3590.

Gray, J.M., Hill, J.J., and Bargmann, C.I. (2005). A circuit for navigation in Caenorhabditis elegans. Proc Natl Acad Sci U S A *102*, 3184-3191.

Grove, C.A., De Masi, F., Barrasa, M.I., Newburger, D.E., Alkema, M.J., Bulyk, M.L., and Walhout, A.J. (2009). A multiparameter network reveals extensive divergence between C. elegans bHLH transcription factors. Cell *138*, 314-327.

Gruninger, T.R., Gualberto, D.G., and Garcia, L.R. (2008). Sensory perception of food and insulin-like signals influence seizure susceptibility. PLoS Genet *4*, e1000117.

Hamm, H.E. (1998). The many faces of G protein signaling. J Biol Chem *273*, 669-672.

Havula, E., and Hietakangas, V. (2012). Glucose sensing by ChREBP/MondoA-Mlx transcription factors. Semin Cell Dev Biol *23*, 640-647.

Hertweck, M., Gobel, C., and Baumeister, R. (2004). C. elegans SGK-1 is the critical component in the Akt/PKB kinase complex to control stress response and life span. Dev Cell *6*, 577-588.

Hilliard, M.A., Apicella, A.J., Kerr, R., Suzuki, H., Bazzicalupo, P., and Schafer, W.R. (2005). In vivo imaging of C. elegans ASH neurons: cellular response and adaptation to chemical repellents. Embo J *24*, 63-72.

Hilliard, M.A., and Bargmann, C.I. (2006). Wnt signals and frizzled activity orient anterior-posterior axon outgrowth in C. elegans. Dev Cell *10*, 379-390.

Hilliard, M.A., Bargmann, C.I., and Bazzicalupo, P. (2002). C. elegans responds to chemical repellents by integrating sensory inputs from the head and the tail. Curr Biol *12*, 730-734.

Hills, T., Brockie, P.J., and Maricq, A.V. (2004). Dopamine and glutamate control area-restricted search behavior in Caenorhabditis elegans. J Neurosci *24*, 1217-1225.

Hobert, O. (2013). The neuronal genome of Caenorhabditis elegans. WormBook, 1-106.

Hung, W.L., Wang, Y., Chitturi, J., and Zhen, M. (2014). A Caenorhabditis elegans developmental decision requires insulin signaling-mediated neuron-intestine communication. Development *141*, 1767-1779.

Husson, S.J., Janssen, T., Baggerman, G., Bogert, B., Kahn-Kirby, A.H., Ashrafi, K., and Schoofs, L. (2007). Impaired processing of FLP and NLP peptides in carboxypeptidase E (EGL-21)-deficient Caenorhabditis elegans as analyzed by mass spectrometry. J Neurochem *102*, 246-260.

Iino, Y., and Yoshida, K. (2009). Parallel use of two behavioral mechanisms for chemotaxis in Caenorhabditis elegans. J Neurosci *29*, 5370-5380.

Inagaki, H.K., Panse, K.M., and Anderson, D.J. (2014). Independent, reciprocal neuromodulatory control of sweet and bitter taste sensitivity during starvation in Drosophila. Neuron *84*, 806-820.

Ishihara, T., Iino, Y., Mohri, A., Mori, I., Gengyo-Ando, K., Mitani, S., and Katsura, I. (2002). HEN-1, a secretory protein with an LDL receptor motif, regulates sensory integration and learning in Caenorhabditis elegans. Cell *109*, 639-649.

Jansen, G., Thijssen, K.L., Werner, P., van der Horst, M., Hazendonk, E., and Plasterk, R.H. (1999). The complete family of genes encoding G proteins of Caenorhabditis elegans. Nat Genet *21*, 414-419.

Johnson, D.W., Llop, J.R., Farrell, S.F., Yuan, J., Stolzenburg, L.R., and Samuelson, A.V. (2014). The Caenorhabditis elegans Myc-Mondo/Mad complexes integrate diverse longevity signals. PLoS Genet *10*, e1004278.

Jones, K.T., Greer, E.R., Pearce, D., and Ashrafi, K. (2009). Rictor/TORC2 regulates Caenorhabditis elegans fat storage, body size, and development through sgk-1. PLoS Biol *7*, e60.

Jordan, S.D., Konner, A.C., and Bruning, J.C. (2010). Sensing the fuels: glucose and lipid signaling in the CNS controlling energy homeostasis. Cell Mol Life Sci *67*, 3255-3273.

Kawai, K., Sugimoto, K., Nakashima, K., Miura, H., and Ninomiya, Y. (2000). Leptin as a modulator of sweet taste sensitivities in mice. Proc Natl Acad Sci U S A *97*, 11044-11049.

Kojima, M., Hosoda, H., Date, Y., Nakazato, M., Matsuo, H., and Kangawa, K. (1999). Ghrelin is a growth-hormone-releasing acylated peptide from stomach. Nature *402*, 656-660.

Lapierre, L.R., and Hansen, M. (2012). Lessons from C. elegans: signaling pathways for longevity. Trends Endocrinol Metab *23*, 637-644.

Leinwand, S.G., and Chalasani, S.H. (2013). Neuropeptide signaling remodels chemosensory circuit composition in Caenorhabditis elegans. Nat Neurosci *16*, 1461-1467.

Li, C., and Kim, K. (2008). Neuropeptides. WormBook, 1-36.

Li, M.V., Chen, W., Harmancey, R.N., Nuotio-Antar, A.M., Imamura, M., Saha, P., Taegtmeyer, H., and Chan, L. (2010). Glucose-6-phosphate mediates activation of the carbohydrate responsive binding protein (ChREBP). Biochem Biophys Res Commun *395*, 395-400.

Lipton, J., Kleemann, G., Ghosh, R., Lints, R., and Emmons, S.W. (2004). Mate searching in Caenorhabditis elegans: a genetic model for sex drive in a simple invertebrate. J Neurosci *24*, 7427-7434.

Ludewig, A.H., and Schroeder, F.C. (2013). Ascaroside signaling in C. elegans. WormBook, 1-22.

Maduro, M., and Pilgrim, D. (1995). Identification and cloning of unc-119, a gene expressed in the Caenorhabditis elegans nervous system. Genetics *141*, 977-988.

Mahoney, T.R., Luo, S., Round, E.K., Brauner, M., Gottschalk, A., Thomas, J.H., and Nonet, M.L. (2008). Intestinal signaling to GABAergic neurons regulates a rhythmic behavior in Caenorhabditis elegans. Proc Natl Acad Sci U S A *105*, 16350-16355.

Malik, S., McGlone, F., Bedrossian, D., and Dagher, A. (2008). Ghrelin modulates brain activity in areas that control appetitive behavior. Cell Metab *7*, 400-409.

McGhee, J.D. (2007). The C. elegans intestine. WormBook, 1-36.

McGlone, F., and Reilly, D. (2010). The cutaneous sensory system. Neurosci Biobehav Rev *34*, 148-159.

Mease, R.A., Famulare, M., Gjorgjieva, J., Moody, W.J., and Fairhall, A.L. (2013). Emergence of adaptive computation by single neurons in the developing cortex. J Neurosci *33*, 12154-12170.

Mello, C., and Fire, A. (1995). DNA transformation. Methods Cell Biol *48*, 451-482.

Mercer, R.E., Chee, M.J., and Colmers, W.F. (2011). The role of NPY in hypothalamic mediated food intake. Front Neuroendocrinol *32*, 398-415.

Mizunuma, M., Neumann-Haefelin, E., Moroz, N., Li, Y., and Blackwell, T.K. (2014). mTORC2-SGK-1 acts in two environmentally responsive pathways with opposing effects on longevity. Aging Cell *13*, 869-878.

Moerman, D.G., and Williams, B.D. (2006). Sarcomere assembly in C. elegans muscle. WormBook, 1-16.

Muller, T.D., Nogueiras, R., Andermann, M.L., Andrews, Z.B., Anker, S.D., Argente, J., Batterham, R.L., Benoit, S.C., Bowers, C.Y., Broglio, F., Casanueva, F.F., D'Alessio, D., Depoortere, I., Geliebter, A., Ghigo, E., Cole, P.A., Cowley, M., Cummings, D.E., Dagher, A., Diano, S., Dickson, S.L., Dieguez, C., Granata, R., Grill, H.J., Grove, K.,

Habegger, K.M., Heppner, K., Heiman, M.L., Holsen, L., Holst, B., Inui, A., Jansson, J.O., Kirchner, H., Korbonits, M., Laferrere, B., LeRoux, C.W., Lopez, M., Morin, S., Nakazato, M., Nass, R., Perez-Tilve, D., Pfluger, P.T., Schwartz, T.W., Seeley, R.J., Sleeman, M., Sun, Y., Sussel, L., Tong, J., Thorner, M.O., van der Lely, A.J., van der Ploeg, L.H., Zigman, J.M., Kojima, M., Kangawa, K., Smith, R.G., Horvath, T., and Tschop, M.H. (2015). Ghrelin. Molecular metabolism *4*, 437-460.

Murphy, C.T., and Hu, P.J. (2013). Insulin/insulin-like growth factor signaling in C. elegans. WormBook, 1-43.

Nassel, D.R., and Wegener, C. (2011). A comparative review of short and long neuropeptide F signaling in invertebrates: Any similarities to vertebrate neuropeptide Y signaling? Peptides *32*, 1335-1355.

Okkema, P.G., Harrison, S.W., Plunger, V., Aryana, A., and Fire, A. (1993). Sequence requirements for myosin gene expression and regulation in Caenorhabditis elegans. Genetics *135*, 385-404.

Pierce, S.B., Costa, M., Wisotzkey, R., Devadhar, S., Homburger, S.A., Buchman, A.R., Ferguson, K.C., Heller, J., Platt, D.M., Pasquinelli, A.A., Liu, L.X., Doberstein, S.K., and Ruvkun, G. (2001). Regulation of DAF-2 receptor signaling by human insulin and ins-1, a member of the unusually large and diverse C. elegans insulin gene family. Genes Dev *15*, 672-686.

Pierce-Shimomura, J.T., Morse, T.M., and Lockery, S.R. (1999). The fundamental role of pirouettes in Caenorhabditis elegans chemotaxis. J Neurosci *19*, 9557-9569.

Ramot, D., Johnson, B.E., Berry, T.L., Jr., Carnell, L., and Goodman, M.B. (2008). The Parallel Worm Tracker: a platform for measuring average speed and drug-induced paralysis in nematodes. PLoS One *3*, e2208.

Sawin, E.R., Ranganathan, R., and Horvitz, H.R. (2000). C. elegans locomotory rate is modulated by the environment through a dopaminergic pathway and by experience through a serotonergic pathway. Neuron *26*, 619-631.

Schrodel, T., Prevedel, R., Aumayr, K., Zimmer, M., and Vaziri, A. (2013). Brain-wide 3D imaging of neuronal activity in Caenorhabditis elegans with sculpted light. Nat Methods *10*, 1013-1020.

Sengupta, P. (2013). The belly rules the nose: feeding state-dependent modulation of peripheral chemosensory responses. Curr Opin Neurobiol *23*, 68-75.

Sheng, M., Hosseinzadeh, A., Muralidharan, S.V., Gaur, R., Selstam, E., and Tuck, S. (2015). Aberrant fat metabolism in Caenorhabditis elegans mutants with defects in the defecation motor program. PLoS One *10*, e0124515.

Shioi, G., Shoji, M., Nakamura, M., Ishihara, T., Katsura, I., Fujisawa, H., and Takagi, S. (2001). Mutations affecting nerve attachment of Caenorhabditis elegans. Genetics *157*, 1611-1622.

Soukas, A.A., Kane, E.A., Carr, C.E., Melo, J.A., and Ruvkun, G. (2009). Rictor/TORC2 regulates fat metabolism, feeding, growth, and life span in Caenorhabditis elegans. Genes Dev *23*, 496-511.

Speese, S., Petrie, M., Schuske, K., Ailion, M., Ann, K., Iwasaki, K., Jorgensen, E.M., and Martin, T.F. (2007). UNC-31 (CAPS) is required for dense-core vesicle but not synaptic vesicle exocytosis in Caenorhabditis elegans. J Neurosci *27*, 6150-6162.

Speidel, D., Varoqueaux, F., Enk, C., Nojiri, M., Grishanin, R.N., Martin, T.F., Hofmann, K., Brose, N., and Reim, K. (2003). A family of Ca2+-dependent activator proteins for secretion: comparative analysis of structure, expression, localization, and function. J Biol Chem *278*, 52802-52809.

Sternson, S.M., Nicholas Betley, J., and Cao, Z.F. (2013). Neural circuits and motivational processes for hunger. Curr Opin Neurobiol *23*, 353-360.

Stoeckman, A.K., Ma, L., and Towle, H.C. (2004). Mlx is the functional heteromeric partner of the carbohydrate response element-binding protein in glucose regulation of lipogenic enzyme genes. J Biol Chem *279*, 15662-15669.

Stoltzman, C.A., Peterson, C.W., Breen, K.T., Muoio, D.M., Billin, A.N., and Ayer, D.E. (2008). Glucose sensing by MondoA:Mlx complexes: a role for hexokinases and direct regulation of thioredoxin-interacting protein expression. Proc Natl Acad Sci U S A *105*, 6912-6917.

Taghert, P.H., and Nitabach, M.N. (2012). Peptide neuromodulation in invertebrate model systems. Neuron *76*, 82-97.

Trent, C., Tsuing, N., and Horvitz, H.R. (1983). Egg-laying defective mutants of the nematode Caenorhabditis elegans. Genetics *104*, 619-647.

Troemel, E.R., Chou, J.H., Dwyer, N.D., Colbert, H.A., and Bargmann, C.I. (1995). Divergent seven transmembrane receptors are candidate chemosensory receptors in C. elegans. Cell *83*, 207-218.

Tschop, M., Smiley, D.L., and Heiman, M.L. (2000). Ghrelin induces adiposity in rodents. Nature *407*, 908-913.

Wark, B., Fairhall, A., and Rieke, F. (2009). Timescales of inference in visual adaptation. Neuron *61*, 750-761.

Wark, B., Lundstrom, B.N., and Fairhall, A. (2007). Sensory adaptation. Curr Opin Neurobiol *17*, 423-429.

Warren, C.E., Krizus, A., and Dennis, J.W. (2001). Complementary expression patterns of six nonessential Caenorhabditis elegans core 2/I N-acetylglucosaminyltransferase homologues. Glycobiology *11*, 979-988.

White, J.G., Southgate, E., Thomson, J.N., and Brenner, S. (1986). The structure of the nervous system of the nematode Caenorhabditis elegans. Philos Trans R Soc Lond B Biol Sci *314*, 1-340.

CHAPTER 3.

Varying bacterial diet modifies chemosensory behavior via neuropeptide signaling in *Caenorhabditis elegans*

ABSTRACT

Changing an animal's diet has a major influence on its neural circuits and behavior. Despite this, less is known about the precise nature of the molecular mechanisms that integrate food signals and drive behavior. Here, we use the bacteria feeding nematode, *Caenorhabditis elegans* to probe the molecular pathways integrating diet signals into behavioral circuits. We analyzed the behavior of animals that have been acutely fed different bacteria diets. Animals fed *Pseudomonas* and *Serratia* species for 3 hours altered their food-seeking behavior in an assay integrating repellent and attractant signals. While these bacteria are pathogenic to *C. elegans*, we show that pathogenesis is not a requirement for the diet-induced behavioral change. Further, we demonstrate that multiple tissues including neurons and intestine use AEX-5 processed peptides to relay information about the altered diet. Additionally, we find that animals missing three neuropeptides NLP-2, NLP-3 and FLP-8 do not alter their behavior in response to the altered diet. These results show that transiently altering *C. elegans* diet modifies its food-seeking behavior. Also, we suggest that neuropeptides might relay information about the altered diet. More generally, our results argue that altering an animal's diet might lead to a change in peptide signals between tissues leading to changes in neural circuitry and behavior.

INTRODUCTION

Animals are exposed to a variety of food sources in their environment and use a feeding strategy to maximize their survival, fecundity and lifespan (Martin et al., 2008; Piper et al., 2005; Tilly and Sinclair, 2013; Wilkinson et al., 2012; Willett, 1994). An optimal strategy involves selecting a diet that provides a balance of nutrients. Moreover,

in the absence of a particular element, animals develop a drive to supplement that nutrient. For example, rats deprived of vitamin B develop a strong appetite for it (Richter et al., 1937). Apart from feeding behaviors, dietary changes can also alter higher brain functions including anxiety, cognition and memory (Attuquayefio and Stevenson, 2015; Kanoski and Davidson, 2011; Rivera et al., 2015). These results suggest that an animal's diet can have broad influence on a number of neural circuits and the associated behaviors. A complete understanding of this process requires an ability to identify and manipulate the participating neurons, their connections and their interactions with other tissues including the circulatory system, intestine and musculature, a difficult task in the complex vertebrate. We approach this problem by analyzing the effects of different bacterial diets on an invertebrate.

The nematode, *C. elegans*, has a small nervous system consisting of just 302 neurons and a fully mapped connectome (White et al., 1986), 20 cells in its intestine (McGhee, 2007) and 95 body wall muscle cells (Moerman and Williams, 2006). With a complete lineage (Sulston et al., 1983) and powerful genetic tools (Boulin and Hobert, 2012), this animal provides a unique opportunity to dissect the molecular pathways integrating dietary changes with neural circuitry and behavior. In the wild, *C. elegans* is typically found in compost heaps foraging for bacterial food (Felix and Duveau, 2012). Consistently, almost all *C. elegans* behaviors are affected by the presence or absence of bacteria (de Bono and Maricq, 2005; Gray et al., 2005; Sawin et al., 2000) and *C. elegans* has been shown to seek bacteria that best support its growth (Shtonda and Avery, 2006; Yu et al., 2015), suggesting that changes in diet might similarly affect worms and mammals. Additionally, previous studies have shown that altering bacterial lawns affects

C. elegans physiology, behavior, lifespan and fecundity (Gusarov et al., 2013; MacNeil et al., 2013; Reinke et al., 2010). *C. elegans'* food preferences are often quantified using behavioral assays measuring the probability of lawn occupancy or lawn leaving (Meisel et al., 2014; Shtonda and Avery, 2006). Although *C. elegans* exhibit an innate preference for pathogenic bacteria (Glater et al., 2014), prolonged exposure results in learning where the animals avoid subsequent exposures (Meisel et al., 2014; Pradel et al., 2007; Zhang et al., 2005). While these studies illustrating the importance of the *C. elegans* model in understanding host-bacteria experiences, less is known about how acute changes in the diet affect animal behavior.

Here, we developed a behavioral paradigm combining acute changes in bacterial food with a complex behavioral assay that requires animals to evaluate both attractive and repulsive chemosensory cues. In the sensory integration assays, animals cross a repellent (copper) barrier and chemotax towards a point source of a volatile attractant (Ishihara et al., 2002). Using this assay, we show that animals previously experienced pathogenic bacteria are more likely to cross the repellent compared to animals feeding on *E. coli* bacteria (normal food source). Additionally, we show that pathogenesis is not a requirement for this behavioral change. Finally, we map the neuropeptide signals relaying information about dietary changes and modifying behaviors.

RESULTS

Pathogenic and non-pathogenic bacteria modify *C. elegans* behavior

Animals including *C. elegans* encounter a variety of food sources in their environment. We developed a new behavioral paradigm by combining acute exposure to

different bacteria and the sensory integration assay (Figure 3.1A). To test the effects of different bacteria on *C. elegans* behavior, we selected both pathogenic and non-pathogenic bacterial strains. Previous studies have shown that three bacterial pathogens *Pseudomonas areuginosa* (PA14), *Serratia marcescens* and *Staphylococcus aure*us can infect and kill *C. elegans* (Pradel et al., 2007; Sifri et al., 2003; Tan et al., 1999). We also tested four non-pathogenic strains *Pseudomonas fluorescens*, *Bacillus subtilis* and *E. coli* strains OP50 (normal food) and HB101 (Brenner, 1974; Sanchez-Blanco and Kim, 2011; Yu et al., 2015). To differentiate from pathogen-induced effects on *C. elegans* behavior such as learned pathogen avoidance, we acutely exposed adults to either *E. coli* OP50 or one of these other bacteria for 3 hours before analyzing animal behavior. Previous studies have shown that, *C. elegans* can learn to avoid PA14 after a 4-hour exposure (Zhang et al., 2005). We used a sensory integration assay to test the effect of acute changes in bacterial diet on *C. elegans* behavior (Figure 3.1A). This assay allows us to measure the animal responsiveness to both attractants and repellents simultaneously. We found that when adults raised on *E. coli* OP50 lawns were transferred to new OP50 lawns for 3 hours, about 35% of the animals crossed the repellent copper barrier and chemotaxed towards the diacetyl attractant (Figure 3.1B). Surprisingly, we found that when adults were exposed to the pathogenic *P. areuginosa* or *S. marcescens* or the non-pathogenic *P. fluorescens,* significantly more animals crossed the copper barrier (Figure 3.1B). Moreover, pathogenic *S. aureus* or non-pathogenic *B. subtilis* or *E. coli* HB101 had no effect on animal behavior (Figure 3.1B). Taken together, these results suggest an acute change in bacterial diet modifies *C. elegans* chemosensory behavior.

We focused our analysis on the acute change involving *P. areuginosa* (PA14) to probe the underlying molecular machinery. We found that diluting PA14 with *E. coli* OP50 bacteria did not significantly affect the behavior change (Figure 3.1C). However, we found that heat-killing PA14 bacteria completely abrogated the behavioral change (Figure 3.1C). These results suggest that live PA14 bacteria are needed to modify *C. elegans* behavior. We next tested the time course of the acute exposure needed to modify animal behavior. We exposed animals to either *E. coli* (OP50) or *P. areuginosa* (PA14) for different durations and subsequently tested their behavior in the sensory integration assay. We found that animals exposed to PA14 for at least 2 hours showed a significant change in behavior. Also, we observe that the effect was maximal at 3 hours and additional time did not further modify chemosensory behavior (Figure 3.1D). Together, these results suggest that acute exposure to live PA14 for about 3 hours modifies *C. elegans* chemosensory behavior.

Pathogenicity is not required for modifying *C. elegans* sensory integration behavior

Previous studies have shown that *P. areuginosa* PA14 is highly pathogenic and rapidly kills *C. elegans* (Tan et al., 1999). We used two different approaches to test whether PA14 pathogenicity was required to modify *C. elegans* behavior. We first tested a non-pathogenic PA14 mutant, *gacA*, for its ability to modify sensory integration behavior after acute exposure. We found that *gacA* was also able to alter *C. elegans* sensory integration response, suggesting that pathogenicity was not required (Figure 3.2A). Next, we used a small molecule that blocks quorum sensing in *P. areuginosa* and blocks its virulence. mBTL is an analog of the *P. areuginosa* autoinducer, which

represses the expression of pyocyanin and prevents biofilm formation and *C. elegans* killing (Dietrich et al., 2006; O'Loughlin et al., 2013). We found that adding mBTL to the *P. areuginosa* PA14 had no effect on modifying *C. elegans* sensory integration behavior (Fig 3.2B). Collectively, these results argue that PA14 pathogenicity is not a requirement for modifying *C. elegans* chemosensory behavior.

Acute PA14 exposure alters *C. elegans* sensitivity to attractants

An increase in the number of animals crossing the repellent barrier could occur from either an increased attraction to the diacetyl attractant on the other side or a decrease in the sensitivity to the copper repellent barrier. To test these possibilities, we acutely exposed adults to PA14 and then assayed their behavior on plates with just the repellent or attractant alone. We found that PA14 exposed animals showed an increased sensitivity to the attractant, but no effect on repellent responsiveness (Figure 3.3A). However, the increased attractant sensitivity is not sufficient to explain the entire effect (compare Figure 3.3A to Figure 3.1B) suggesting that PA14 exposure might also affect the integration of both attractant and repellent signals.

We then tested whether reducing the concentration of the attractant would have any effect on *C. elegans* integration response. We found OP50-exposed animals showed a dose-dependent effect, with fewer animals crossing the repellent barrier when presented with diluted attractants (grey line, Figure 3.3A). In contrast, PA14-exposed animals continued to maintain a high level of attractiveness even at diluted attractant concentrations (green line, Figure 3.3B). These data suggest that acute PA14 exposure modifies *C. elegans* sensitivity to attractants. Next, we analyzed the *C. elegans* responses

to other volatile attractants. We found that PA14-exposed animals also showed increased attraction to two other volatile attractants, pyrazine and isoamyl alcohol (Fig 3.3C) (Bargmann, 2006). Taken together, these results show that acute exposure to *P. areuginosa* PA14 increases *C. elegans* sensitivity to multiple volatile attractants.

Multiple tissues process peptides to modify *C. elegans* response after PA14 exposure

Our results show that changes in bacterial diet modifies *C. elegans* sensitivity to attractants leading to an increase in integration index. We hypothesized that intestine senses the change in bacterial food and releases signals to modify behavior. To gain insights into the nature of the tissue-released signals, we tested mutants in peptide signaling. The *C. elegans* genome encodes four pro-protein convertases that cleave an overlapping subset of pro-peptides, which are further modified before being released from dense core vesicles (Li and Kim, 2008). We analyzed null mutants in each of these pro-protein convertases (*egl-3*, *bli-4*, *kpc-1* and *aex-5*) for their integration responses after PA14 exposure. We found that *egl-3* mutants did not perform the integration assay in either OP50 or PA14 exposed condition (Figure 3.4A). This is consistent with previous results showing that a neuropeptide receptor is required to generate normal integration response (Ishihara et al., 2002). We found that *kpc-1* and *bli-4* mutants increased their integration response after PA14 exposure (Figure 3.4A). In contrast, *aex-5* mutants did not change their integration behavior after PA14 exposure, suggesting that AEX-5 processing was required for the behavior change. To identify the cognate tissue where AEX-5 processes the relevant peptides, we performed transgenic rescue experiments. We found that restoring AEX-5 to either the intestine or neurons was sufficient to restore

normal behavior to *aex-5* mutants (Figure 3.4B). Taken together, these results suggest that the intestine or neurons detect the change in bacterial diet and release AEX-5 processed peptides to modify attractive behavior.

To identify the cognate neuropeptides we performed a candidate screen and analyzed null mutants in a number of neuropeptide genes. The *C. elegans* genome encodes at least 122 neuropeptides including 42 neuropeptide like proteins (NLPs), 40 FMRFamide related peptides (FLPs) and 40 insulin-like peptides (ILPs) (Hobert, 2013). We predicted that a null mutant in the cognate peptide would not alter its integration response after PA14 exposure. We tested 51 neuropeptide mutants and found that most of them increased their integration response after acute PA14 exposure (Table S3.1). In contrast, *nlp-2*, *nlp-3* and *flp-8* mutants did not change their integration response, suggesting these might be the cognate peptide(s) relaying information about dietary changes (Figure 3.4C). Pro-protein convertases have been previously shown to cleave a basic R-X-X-R motif (Thacker and Rose, 2000). We analyzed the peptide sequences of the three candidate neuropeptide genes. We found that *nlp-3* and *flp-8* have at least one R-X-X-R motif; *nlp-2* did not have this sequence (Table S3.2). These results suggest that AEX-5 might cleave *nlp-3* and *flp-8* in neurons and/or intestine to modify integration response after PA14 exposure.

DISCUSSION

Our results show that acute PA14 exposure increases *C. elegans* sensitivity to multiple attractants leading to greater numbers of animals crossing the repellent barrier in the integration assay. We show that PA14 pathogenicity is not required for this behavior

change. Further, we identify that multiple tissues including intestine and neurons likely detect the change in bacterial diet and release AEX-5 processed peptide(s) to modify behavior. Finally, we identify NLP-3 and FLP-8 as candidate neuropeptides relaying information about dietary changes and modifying behavior (Figure 3.4D). These studies show how changes in bacterial food act via neuropeptide signals to modify *C. elegans* behavior.

Previous studies have shown that *C. elegans* can detect bacterial pathogen-released odors and modify their behavior in order to avoid them (Zhang et al., 2005). In particular, *C. elegans* detect PA14 released phenazine-1-carboxamide and pyochelin along with *S. marcescens* released Serrawettin W2 leading to behavioral changes (Meisel et al., 2014; Pradel et al., 2007). However, we show that pathogenicity is not required and suggest that *C. elegans* might be detecting additional signals from these bacteria. Moreover, we observe the behavioral change to occur after 2-3 hours of exposure, which is shorter than the time required to develop an infection or kill animals (Tan et al., 1999). Additionally, our results showing that biofilm formation is not required to modify *C. elegans* behavior (mBTL does not affect PA14 induced behavior changes) confirm that this increased attraction is independent of pathogenicity or previously identified small molecules. We suggest that *C. elegans* might use multiple signals to detect a change in bacterial diet leading to behavioral change.

We also show that both intestine and neurons are required to process neuropeptide signals required for the PA14 induced behavioral change. AEX-5 has been previously shown to act in the intestine to control the defecation motor program and in motor neurons to regulate signaling at the neuromuscular junction (Doi and Iwasaki, 2002;

Mahoney et al., 2008). Also, *aex-5* mutants are unable to take up fats from the intestinal lumen and have reduced levels of fat in the intestine, which in turns affects defecation (Sheng et al., 2015). We suggest a change in bacterial diet affects the fat content in the intestine leading to a change in AEX-5 function, which in turn releases neuropeptides likely NLP-3 and/or FLP-8 to modify *C. elegans* behavior. There is substantial evidence that neurons can directly sense bacteria. While amphid sensory neuron ASI has been shown to respond to the addition of bacteria, AWC and ASK respond to the removal of bacterial signals (Calhoun et al., 2015; Chalasani et al., 2007). Additionally, ASJ sensory neurons detect PA14-released metabolites and ASI, URX and ADF sensory neurons play a role in pathogenic bacteria induced avoidance behavior (Chen et al., 2013; Meisel et al., 2014; Zhang et al., 2005). We suggest that these amphid sensory or other neurons detect bacterial signals and use AEX-5 to cleave NLP-3 and/or FLP-8 to modify behavior.

We show that upon change in bacterial diet, *C. elegans* increased its sensitivity to multiple volatile attractants. We suggest that altering the bacterial food from the familiar *E. coli* OP50 to a new, perhaps less optimal food leads to the behavioral change. Further, we speculate that *C. elegans* alters its food-seeking strategy before infection. Interestingly, the increase in sensitivity to attractants is also observed in *Drosophila* that are starved (Inagaki et al., 2014). Together, we suggest that *C. elegans* and other species increase their sensitivity to attractants upon exposure to starvation or less nutritious food enabling them to be more successful at foraging. In summary, we link dietary changes with neuropeptide signals from multiple tissues to behavioral changes.

METHODS

C. elegans strains were grown and maintained under standard conditions (Brenner, 1974). A listing of all strains and their genotypes is shown in Table S3.

Strains and Molecular Biology

cDNA corresponding to the entire coding sequence of *aex-5* genomic region was amplified by using the following primers and expressed under tissue specific promoters.

forward 5'TATTTAGCTAGCATGAAATTAATTTTCCTG and

reverse 5'TATTTAGGTACCTTATGACATTGTTCCCAC

Tissue specific expression was achieved with *H20* for all neurons and *gly-19* for the intestine (Shioi et al., 2001; Warren et al., 2001). For all experiments, a splice leader (SL2) fused to *mCherry* or *gfp* transgene was used to confirm expression of the gene of interest in specific tissues. Germline transformations were performed by microinjection of plasmids (Mello and Fire, 1995) at concentrations between 50 ng/µl with 10 ng/µl of *unc-122::rfp*, *unc-122::gfp* or *elt-2::gfp* as co-injection markers. For rescue experiments, DNA was injected into null mutant animals.

Behavior Assays

All animals were grown to adulthood on regular nematode growth medium (NGM) plates with *E. coli* OP50 lawns before they were washed and transferred to new OP50 or test bacteria plates for three hours or indicated durations. Sensory integration assay was performed on 1.6% agar plates containing 5mM potassium phosphate (pH 6), 1mM $CaCl_2$ and 1mM $MgSO_4$. Copper gradients were established by dripping 25µl of

$CuSO_4$ solution across the midline of the plate (Ishihara et al., 2002). Animals were washed from OP50 or test bacteria plates and transferred to assay plates for 45 minutes. After 45 minutes, the integration index was computed as the number of worms in the odor half of the plate minus the worms in origin half of the plate divided by the total number of worms that moved beyond the origin. Five or more assays were performed on at least two different days. Two-tailed unpaired *t* tests were used to obtain statistical information comparing *C. elegans* exposed to OP50 and other types of bacteria.

Bacteria Preparation

Pseudomonas aeruginosa PA14 was grown on slow killing (SK) plates that contain 1.7% agar, 0.35% peptone, 2.5mM potassium phosphate (pH 6), 1mM $CaCl_2$ and 1mM $MgSO_4$ where *C. elegans* killing occurs over several days (Tan et al., 1999). All other bacteria were grown on NGM plates.

mBTL-treated PA14 were prepared as previously described (O'Loughlin et al., 2013). *E. coli* OP50 or *P. areuginosa* PA14 were grown at 37°C overnight to an optical density of ~ 0.5 OD_{600}. 50 μM mBTL or equivalent volume of DMSO was added to plates and bacterial cultures during growth. mBTL treated PA14 was visibly not green which is characteristic of pathogenic PA14 lawns.

ACKNOWLEDGEMENTS

We thank T. Ishihara, V. Nizet, E. Troemel, the National BioResource Project (NBRP, Japan) and Caenorhabditis Genetics Center (CGC) for *C. elegans* and bacteria strains, B. Bassler for mBTL compound. This work was funded by grants from The Rita

Allen Foundation, The W.M. Keck Foundation and NIH R01MH096881-04 to S.H.C. H.E.L. was initially supported by the Socrates Program funded by NSF GK-12 STEM Fellows in Education (Award #NSF-742551) followed by a Graduate Research Fellowship also from the NSF.

Chapter 3 is a reprint of the material as it appears in Lau, H. E., Liu, Z., Chalasani, S.H. (2015). Varying bacterial diet modifies chemosensory behavior via neuropeptide signaling in *Caenorhabditis elegans* (in preparation) and is included with permission from all authors. It has been reformatted for this dissertation. The dissertation author was the primary author of this paper.

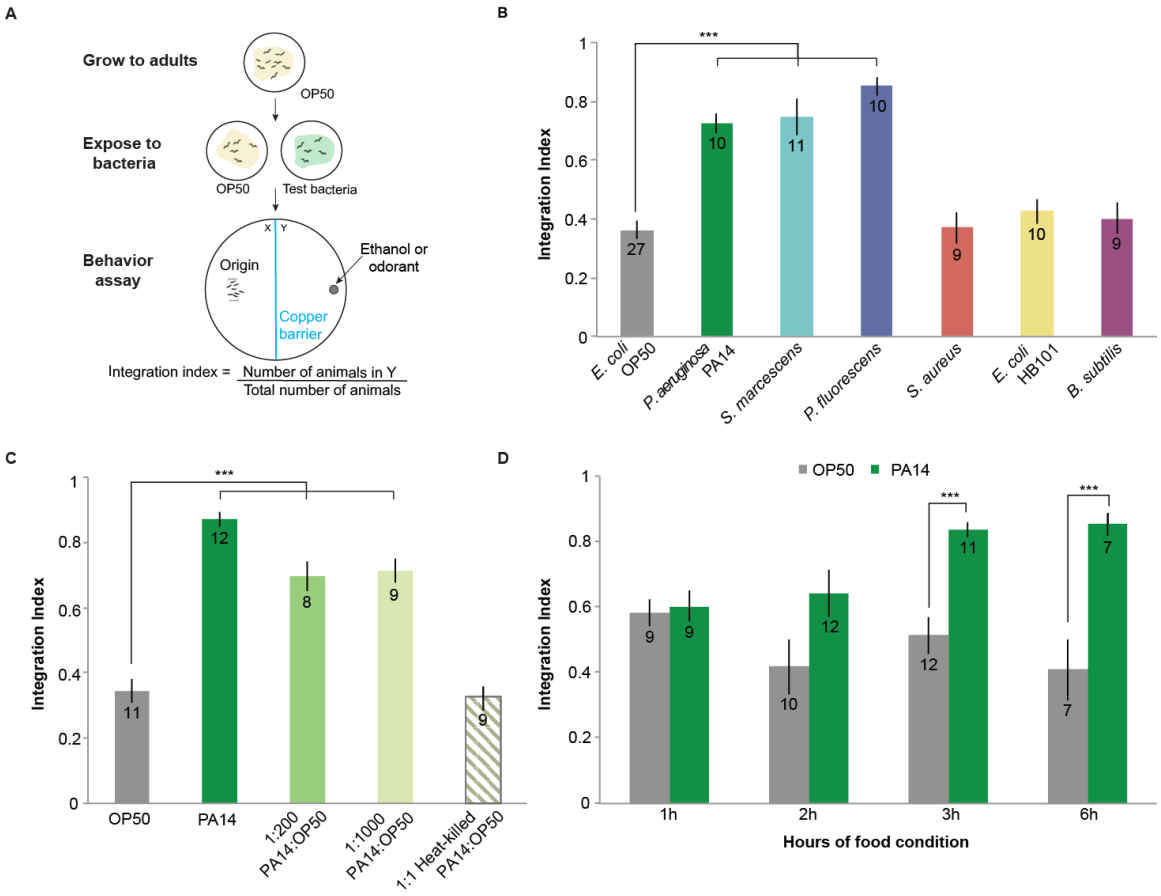

Figure 3.1. Pathogenic and non-pathogenic bacteria modify *C. elegans* behavior.
(A) Schematic of the acute food exposure and sensory integration assay. Here, adults are exposed to *E. coli* OP50 or other bacteria for 3 hours and subsequently analyzed in the sensory integration assay. Integration index is the ratio of animals that crossed the copper barrier to the total number of animals in the assay plate. Average integration index of animals fed (B) indicated bacteria or (C) *P. areuginosa* diluted or heat-killed for 3 hours. (D) Time course of acute bacteria exposure. Animals were exposed to *E. coli* OP50 or *P. areuginosa* PA14 for different times and subsequently analyzed in the sensory integration assay. Averages and s.e.m. are shown with number in each bar representing number of assay plates. Two-tailed *t*-tests were used determine significance with *** indicating $p <$ 0.0001.

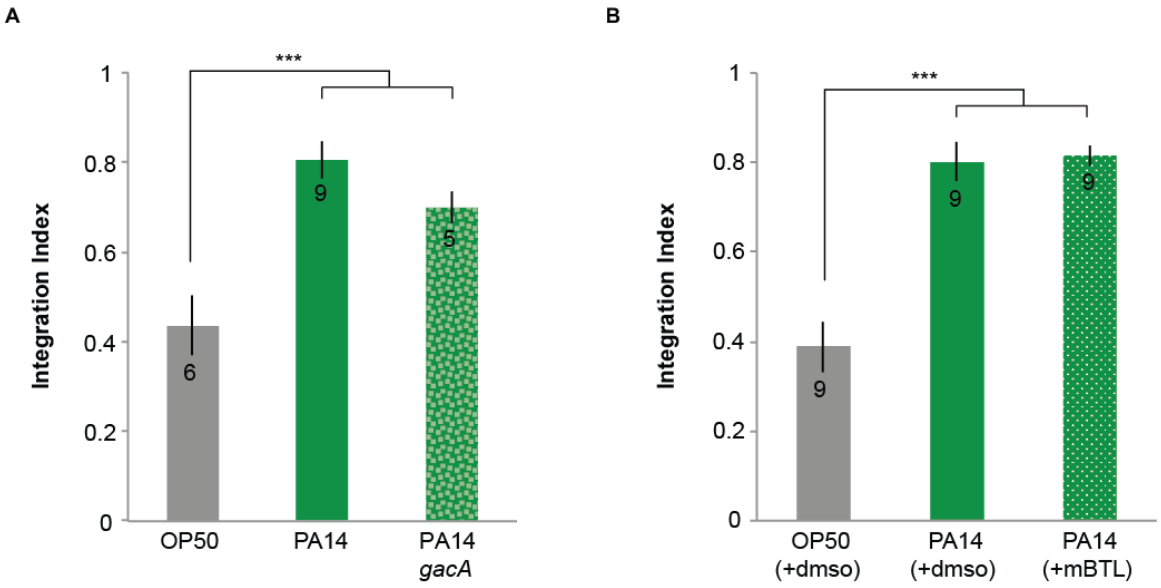

Figure 3.2. PA14 pathogenicity is not required to modify *C. elegans* behavior.
Average integration index of adults exposed to (A) *E. coli* OP50, *P. areuginosa* PA14 and *P. areuginosa gacA* mutants and (B) *E. coli* OP50 and *P. areuginosa* PA14 with and without mBTL. Averages and s.e.m. are shown with number in each bar representing number of assay plates. Two-tailed *t*-tests were used determine significance with *** indicating $p < 0.0001$.

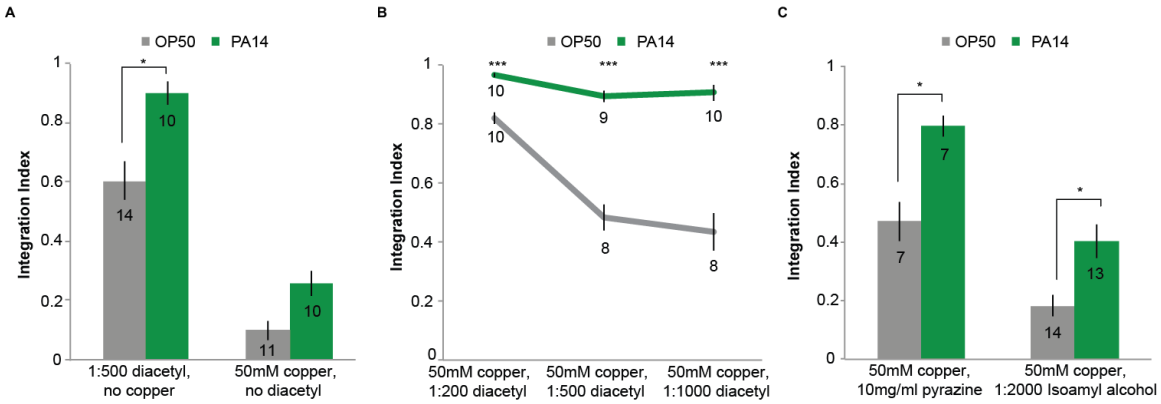

Figure 3.3. PA14 exposure increases *C. elegans* sensitivity to attractants.
(A) *C. elegans* exposed to PA14 are more attracted to diacetyl, but have no effect on copper sensitivity alone. (B) Dose-dependent of *C. elegans* attraction. OP50 exposed animals showed reduced attraction, while PA14 exposed animals maintained a high attraction to diluted attractant when paired with a copper barrier. (C) PA14-exposed animals also show increased integration index when repellent copper barrier is paired with pyrazine or isoamyl alcohol. Averages and s.e.m. are shown with number in each bar representing number of assay plates. Two-tailed *t*-tests were used determine significance with *** indicating $p < 0.0001$ and * indicating $p < 0.05$.

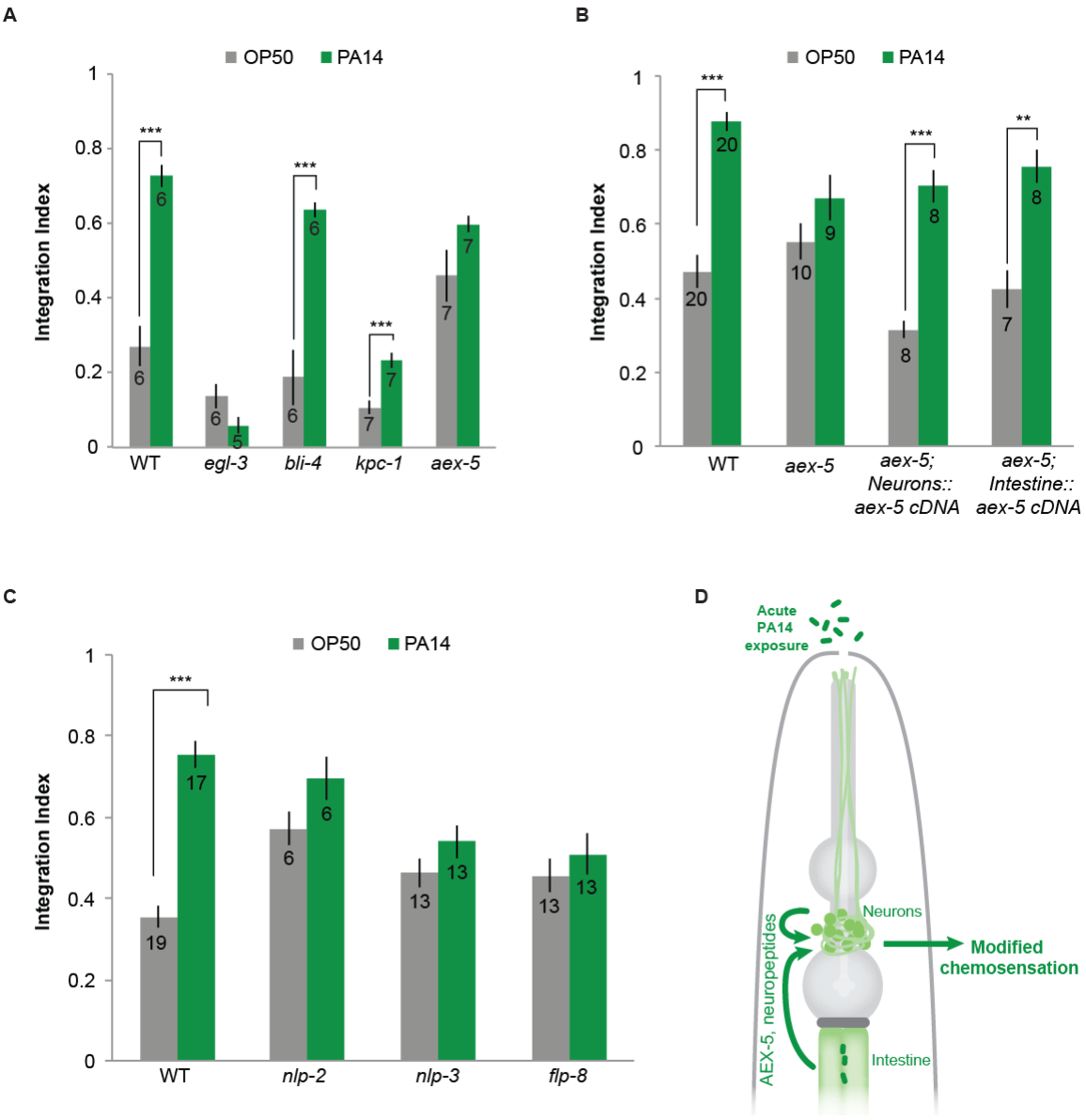

Figure 3.4. Neuropeptide signaling is required to modify *C. elegans* integration response.

(A) Pro-protein convertase mutants have altered integration behavior. While *egl-3* mutants do not show any integration response, *bli-4* and *kpc-1* mutants enhance their integration index after PA14 exposure. *aex-5* mutants do not respond to PA14 exposure. (B) Normal behavior is restored to *aex-5* mutants when full-length AEX-5 cDNA is expressed under intestinal or neuronal promoters. (C) *nlp-2*, *nlp-3* and *flp-8* mutants do not alter their integration response after PA14 exposure. (D) Schematic showing a putative signaling pathway. Intestine and neurons sense the change in bacterial diet and release AEX-5 processed peptides. Averages and s.e.m. are shown with number in each bar representing number of assay plates. Two-tailed *t*-tests were used determine significance with *** indicating $p < 0.0001$ and ** indicating $p < 0.001$.

SUPPLEMENTAL INFORMATION

Table S3.1. Chemotaxis indexes of neuropeptide gene mutants.

Strain	Neuropeptide	3h OP50	3h PA14	Fold change
Controls				
WT	-	0.37	0.83	2.24
IV378	AEX-5 pro-protein convertase	0.60	0.62	1.03
FLP tested				
RB1990	FLP-7	0.43	0.74	1.72
FX741	FLP-8	0.46	0.55	**1.20**
RB2067	FLP-9	O.18	0.77	5.56
RB1989	FLP-10	0.09	0.25	2.78
FX2706	FLP-11	0.54	0.80	1.48
RB1863	FLP-12	0.16	0.80	5.00
FX2448	FLP-13	0.12	0.38	3.17
VC2504	FLP-15	0.15	0.72	6.67
RB2188	FLP-20	0.13	0.42	3.23
RB982	FLP-21	0.06	0.65	10.83
FX4383	FLP-23	0.38	0.68	1.79
VC1982	FLP-25	0.50	0.89	1.78
VC3017	FLP-26	0.15	0.44	2.93
FX4612	FLP-27	0.46	0.84	1.83
VC2423	FLP-33	0.12	0.62	5.17
ILP tested				
FX4467	INS-2	0.57	0.82	1.44
FX2560	INS-5	0.33	0.63	1.91
FX2416	INS-6	0.51	0.74	1.45
FX3618	INS-9	0.43	0.67	1.56
FX3498	INS-10	0.27	0.81	3.00
FX2918	INS-12	0.44	0.78	1.77
FX5129	INS-13	0.24	0.54	2.25
FX4886	INS-14	0.27	0.84	3.11
RB2489	INS-15	0.16	0.33	2.06
RB2159	INS-16	0.15	0.51	3.40
VC1218	INS-18	0.29	0.69	2.38
FX5155	INS-19	0.47	0.76	1.62
FX5634	INS-20	0.41	0.90	2.20
FX1875	INS-23	0.43	0.69	1.60
RB2059	INS-28	0.01	0.13	13.00
FX1922	INS-29	0.13	0.55	4.23
FX6109	INS-32	0.33	0.89	2.70
FX2988	INS33	0.29	0.47	1.62
FX3095	INS-34	0.10	0.20	2.00
RB2412	INS-35	0.07	0.42	6.00
NLP tested				
FX1908	NLP-2	0.57	0.69	**1.21**
FX3023	NLP-3	0.45	0.56	**1.24**
FX1970	NLP-7	0.56	0.79	1.41
FX3572	NLP-9	0.23	0.75	3.26

Table S3.1 Chemotaxis indexes of neuropeptide gene mutants, continued.

Strain	Neuropeptide	3h OP50	3h PA14	Fold change
RB607	NLP-12	0.13	0.32	2.46
FX1880	NLP-14	0.46	0.63	1.37
VC1063	NLP-15	0.17	0.41	2.41
RB1372	NLP-18	0.27	0.73	2.70
RB1396	NLP-20	0.19	0.76	4.00
FX2569	NLP-21	0.44	0.73	1.66
FX5931	NLP-22	0.57	0.93	1.63
FX1712	NLP-29	0.51	0.80	1.57
FX5434	NLP-35	0.02	0.23	11.50
FX5156	NLP-36	0.20	0.73	3.65
FX4393	NLP-37	0.40	0.87	2.18
FX4085	NLP-40	0.12	0.71	5.92

Table S3.2. Peptide cleavage sites. Protein sequences of neuropeptides and highlighted cleavage sites.

Peptide	Protein Sequence	RXXR cleavage site
NLP-2	MRATLVLFALLCAVYSEAVPLQVYRPDESSAVDVVVL ENSPELYDSEDEDEWKQEEEFTEGAMGKRSIALGRSGF RPGKRSMDNFHTVDVSDLIMKRSMAMGRLGLRPGKRS MAYGRQGFRPGKRSMAYGRQGFRPGKRSMAYGRQGF RPGKRSNDMKEVFPQHVPEIYII	No
NLP-3	MSKIVACLVLLALSVMCVYSAPYEFRAKRAINPFLDSM GKRAVNPFLDSIGKRSFRPDMITEEKRYFDSLAGQSLGK RSNNRYEMLENYY	Yes
FLP-8a FLP-8b	MLSGVLFSIFVLAISANASCDVSALTTENEKELGLRICH LEAEMQVVQRALQEVMQQTDVTLYDQEVPVMNKRK NEFIRFGKRSDGMEKRKNEFIRFGKRKNEFIRFGRSDKG LGLDDNDVSSEFFGYTSDVFYL MLSGVLFSIFVLAISANASCDVSALTTENEKELGLRICH LEAEMQVVQRALQEVMQQTDVTLYDQEVPVMNKRK NEFIRFGKSDGMEKRKNEFIRFGKRKNEFIRFGRSDKGL GLDDNDVSMEKRKNEFIRFG	Yes

Table S3.3. Strain list. Table lists genotypes of all strains used.

Strain	**Genotype**	**Name**
Behavior		
N2	Bristol strain	"WT"
CB937	*bli-4(e937) I*	"*bli-4*" in Figure 3.4A
FX1377	*egl-3(tm1377) V*	"*egl-3*" in Figure 3.4A
VC48	*kpc-1(gk8) I*	"*kpc-1*" in Figure 3.4A
IV378	*aex-5(sa23) I*, JT23 outcrossed 4x	"*aex-5*" in Figure 3.4A
IV670	*aex-5(sa23) I; ueEx163 [unc-119::aex-5 sense:sl2mCherry, elt-2::gfp]*	"*aex-5; Neurons::aex-5*" in Figure 3.4B
IV290	*aex-5(sa23) I; ueEx182 [gly-19::aex-5 sense:sl2mCherry, elt-2::gfp]*	"*aex-5; Intestine::aex-5*" in Figure 3.4B
Mutants for neuropeptide screen		
FX4467	*ins-2(tm4467) I*	"INS-2" in Table S3.1
FX2560	*ins-5(tm2560) II*	"INS-5" in Table S3.1
FX2416	*ins-6(tm2416) II*	"INS-6" in Table S3.1
FX3618	*ins-9(tm3618) X*	"INS-9" in Table S3.1
FX3498	*ins-10(tm3498) V*	"INS-10" in Table S3.1
FX2918	*ins-12(tm2918) II*	"INS-12" in Table S3.1
FX5129	*ins-13(tm5129) II*	"INS-13" in Table S3.1
FX4886	*ins-14(tm4886) II*	"INS-14" in Table S3.1
RB2489	*ins-15(ok3444) II*	"INS-15" in Table S3.1

Table S3.3. Strain list, continued.

Strain	**Genotype**	**Name**
RB2159	*ins-16(ok2919) III*	"INS-16" in Table S3.1
IV420 (VC1218 outcrossed)	*ins-18(ok1672) I*	"INS-18" in Table S3.1
FX5155	*ins-19(tm5155) II*	"INS-19" in Table S3.1
FX5634	*ins-20(tm5634) II*	"INS-20" in Table S3.1
FX1975	*ins-23(tm1875) III*	"INS-23" in Table S3.1
RB2059	*ins-28(ok2722) I*	"INS-28" in Table S3.1
FX1922	*ins-29 (tm1922) I*	"INS-29" in Table S3.1
FX6109	*ins-32(tm6109) II*	"INS-32" in Table S3.1
FX2988	*ins-33(tm2988) I*	"INS-33" in Table S3.1
FX3095	*ins-34(tm3095) IV*	"INS-34" in Table S3.1
RB2412	*ins-35(ok3297) V*	"INS-35" in Table S3.1
FX1908	*nlp-2(tm1908) X*	"NLP-2" in Table S3.1 and Figure 3.4C
FX3023	*nlp-3(tm3023) X*	"NLP-3" in Table S3.1 and Figure 3.4C
FX1970	*nlp-7(tm1970) X*	"NLP-7" in Table S3.1
FX3572	*nlp-9(tm3572) V*	"NLP-9" in Table S3.1
RB607	*nlp-12(ok335) I*	"NLP-12" in Table S3.1
FX1880	*nlp-14(tm1880) X*	"NLP-14" in Table S3.1
VC1063	*nlp-15(ok1512) I*	"NLP-15" in Table S3.1
RB1372	*nlp-18(ok1557) II*	"NLP-18" in Table S3.1

Table S3.3. Strain list, continued.

Strain	**Genotype**	**Name**
RB1396	*nlp-20(ok1591) IV*	"NLP-20" in Table S3.1
FX2569	*nlp-21(tm2569) III*	"NLP-21" in Table S3.1
FX5931	*nlp-22(tm5931) X*	"NLP-22" in Table S3.1
FX1712	*nlp-29(tm1712) V*	"NLP-29" in Table S3.1
FX5434	*nlp-35(tm5434) IV*	"NLP-35" in Table S3.1
FX5156	*nlp-36(tm5156) III*	"NLP-36" in Table S3.1
FX4393	*nlp-37(tm4393) X*	"NLP-37" in Table S3.1
FX4085	*nlp-40(tm4085) I*	"NLP-40" in Table S3.1
RB1990	*flp-7(ok2626) X*	"FLP-7" in Table S3.1
FX741	*flp-8(tm741) X*	"FLP-8" in Table S3.1 and Figure 3.4C
RB2067	*flp-9(ok2730) IV*	"FLP-9" in Table S3.1
RB1989	*flp-10(ok2624) IV*	"FLP-10" in Table S3.1
FX2706	*flp-11(tm2706) X*	"FLP-11" in Table S3.1
RB1863	*flp-12(ok2409) X*	"FLP-12" in Table S3.1
FX2448	*flp-13(tm2448)*	"FLP-13" in Table S3.1
VC2504	*flp-15(gk1186) III*	"FLP-15" in Table S3.1
RB2188	*flp-20(ok2964) X*	"FLP-20" in Table S3.1
RB982	*flp-21(ok889) V*	"FLP-21" in Table S3.1
FX4383	*flp-23(tm4383) III*	"FLP-23" in Table S3.1
VC1982	*flp-25(gk1016) III*	"FLP-25" in Table S3.1

Table S3.3. Strain list, continued.

Strain	**Genotype**	**Name**
VC3017	*flp-26(gk3015) X*	"FLP-26" in Table S3.1
FX4612	*flp-27(tm4612) II*	"FLP-27" in Table S3.1
VC2423	*flp-33(gk1038) I*	"FLP-33" in Table S3.1

REFERENCES

Attuquayefio, T., and Stevenson, R.J. (2015). A systematic review of longer-term dietary interventions on human cognitive function: Emerging patterns and future directions. Appetite *95*, 554-570.

Bargmann, C.I. (2006). Chemosensation in C. elegans. WormBook, 1-29.

Boulin, T., and Hobert, O. (2012). From genes to function: the C. elegans genetic toolbox. Wiley interdisciplinary reviews Developmental biology *1*, 114-137.

Brenner, S. (1974). The genetics of Caenorhabditis elegans. Genetics *77*, 71-94.

Calhoun, A.J., Tong, A., Pokala, N., Fitzpatrick, J.A., Sharpee, T.O., and Chalasani, S.H. (2015). Neural Mechanisms for Evaluating Environmental Variability in Caenorhabditis elegans. Neuron *86*, 428-441.

Chalasani, S.H., Chronis, N., Tsunozaki, M., Gray, J.M., Ramot, D., Goodman, M.B., and Bargmann, C.I. (2007). Dissecting a circuit for olfactory behaviour in Caenorhabditis elegans. Nature *450*, 63-70.

Chen, Z., Hendricks, M., Cornils, A., Maier, W., Alcedo, J., and Zhang, Y. (2013). Two insulin-like peptides antagonistically regulate aversive olfactory learning in C. elegans. Neuron *77*, 572-585.

de Bono, M., and Maricq, A.V. (2005). Neuronal substrates of complex behaviors in C. elegans. Annu Rev Neurosci *28*, 451-501.

Dietrich, L.E., Price-Whelan, A., Petersen, A., Whiteley, M., and Newman, D.K. (2006). The phenazine pyocyanin is a terminal signalling factor in the quorum sensing network of Pseudomonas aeruginosa. Mol Microbiol *61*, 1308-1321.

Doi, M., and Iwasaki, K. (2002). Regulation of retrograde signaling at neuromuscular junctions by the novel C2 domain protein AEX-1. Neuron *33*, 249-259.

Felix, M.A., and Duveau, F. (2012). Population dynamics and habitat sharing of natural populations of Caenorhabditis elegans and C. briggsae. BMC Biol *10*, 59.

Glater, E.E., Rockman, M.V., and Bargmann, C.I. (2014). Multigenic natural variation underlies Caenorhabditis elegans olfactory preference for the bacterial pathogen Serratia marcescens. G3 (Bethesda) *4*, 265-276.

Gray, J.M., Hill, J.J., and Bargmann, C.I. (2005). A circuit for navigation in Caenorhabditis elegans. Proc Natl Acad Sci U S A *102*, 3184-3191.

Gusarov, I., Gautier, L., Smolentseva, O., Shamovsky, I., Eremina, S., Mironov, A., and Nudler, E. (2013). Bacterial nitric oxide extends the lifespan of C. elegans. Cell *152*, 818-830.

Hobert, O. (2013). The neuronal genome of Caenorhabditis elegans. WormBook, 1-106.

Inagaki, H.K., Panse, K.M., and Anderson, D.J. (2014). Independent, reciprocal neuromodulatory control of sweet and bitter taste sensitivity during starvation in Drosophila. Neuron *84*, 806-820.

Ishihara, T., Iino, Y., Mohri, A., Mori, I., Gengyo-Ando, K., Mitani, S., and Katsura, I. (2002). HEN-1, a secretory protein with an LDL receptor motif, regulates sensory integration and learning in Caenorhabditis elegans. Cell *109*, 639-649.

Kanoski, S.E., and Davidson, T.L. (2011). Western diet consumption and cognitive impairment: links to hippocampal dysfunction and obesity. Physiol Behav *103*, 59-68.

Li, C., and Kim, K. (2008). Neuropeptides. WormBook, 1-36.

MacNeil, L.T., Watson, E., Arda, H.E., Zhu, L.J., and Walhout, A.J. (2013). Diet-induced developmental acceleration independent of TOR and insulin in C. elegans. Cell *153*, 240-252.

Mahoney, T.R., Luo, S., Round, E.K., Brauner, M., Gottschalk, A., Thomas, J.H., and Nonet, M.L. (2008). Intestinal signaling to GABAergic neurons regulates a rhythmic behavior in Caenorhabditis elegans. Proc Natl Acad Sci U S A *105*, 16350-16355.

Martin, B., Golden, E., Carlson, O.D., Egan, J.M., Mattson, M.P., and Maudsley, S. (2008). Caloric restriction: impact upon pituitary function and reproduction. Ageing Res Rev *7*, 209-224.

McGhee, J.D. (2007). The C. elegans intestine. WormBook, 1-36.

Meisel, J.D., Panda, O., Mahanti, P., Schroeder, F.C., and Kim, D.H. (2014). Chemosensation of bacterial secondary metabolites modulates neuroendocrine signaling and behavior of C. elegans. Cell *159*, 267-280.

Mello, C., and Fire, A. (1995). DNA transformation. Methods Cell Biol *48*, 451-482.

Moerman, D.G., and Williams, B.D. (2006). Sarcomere assembly in C. elegans muscle. WormBook, 1-16.

O'Loughlin, C.T., Miller, L.C., Siryaporn, A., Drescher, K., Semmelhack, M.F., and Bassler, B.L. (2013). A quorum-sensing inhibitor blocks Pseudomonas aeruginosa virulence and biofilm formation. Proc Natl Acad Sci U S A *110*, 17981-17986.

Piper, M.D., Skorupa, D., and Partridge, L. (2005). Diet, metabolism and lifespan in Drosophila. Exp Gerontol *40*, 857-862.

Pradel, E., Zhang, Y., Pujol, N., Matsuyama, T., Bargmann, C.I., and Ewbank, J.J. (2007). Detection and avoidance of a natural product from the pathogenic bacterium Serratia marcescens by Caenorhabditis elegans. Proc Natl Acad Sci U S A *104*, 2295-2300.

Reinke, S.N., Hu, X., Sykes, B.D., and Lemire, B.D. (2010). Caenorhabditis elegans diet significantly affects metabolic profile, mitochondrial DNA levels, lifespan and brood size. Molecular genetics and metabolism *100*, 274-282.

Richter, C.P., Holt, L.E., Jr., and Barelare, B., Jr. (1937). Vitamin B1 Craving in Rats. Science *86*, 354-355.

Rivera, H.M., Christiansen, K.J., and Sullivan, E.L. (2015). The role of maternal obesity in the risk of neuropsychiatric disorders. Front Neurosci *9*, 194.

Sanchez-Blanco, A., and Kim, S.K. (2011). Variable pathogenicity determines individual lifespan in Caenorhabditis elegans. PLoS Genet *7*, e1002047.

Sawin, E.R., Ranganathan, R., and Horvitz, H.R. (2000). C. elegans locomotory rate is modulated by the environment through a dopaminergic pathway and by experience through a serotonergic pathway. Neuron *26*, 619-631.

Sheng, M., Hosseinzadeh, A., Muralidharan, S.V., Gaur, R., Selstam, E., and Tuck, S. (2015). Aberrant fat metabolism in Caenorhabditis elegans mutants with defects in the defecation motor program. PLoS One *10*, e0124515.

Shioi, G., Shoji, M., Nakamura, M., Ishihara, T., Katsura, I., Fujisawa, H., and Takagi, S. (2001). Mutations affecting nerve attachment of Caenorhabditis elegans. Genetics *157*, 1611-1622.

Shtonda, B.B., and Avery, L. (2006). Dietary choice behavior in Caenorhabditis elegans. J Exp Biol *209*, 89-102.

Sifri, C.D., Begun, J., Ausubel, F.M., and Calderwood, S.B. (2003). Caenorhabditis elegans as a model host for Staphylococcus aureus pathogenesis. Infect Immun *71*, 2208-2217.

Sulston, J.E., Schierenberg, E., White, J.G., and Thomson, J.N. (1983). The embryonic cell lineage of the nematode Caenorhabditis elegans. Dev Biol *100*, 64-119.

Tan, M.W., Mahajan-Miklos, S., and Ausubel, F.M. (1999). Killing of Caenorhabditis elegans by Pseudomonas aeruginosa used to model mammalian bacterial pathogenesis. Proc Natl Acad Sci U S A *96*, 715-720.

Thacker, C., and Rose, A.M. (2000). A look at the Caenorhabditis elegans Kex2/Subtilisin-like proprotein convertase family. Bioessays *22*, 545-553.

Tilly, J.L., and Sinclair, D.A. (2013). Germline energetics, aging, and female infertility. Cell Metab *17*, 838-850.

Warren, C.E., Krizus, A., and Dennis, J.W. (2001). Complementary expression patterns of six nonessential Caenorhabditis elegans core 2/I N-acetylglucosaminyltransferase homologues. Glycobiology *11*, 979-988.

White, J.G., Southgate, E., Thomson, J.N., and Brenner, S. (1986). The structure of the nervous system of the nematode Caenorhabditis elegans. Philos Trans R Soc Lond B Biol Sci *314*, 1-340.

Wilkinson, D.S., Taylor, R.C., and Dillin, A. (2012). Analysis of aging in Caenorhabditis elegans. Methods Cell Biol *107*, 353-381.

Willett, W.C. (1994). Diet and health: what should we eat? Science *264*, 532-537.

Yu, L., Yan, X., Ye, C., Zhao, H., Chen, X., Hu, F., and Li, H. (2015). Bacterial Respiration and Growth Rates Affect the Feeding Preferences, Brood Size and Lifespan of Caenorhabditis elegans. PLoS One *10*, e0134401.

Zhang, Y., Lu, H., and Bargmann, C.I. (2005). Pathogenic bacteria induce aversive olfactory learning in Caenorhabditis elegans. Nature *438*, 179-184.

CHAPTER 4.

Conclusions and future directions

In this dissertation, I present findings of molecular and cellular mechanisms that allow the nervous system to respond to changing environmental conditions by generating flexible behaviors. In Chapter 2, I show that internal states such as hunger can modify neural functions using conserved molecular signals for sensing and relaying energy status. In Chapter 3, I demonstrate that dietary changes in bacteria food sources alter behavior via neuropeptide signaling. In both scenarios, I reveal a crucial role for neuropeptide signaling between different tissues in transient modification of behaviors. Together, my work suggests that animal nervous systems respond to different types of environmental perturbations by generating flexible and appropriate behaviors. In this chapter, I will discuss how my research contributes to the existing body of knowledge. While this dissertation presents novel mechanisms linking genes, molecules and cells in the context of prior experience modification of behavior, much remains to be explored. I will highlight some areas of interest that remain incompletely understood and inform how research can further contribute to the biology of how animals respond appropriately to the surrounding, ever-changing world.

Internal states modify neural circuits

Using food deprivation as a way to alter internal state, I reveal mechanisms that allow organisms to respond to environmental change. Animals must be able to sense and regulate food status on multiple levels including cellular metabolism and tissue homeostasis. For detecting a drop in energy levels upon food deprivation, I identified a role for MondoA, a transcription factor in the Myc family. Further, I show that MondoA allows multiple tissues including the intestine and body wall muscles to detect a change

in glucose levels. Recently, RNA sequencing has been used to reveal the role of the Mondo-Mlx complex. Detecting gene expression changes induced by sugar intake *in vivo* revealed that Mondo-Mlx regulates genes for nutrient digestion, biosynthesis, triglyceride homeostasis, fatty acid biosynthesis and desaturation (Mattila et al., 2015). This research further characterizes the role of MondoA as a master regulator of sugar-responsive genes that allows animal metabolism to adapt to the amount of sugar available in its diet. Having revealed a connection between the MondoA glucose sensing transcription factor and neural function in my studies, it would be interesting to extend the RNA sequencing approach beyond metabolism-related gene transcription. More specifically, it may be interesting to identify RNA transcript changes regulated by MondoA that are also related to neuropeptide signaling, which is required for modifying behavior upon food deprivation.

Beyond sugar sensing molecules, it is likely that proteins also sense and regulate the condition other types of energy stores in various tissues. While MondoA directly binds glucose-6-phosphate (Havula and Hietakangas, 2012), other molecules such as amino acids, fatty acids, coenzymes and metabolic intermediates are core components of glycolysis, the citric acid cycle and cellular metabolism. Depending on the metabolic needs of the organism, it may be possible that behaviors are further fine-tuned to appropriately replenish specific classes of macromolecules. In Chapter 2, I find that the timeline of behavior change is fast relative to large-scale physiological effects of food deprivation such as depletion of fat stores. This data suggests that behavior modification is employed as a first line of defense against starvation effects that can harm the body. I

speculate that subtle changes in gene expression at early stages of food deprivation can reveal key events affecting behavior.

My studies provide a link between multiple scales of biology from glucose sensing in cells, to relaying internal state in multiple tissues, to convergence of signals in neurons affecting behaviors. While more is known about how sensory neurons are altered in response to food conditions (Chalasani et al., 2010; Chao et al., 2004; Ezcurra et al., 2011), this focus on the sensory system neglects to address many other changes happening in the body. To further advance our understanding of how organisms cope with food deprivation as a system, an interdisciplinary approach involving techniques used in the fields of metabolism, cellular, molecular biology and neurobiology would be useful.

Interactions between species modifies behavior

Using different bacterial diets to modify external signals experienced by animals, I demonstrated that specific strains of bacteria acutely alter neural circuits and behavior. Using my food experience paradigm, I have provided an approach for investigating how external signals from interactions between species can modify animal behavior. *C. elegans* also interact with fungi and yeast in the environment (Jansson, 1994; Mylonakis et al., 2002), and understanding these external signals can aid our understanding of how prior experience affects animal behavior. Previous studies investigating the effect of bacteria signals on *C. elegans* behavioral responses to external stimuli have often been focused on and isolated at the sensory level. For example, *C. elegans* neuropeptides INS-6 and INS-7 work in a peptide-to-peptide loop between two pairs of sensory neurons.

Further effects of this loop is relayed to a pair of downstream interneurons where the insulin signaling cascade functions (Chen et al., 2013). As limited by this approach, the link between the intestine and the nervous system for altering behavior remains elusive. I have shown that exposure to PA14 induces behavioral change that is dependent on AEX-5 function in the intestine. This data suggests that bacteria action in the intestine is relayed to the neural circuits that generate behavior. Multiple immune signaling pathways have been shown to be activated incoordination of pathogen specific immune responses including insulin signaling and MAP kinase pathway. While some immune defense mechanisms have been elucidated (Pukkila-Worley and Ausubel, 2012), further studies revealing how bacteria interactions with intestinal cells specifically affect the nervous system and behavior would be interesting.

While the interaction between pathogenic bacteria and host can be characterized as defense and invasion, bacteria and hosts can also share a commensal relationship. An emerging field studying the commensal relationship of bacteria and host shifts the focus to understanding the microbiota-gut-brain axis. Microbiome interactions with the nervous system can have varied effects on animal physiology and conditions. These long range interactions from the gut to the brain have been shown to affect fundamental processes impacted in neurodevelopmental disorders (Hsiao et al., 2013). Furthermore, gut-brain communication between microbiota and the nervous system has also been shown to have profound effects on brain development, behavior and disorders relating to anxiety and autism (Collins et al., 2012). In addition to the effects of microbiota on the central nervous system, the reciprocal effects of stress on microbiota composition also have important implications for health and physiology (Cryan and Dinan, 2012). Studies in

mammals have begun to unravel the bidirectional effects between microbiota and hosts. In one example, studies in humans that show consumption of probiotic milk products modulates brain activity (Tillisch et al., 2013). In rodents, isolation in a germ free environment has been shown to lead to behavioral and neurochemical consequences (Cryan and O'Mahony, 2011). However, due to the complexity of the mammalian system, I propose that use of simpler model organisms will be beneficial in understanding the cause and effect relationship between microbes and hosts. Pathways that have been implicated in the bidirectional communication between microbiota and the nervous system involve cytokines, cortisol, neurotransmitters and fatty acids (Cryan and Dinan, 2012). From its natural environment, *C. elegans* strains isolated from the wild have been shown to encounter and host various types of bacteria and yeast (Felix and Duveau, 2012). I propose that it would be feasible to use the simple *C. elegans* model with powerful genetics and molecular tools to identify tissues, signals and cellular responses involved. Further research into how bacteria interact with hosts will provide a greater understanding of the body as an ecosystem.

Multiple tissue-released neuropeptides

My analysis demonstrates a role for proprotein convertases in modifying behavior upon both food deprivation and bacteria exposure in Chapters 2 and 3. I show that *aex-5* proprotein convertase mutants are defective in modifying behavior after acute food deprivation and exposure to bacteria diets. Proteolytic cleavage at basic amino acid sites to release active peptides by proprotein convertases have been identified in all eukaryotes examined from nematodes to mammals (Seidah and Chrétien, 1997). My results also

demonstrate a role for non-neuronal tissue released neuropeptides via dense core vesicles. My studies reveal that as conditions change on the timescale of hours, neuropeptides can be released from multiple tissues to respond to changes in the environment. However, it remains a question as to how neuropeptide function is *regulated* to dynamically respond to changes in the body. A deeper understanding of neuropeptide regulation including key proteins involved in processing and release will be useful. One additional mechanism for regulating peptide action comes from the receptor where expression or transport of the receptor to the membrane can be regulated. For example, 24 hours of starvation down regulates the *C. elegans* insulin receptor DAF-2 (Kimura et al., 2011). Understanding these various levels of regulation for peptide processing, packing, release and binding will allow a better understanding of peptide action.

While I demonstrate a role for neuropeptide processing and release in relaying food deprived internal state, performing a screen to identify the cognate peptide revealed that no single insulin-like peptide alone was responsible for the modified behavioral phenotype. I speculate that multiple neuropeptides synergistically act together in this context. In a similar manner, although insulin receptor *daf-2* mutants show a strong dauer phenotype, no single insulin-like peptide mutant recapitulates the phenotype (Ritter et al., 2013). With 40 insulin-like peptide genes identified in the *C. elegans* genome, I propose that this expansive repertoire of peptides allows for combinatorial uses for achieving greater flexibility in encoding different conditions. Previous studies have also identified neuropeptides that work together in the context of modulating excitation and inhibition in locomotion (Stawicki et al., 2013) and in aversive olfactory learning (Chen et al., 2013). With a highly diversified family of peptides, parsing out the specific functions of each

peptide and further understanding how they work together remains a challenge. New genomic approaches can accelerate research in these areas. Complex and dynamic peptide expression have been observed in contexts such as development, starvation, aging and heat stress (Ritter et al., 2013). Using a mass-spectrometry based proteomic approach to profile and analyze large numbers of peptides would provide a high throughput method for screening peptide signaling responses to environmental changes. Resolution at the tissue or cellular level combined with peptidomics profiling would allow an unbiased way to capture information about the use of peptides in specific contexts.

Taken together, the work presented in my dissertation contributes to an understanding of how prior experience alters animal behavior. As a response to environmental changes, animals' neural circuits are modified to generate context-dependent behaviors that maximize survival. This research highlights how an approach combining genetic and molecular methods in studying robust behaviors can be fruitful in revealing key insights into complex biological processes. By gaining an understanding at different levels, whether it is between organisms and the environment, interactions between organisms, the signaling between tissues, or the inputs and outputs of a neural circuit, these connections can allow a more complete understanding of underlying biological mechanisms.

REFERENCES

Chalasani, S.H., Kato, S., Albrecht, D.R., Nakagawa, T., Abbott, L.F., and Bargmann, C.I. (2010). Neuropeptide feedback modifies odor-evoked dynamics in Caenorhabditis elegans olfactory neurons. Nat Neurosci *13*, 615-621.

Chao, M.Y., Komatsu, H., Fukuto, H.S., Dionne, H.M., and Hart, A.C. (2004). Feeding status and serotonin rapidly and reversibly modulate a Caenorhabditis elegans chemosensory circuit. Proc Natl Acad Sci U S A *101*, 15512-15517.

Chen, Z., Hendricks, M., Cornils, A., Maier, W., Alcedo, J., and Zhang, Y. (2013). Two insulin-like peptides antagonistically regulate aversive olfactory learning in C. elegans. Neuron *77*, 572-585.

Collins, S.M., Surette, M., and Bercik, P. (2012). The interplay between the intestinal microbiota and the brain. Nature Reviews Microbiology.

Cryan, J.F., and Dinan, T.G. (2012). Mind-altering microorganisms: the impact of the gut microbiota on brain and behaviour. Nature reviews neuroscience.

Cryan, J.F., and O'Mahony, S.M. (2011). The microbiome‐gut‐brain axis: from bowel to behavior. Neurogastroenterology & Motility *23*, 187-192.

Ezcurra, M., Tanizawa, Y., Swoboda, P., and Schafer, W. (2011). Food sensitizes C. elegans avoidance behaviours through acute dopamine signalling. The EMBO journal *30*, 1110-1122.

Felix, M.A., and Duveau, F. (2012). Population dynamics and habitat sharing of natural populations of Caenorhabditis elegans and C. briggsae. BMC Biol *10*, 59.

Havula, E., and Hietakangas, V. (2012). Glucose sensing by ChREBP/MondoA-Mlx transcription factors. Semin Cell Dev Biol *23*, 640-647.

Hsiao, E.Y., McBride, S.W., Hsien, S., Sharon, G., Hyde, E.R., McCue, T., Codelli, J.A., Chow, J., Reisman, S.E., Petrosino, J.F., Patterson, P.H., and Mazmanian, S.K. (2013). Microbiota Modulate Behavioral and Physiological Abnormalities Associated with Neurodevelopmental Disorders. Cell *155*.

Jansson, H.B. (1994). Adhesion of Conidia of Drechmeria coniospora to Caenorhabditis elegans Wild Type and Mutants. Journal of nematology *26*, 430-435.

Kimura, K.D., Riddle, D.L., and Ruvkun, G. (2011). The C. elegans DAF-2 insulin-like receptor is abundantly expressed in the nervous system and regulated by nutritional status. Cold Spring Harbor symposia on quantitative biology *76*, 113-120.

Mattila, J., Havula, E., Suominen, E., Teesalu, M., Surakka, I., Hynynen, R., Kilpinen, H., Väänänen, J., Hovatta, I., Käkelä, R., Ripatti, S., Sandmann, T., and Hietakangas, V.

(2015). Mondo-Mlx Mediates Organismal Sugar Sensing through the Gli-Similar Transcription Factor Sugarbabe. Cell reports *13*, 350-364.

Mylonakis, E., Ausubel, F.M., Perfect, J.R., Heitman, J., and Calderwood, S.B. (2002). Killing of Caenorhabditis elegans by Cryptococcus neoformans as a model of yeast pathogenesis. Proc Natl Acad Sci U S A *99*, 15675-15680.

Pukkila-Worley, R., and Ausubel, F.M. (2012). Immune defense mechanisms in the Caenorhabditis elegans intestinal epithelium. Current opinion in immunology *24*, 3-9.

Ritter, A., Shen, Y., Fuxman Bass, J., Jeyaraj, S., Deplancke, B., Mukhopadhyay, A., Xu, J., Driscoll, M., Tissenbaum, H., and Walhout, A. (2013). Complex expression dynamics and robustness in C. elegans insulin networks. Genome research *23*, 954-965.

Seidah, N.G., and Chrétien, M. (1997). Eukaryotic protein processing: endoproteolysis of precursor proteins. Current opinion in biotechnology *8*, 602-607.

Stawicki, T.M., Takayanagi-Kiya, S., Zhou, K., and Jin, Y. (2013). Neuropeptides function in a homeostatic manner to modulate excitation-inhibition imbalance in C. elegans. PLoS genetics *9*.

Tillisch, K., Labus, J., Kilpatrick, L., Jiang, Z., and Stains, J. (2013). Consumption of fermented milk product with probiotic modulates brain activity. Gastroenterology.